Title	Mechanism of Protein Misfolding
Author(s)	Goda, Shuichiro
Citation	大阪大学, 2000, 博士論文
Version Type	VoR
URL	https://doi.org/10.11501/3169139
rights	
Note	
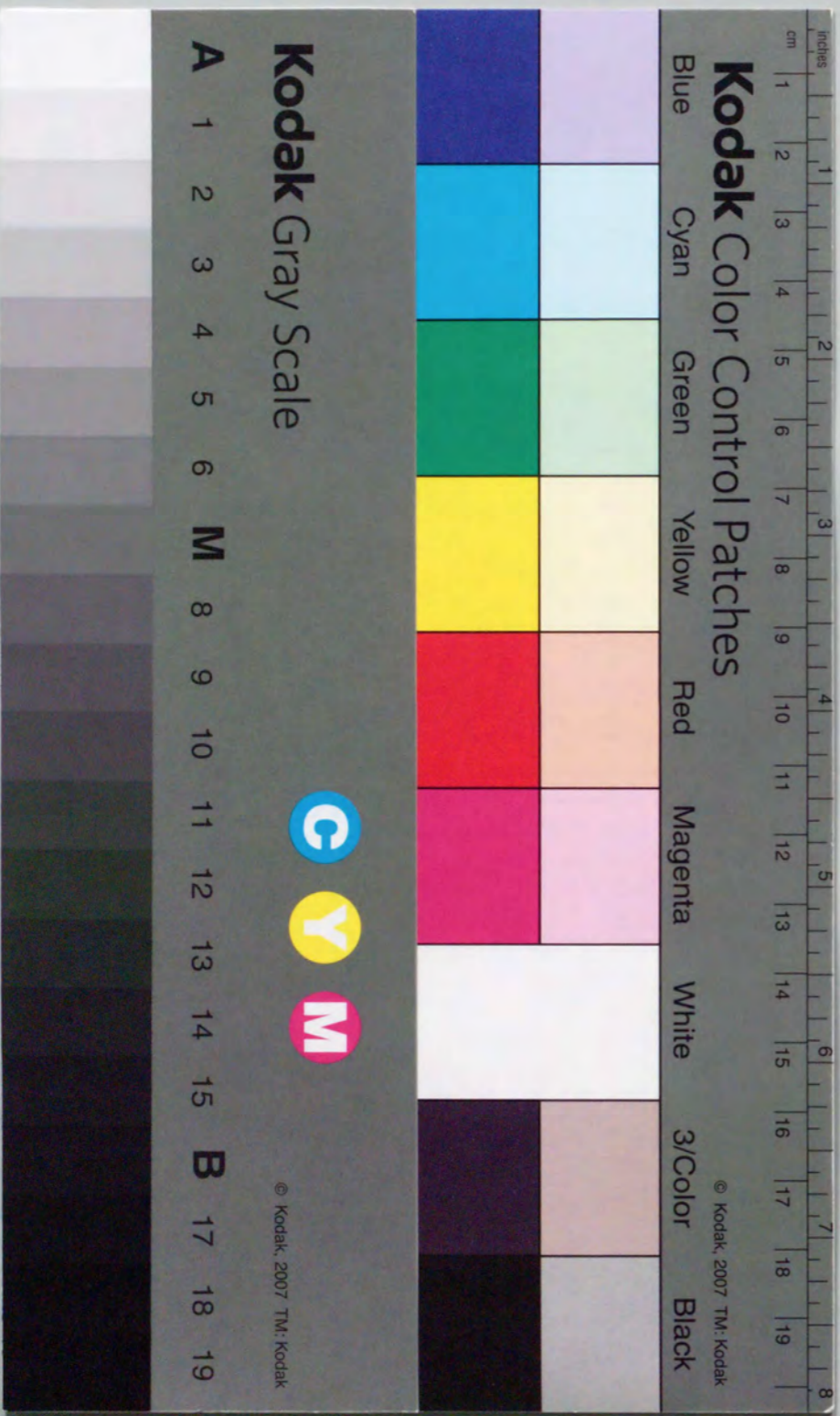
Mechanism of Protein Misfolding

A Doctoral Thesis

by

Shuichiro Goda

Submitted to

the Graduate School of Science,

Osaka University

February, 2000

Mechanism of Protein Misfolding

A Doctoral Thesis

by

Shuichiro Goda

Submitted to

the Graduate School of Science,

Osaka University

February, 2000

Acknowledgments

Shuichiro Goda

Contents

Abbreviations Used in This Thesis

ASA   accessible surface area

B-factor   temperature factor

CD   circular dichroism

CR   Congo red

ΔC_p heat capacity change between native and denatured states

ΔG Gibbs energy change of denaturation

ΔH enthalpy change of denaturation

ΔS entropy change of denaturation

DSC   differential scanning calorimetry

EAEA-lysozyme   human lysozyme with four extra residues (Glu-Ala-Glu-Ala-) at N-terminal residue

EAEA-I56T   human lysozyme with four extra residues and point mutated at 56 Ile to Thr

I56T   human lysozyme point mutated at 56 Ile to Thr

NMR   nuclear magnetic resonance

T_d denaturation temperature

r.m.s.   root mean square

R factor $\Sigma||F_o|-|F_c||/\Sigma|F_o|$, where F_o and F_c are the observed and calculated structure factor amplitudes, respectively.

R_{merge} $100\Sigma|I_{h,i}<I_h>|/\Sigma I_{h,i}I_{h,I}$, where $I_{h,i}$ is individual values, and $<I_h>$ is the mean intensity of the reflection h.

Chapter I

General Introduction

Protein Folding

Proteins are produced to play their specific roles in organisms; some catalyze physiological reactions with their own specificity, some are used as constructional materials of bodies and some are involved in electron transfer or transport of physiological materials and products. In this context, proteins consisting of 20 kinds of amino acids can be regarded as ultimate functional and sophisticated macromolecules.

Twenty kinds of natural L-amino acids are polymerized to make a single polypeptide chain without branching. This chain folds into its intrinsic native conformation to exert its proper function. In other words, forming the tertiary structure of a polypeptide (folding) is essential for exhibiting its physiological function. What a gene governs is only an amino acid sequence. However, when a gene is translated into amino acid residues, the given polypeptide chain can fold spontaneously to gain its inherent activity even *in vitro*. Understanding how a protein molecule folds a unique functional three-dimensional structure based only on the information of an amino acid sequence is a question that has intrigued scientists for decades. Since Anfinsen's proposal (1973) that the tertiary structure of a protein is determined by its amino acid sequence, a huge number of studies on protein folding have been performed to clarify the mechanism of how proteins adopt the native folding (Kuwajima, 1989).

What is Protein Misfolding?

Several diverse disorders, including the prevalent dementias and encephalopathies, are now believed to arise from the same general disease mechanism (Tan & Pepys, 1994; Kelly, 1996). In each, there is abnormal folding of proteins and then aggregation of an underlying protein. The gradual

accumulation of these aggregates and the acceleration of their formation by stress explain the characteristic late or episodic onset of the clinical disease. The understanding of these processes at the molecular level is opening prospects of more rational approaches to investigation and therapy (Peterson *et al.*, 1998).

Understanding of individual disorders is greatly helped by grouping them on the basis of their pathology, into categories such as inflammatory, degenerative, infectious, or neoplastic disease. Carrell & Lomas, (1997) have proposed the addition of a new entity, "conformational disease", which is an otherwise diverse group of disorders (Table I-1) that includes some of the currently most perplexing medical problems such as Alzheimer's disease (Bayreuther & Masters, 1996) and the prion encephalopathies (Collinge & Rosser, 1996; Collee, 1996).

Conformational diseases arise when a constituent protein undergoes a change in size or fluctuation in shape, with resultant self-association and tissue deposition. Although such changes can occur with normal proteins, there is commonly an interacting genetic contribution, which may sometimes be dominant. There is a clear differentiation between the conformational diseases and most other genetic diseases which are directly due to a failure of production of a protein as occurs with haemoglobin in the thalassaemias. Such failure in production may be due to an initial misfolding of the newly synthesized protein. The differentiating feature of the conformational disease is that at least some of the proteins are correctly folded and released in their normal form. The conformational disease arises from subsequent changes that lead to the aggregation and deposition of the protein, with consequent late or episodic onset of the disorder as with haemoglobin in sickle-cell disease, for example.

The risk of self-association and aggregation, whether it is associated with a genetic defect or not, is greatly increased with proteins that are inherently able to

Table I-1   *List of conformational diseases*

Fibrils and aggregates

Haemoglobin:	Sickle cell anaemia
	Unstable haemoglobin inclusion-body haemolysis
	Drug-induced inclusion body haemolysis
Prion proteins:	Creutzfeld-Jakob disease (CJD)
	New variant CJD (? Bovine spongiform encephalopathy)
	Gerstmann-Straussler-Scheinker disease
	Fatal familial insomnia
	Kuru
Serpins:	α_1-antitrypsin deficiency-emphysema.cirrhosis
	Antithrombin deficiency thromboembolic disease
	C_1-inhibitor deficiency angioedema
Glutamine-repeats:	Inherited neurodegenerative disorders
	Huntington's disease
	Spinocerebellar ataxin
	Dentato-ubro-pallido-luysian atrophy
	Machado-Joseph atrophy
β-amyloid protein:	Alzheimer's disease
	Down's syndrome
	Familial Alzheimer's-β-amyloid precursor
	Presenilins 1 and 2

Table I-1 *(continued)*

Amyloidoses

Immunoglobulin light chain:	Systemic AL amyloidosis
	Nodular AL amyloidosis
Serum amyloid A protein:	Reactive systemic AA amyloidosis
	Chroric inflammatory disease
Transthyretin:	Senile systemic amyloidosis
	Familial amyloid neuropathy
	Familial cardiac amyloid
$\beta_2$microglobulin:	Haemodialysis amyloidosis
	Prostatic amyloid
Apolipoprotein AI:	Familial amyloid polyneuropathy
	Familial visceral amyloid
Cystatin C:	Hereditary (Icelandic) cerebral angiopathy
Lysozyme:	Familial visceral amyloidosis

undergo radical changes in their conformation. This point is true both of the prion proteins, in which the change in shape can be propagated by induction, and of the plasma serpins, where fibril formation results from the premature occurrence of a physiological conformational transition.

In the case of diseases caused by protein misfolding (Table I-1), fibrils which consist of proteins are seen at the diseased part in many cases. The fibrils have the same common feature as that of amyloid fibrils. Therefore, studies on the formation of amyloids fibril are important.

Amyloidosis

Amyloidosis is a disorder of protein metabolism, which may be either acquired or hereditary, characterized by extracellular deposition of abnormal protein fibrils (Pepys, 1996). Many different proteins can form amyloid fibrils. At least 16 different proteins and polypeptides have been identified in amyloid deposits to date (Tan & Pepys, 1994; Kelly, 1996). Proteins known to form amyloid fibrils *in vivo* have no obvious sequence or structural similarities, and where the soluble folds of the amyloidgenic precursors are known, they span the range of secondary, tertiary, and quaternary structural elements. In spite of this diversity, there is a body of evidence that indicates that all amyloid fibrils have a common core structure (Sunde & Blake, 1997). All amyloid fibrils are long, straight, and unbranching, with a diameter of 70-120 Å, and they all exhibit a cross-β diffraction pattern. Recent high-resolution fiber diffraction studies of different amyloid fibrils have shown a detailed molecular similarity at the level of the protofilament skeleton. The model initially proposed for the core structure of the transthyretin amyloid (Blake & Serpell, 1996), which is a continuous β-sheet helix, can be extended to other amyloids formed by proteins as diverse as

lysozyme and Immunoglobulin light chain (Sunde *et al.*, 1997). Current structural models suggest that the main molecular feature of these amyloid fibrils involve β-sheets organized as extended cross-β structures with a helical twist (Blake & Serpell, 1996; Sunde & Blake, 1997), as a helix with between 9 and 24 residues per turn (Lazo & Downing, 1998), or short, non-twisted β-sheets linked by loops (Jimenez *et al.*, 1999). The mechanism of the formation of such proteinaceous fibrils is not known in molecular detail, although general models for specific cases have been proposed (Arvinte *et al.*, 1993).

In addition, the deposits contain glycosaminoglycans, some of which are tightly associated with the fibrils, and also a non-fibrillar plasma glycoprotein, amyloid P component (AP). Small focal and clinically silent amyloid deposits in the brain, heart, seminal vesicles, and joints are a universal accompaniment of aging. However, systemic or significant local amyloid deposits usually accumulate progressively, disrupting the structure and function of affected tissues and leading inexorably to organ failure and death. No treatment yet exists which specifically causes resolution, but intervention which reduces availability of the protein precursors of amyloid fibrils may lead to regression.

Human Lysozyme Variants Causes Amyloidosis

Lysozyme (EC 3.2.1.17) is the classic bacteriolytic enzyme of external secretions, discovered by Fleming in 1922. It is also present at high concentration within articular cartilage and in the granules of polymorphonuclear leukocytes and is the major secreted product of macrophages. Lysozymes are present in most organisms in which they have been sought, although their physiological role is not always clear. The mutations which cause amyloid produce a substitution of Thr for Ile56 in one family and His for Asp67 in the other. The complete structures of

hen egg white and human lysozymes are known at atomic resolution, and their catalytic mechanism, epitopes, folding and other aspects of structure-function relationship have been analyzed exhaustively. This contrasts with the absence of detailed three-dimensional structural information on all other amyloid fibril proteins and their precursors, except transthyretin and β_2-microglobulin. Lysozyme, unlike transthyretin and β_2-microglobulin, is not inherently amyloidgenic and may therefore become a particularly valuable model for investigation of amyloid fibrillogenesis. Funahashi *et al.* (1996) has found that the physicochemical properties of the mutant human lysozyme in the native state were not different from those of the wild-type human lysozyme. On the other hand, the equilibrium and kinetic stabilities of the mutant human lysozyme were remarkably decreased due to the introduction of a polar residue (Thr) in the interior of the molecule. Funahashi *et al.* (1996) has concluded that the amyloid formation of the mutant human lysozyme is due to a tendency to favor (partly or completely) denatured structures.

Three Hallmarks of Amyloid Fibrils

Congo Red Staining

The initial steps in the structural characterization of amyloid were a consequence of the specific chemical staining of the material, at first using iodine, whose similarity to that observed in the iodine staining of cellulose gave rise to the name "amyloid" meaning starchlike (Virchow, 1854). Much later, staining with the dye Congo red has been observed to produce a characteristic green birefringence under cross-polarized light (Missmahl & Hartwig, 1953; Cohen, 1965; Missmahl, 1968), and this method is still used as a diagnostic test for amyloid (Fig. I-1). Early electron microscope studies of amyloid by Cohen &
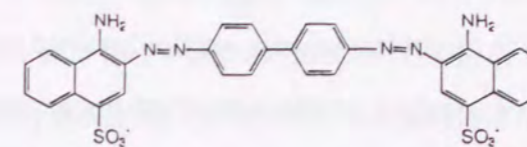
Fig. I-1. Structure of the dye, Congo red.
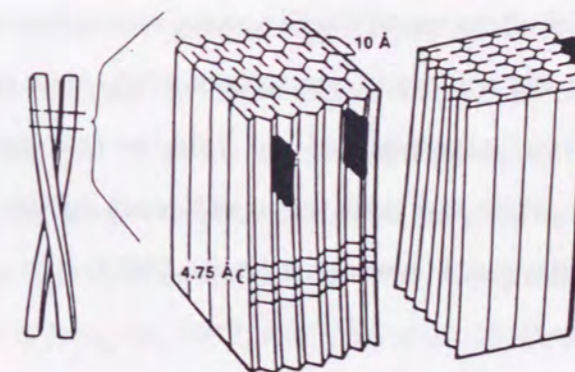
Fig. I-2. Modeled structure by Glenner (1980). Twisted β-pleated sheet antiparallel configuration of paired filaments of an amyloid fibril in acquired systemic amyloidosis. The sites of binding of the planar Congo red dye are indicated by the dark blocks. In this model, the smallest amyloidgenic building block is a bilaminar β-sheet containing a small number of β-strands, which can associate in a linear fashion with other such monomers by intermolecular hydrogen bonding (spacing 4.7 Å) between adjacent edge strands. This results in extension of the polymer in the direction of the fiber axis. These two-sheeted protofilaments can then associate with each other, stacking face-to-face, with an intersheet spacing of approximately 10 Å, and this increase the thickness of the protofilament.

Calkins (1959) have demonstrated that a variety of amyloids all have a similar morphology and ultrastructure, consisting of uniform fibrils about 100 Å wide, which are rigid and nonbranching. The fibrillar nature of the deposits, combined with the observation of birefringence in amyloid stained with Congo red, suggests that components of amyloid would consist of linear structures arranged in an orderly and parallel fashion (Fig. I-2) (Puchtler *et al.*, 1962; Wolman & Bubis, 1965). A comparison of amyloid staining by a variety of related dyes indicates that the binding of Congo red by amyloid is probably through hydrogen bonds, rather than ionic interactions, and that it would be favored by a substrate having a regular and linear arrangement of reactive groups (Puchtler *et al.*, 1962). The development of green birefringence appears to be dependent on two factors: (1) near-perfect parallel alignment of the Congo red molecule and (2) a thickness of the stained sample that will result in retardation of the slow rays of the polarized light by one-half the wavelength of red light, so that extinction of the red component of the white rays will occur and result in the appearance of the complementary color, green (Wolman & Bubis, 1965).

Electron microscopy

The principal characteristics of the amyloid fibril observable by electron microscopy have been comprehensively described by Shirahama & Cohen (1967). Working with *ex vivo* fibrils isolated from patients with secondary amyloidosis [composed of fragments of the serum amyloid A (SAA) protein or the immumoglobulin light chain], they have described the fibrils as being 75-80 Å in diameter and composed of five (or less likely, six) protofilaments, each about 25-35 Å wide, arranged parallel to one another, longitudinal or slightly oblique to the long axis of the fibril. Generally, amyloid fibrils are straight, unbranched fibrils, about 100 Å in diameter and of indefinite length, which appear to be composed of two or more protofilaments, each 25-35 Å in diameter. In turn, the protofilaments appear to be composed of two or three subunit strands 10-15 Å wide (termed subprotofilaments), arranged helically with a 35-50 Å repeat. It is, however, interesting to note that while the subprotofilament is not mentioned in the later work, the X-ray model of the transthyretin amyloid fibril core (Blake & Serpell, 1996) includes a helical substructure to the protofilament that is dimensionally similar to that described by Shirahama & Cohen in 1967. It therefore may need to be reinstituted as an element in the ultrastructure of the amyloid fibril.

X-ray diffraction

X-ray diffraction measurement is used to probe the molecular structure of the fibrils. The X-ray diffraction patterns suggest that the fibrils are composed of polypeptide chains extended in the so-called cross-β conformation (Eanes & Glenner, 1968; Bonar *et al.*, 1969), a structure that has earlier been identified as a possible conformation for polypeptide chains on the grounds of model building by Pauling & Corey (1951). Subsequent analyses by X-ray diffraction of a variety of amyloids (Burke & Rougvie, 1972; Kirschner *et al.*, 1986; Turnell *et al.*, 1986; Gilchrist & Bradshaw, 1993; Nguyen *et al.*, 1995; Blake & Serpell 1996), and also by NMR analysis (Lansbury *et al.*, 1995), have confirmed that the protein chains in all amyloid fibrils are predominantly in the cross-β-conformation.

Amyloid samples are usually exposed to the X-ray beam with the long axis of the fibrils more or less perpendicular to the direction of the beam. The X-ray reflections are then distinguished by their direction with reference to the fibril axis and their distance from the center of the pattern: meridional reflections are defined as those lying parallel to the fiber axis, and equatorial reflections are defined as those lying parallel to the fiber axis. If the long axes of the individual

fibrils within a bundle of fibrils or the bundles themselves deviate from the mean fiber axis, the corresponding reflections will be drawn out into arcs whose angular dispersion is related to the relative dispersion within the fibrillar bundles. In the most extreme unaligned case, where the fibrils lie at all possible angles, the reflections are drawn out into complete rings giving no indication as to whether they are meridional or equatorial.

The earliest reported fiber diffraction investigations, of serum amyloid A and light chain amyloid, have reported meridional reflections at 4.68 Å and equatorial reflections at 9.8 Å (Fig. I-2) (Eanes & Glenner, 1968; Bonar *et al.*, 1969; Glenner *et al.*, 1972). This pattern is characteristic of the cross-β structure, in that the meridional reflection indicates a regular structural repeat of 4.68 Å along the fibril axis and the equatorial reflection indicates a structural spacing of 9.8 Å perpendicular to the fiber axis. A β-sheet structure organized so that the sheet axis is parallel to the fibril axis, with its constituent β-strands perpendicular to the fibril axis, would fulfill the spacing requirements. The structural repeat of 4.68 Å along the fiber axis then corresponds to the spacing of adjacent β-strands, and the 9.8 Å spacing perpendicular to the fiber axis corresponds to the face-to-face separation of the β-sheets. The latter, of course, can only occur if the amyloid fibrils, or protofilaments, are composed of two or more β-sheets. The fiber diffraction data indicate that the β-sheets in amyloid probably contain a mixture of parallel and antiparallel hydrogen-bonded β-strands. A purely antiparallel arrangement of strands would give rise to the smallest repeat spacing, 9.6 Å, which is not observed. This indicates that at least some of the strands must be hydrogen-bonded in a parallel manner.

Physico-chemical Studies on Amyloidosis

Various methods have been exploited to elucidate the mechanism of amyloid fibril formation *in vitro*.

To estimate the stability of the protein, calorimetry has been used to directly evaluate the thermodynamic stability of a protein (Funahashi *et al.*, 1996). Under the equilibrium conditions, the conformational stability of a protein, the Gibbs energy change in denaturation (ΔG), can be estimated by differential scanning calorimetry (DSC) (Privalov & Khechinashvili, 1974; Becktel & Schellman, 1987), or by analyses of heat or denaturant denaturation curves of a protein using spectroscopic techniques (Hawkers *et al.*, 1984; Pace 1986). The exact thermodynamic parameters, Gibbs energy change (ΔG), enthalpy change (ΔH), and entropy change (ΔS), of denaturation are directly obtained only from the measurement of adiabatic DSC (Privalov, 1974; Privalov & Potekhin, 1986). The recent developments in sensitive calorimeters have allowed reliable measurements of the energetics for the denaturation process of a protein (Privalov & Khechinashvili, 1974; Privalov *et al.*, 1995; Plotnikov *et al.*, 1997). With this technique, the heat capacity of a protein solution can be measured during heating at a constant rate. The excess heat capacities are accompanied by denaturation of a protein. The denaturation temperature (T_d), calorimetric enthalpy change (ΔH_{cal}), van't Hoff enthalpy (ΔH_{vH}) and heat capacity change (ΔC_p) of denaturation can be directly obtained from analysis of the DSC curve. The temperature functions of the thermodynamic parameters of denaturation can be calculated using the following equations.

$$\Delta H(T) = \Delta H(T_d) - \Delta C_p (T_d - T) \qquad (I\text{-}1)$$

$$\Delta S(T) = \Delta H(T_d) / T_d - \Delta C_p \ln (T_d / T) \qquad (I\text{-}2)$$

$$\Delta G(T) = \Delta H(T) - T\Delta S(T) \qquad\qquad (I\text{-}3)$$

where ΔC_p is assumed to be independent of temperature (Privalov & Khechinashvili, 1974). DSC measurements should allow us to investigate the thermodynamic parameters for the denaturation of a protein.

On the other hand, kinetic and statistic aspects of a protein have been revealed by means of procedures in physical chemistry, such as spectroscopic; ultraviolet visible (UV) absorption, circular dichroism (CD), tryptophan fluorescence, infrared (IR), nuclear magnetic resonance (NMR) (Funahashi *et al.*, 1996; Booth *et al.*, 1997; Canet *et al.*, 1999). X-ray fibril diffraction and cryo-electron microscopy have been carried out to elucidate the structure of the amyloid fibrils in detail, described above (Sunde *et al.*, 1997; Jimenez *et al.*, 1999). Quasielastic light scattering (QLS) have been used (Shen *et al.*, 1993; Lomakin *et al.*, 1997) to elucidate the structural change in amyloid formation. Atomic force microscopy have been used to watch the amyloid fibril growth (Goldsbury *et al.*, 1999; Kowalewski & Holtzman, 1999). Ultracentrifugation have been used to elucidate the association of amyloid fibril formation (Lashuel *et al.*, 1998). In parallel with such experimental studies, theoretical works in molecular dynamics or calculation of stability have made progress in the simulation for protein folding exhibiting the behavior of a real protein (Radford & Dobson, 1999).

Amyloid-like Fibril Formation by Non-amyloidosis Related Proteins

It has been found that non-amyloidosis related proteins form amyloid fibril in extreme environments. One case is insulin which is a globular protein under physiological condition. By heating in a water bath at between 80 and 100 °C, insulin has been reported to form submicroscopic fibrils with the three hallmarks of amyloid (Burke & Rougvie, 1972; Klunk *et al.*, 1989). The fibrils can be transformed back to biologically active and crystallizable insulin (Waugh, 1957).

Recently, amyloid fibril formation of non-amyloidosis related proteins have been found for the SH3 domain of the p85α subunit of bovine phosphatidylinositol 3-kinase at acidic pH (Guijarro *et al.*, 1998), acylphosphatase in trifluoroethanol (Chiti *et al.*, 1999), the peptides corresponding to the cold shock protein of Bacillus subtilis (CspB) in acetonitrile at pH 4.0 (Gross *et al.*, 1999) and monellin from plant protein at pH 2.5 and 85 °C. Even a protein derived from hyperthermophile (methionine aminopeptidase from *Pyrococcus furiosus*) forms amyloid fibrils in the presence of guanidine hydrochloride in the acidic region (Yutani *et al.*, 2000). These results also indicate that all conditions forming amyloid are in extreme environments far from the physiological condition and suggest that the amyloid fibril formation occurs via the denaturation process of proteins. Furthermore, these results suggest that the potential for amyloid deposition may be a common property of proteins and not only of a few proteins associated with disease.

Purpose and Outline of This Thesis

The final goal of this thesis is to understand the mechanism of amyloid fibril formation. The relationship between amyloidgenecity and thermal stability suggests that the instability of the protein is the driving force of amyloid fibril formation (Funahashi *et al.*, 1996). However, these experiments do not estimate the stability between the native and amyloid fibril forms. It is important to understand the transition process from the native to amyloid forms. Therefore, determining the conditions of amyloid fibril formation *in vitro* should be attempted. The complete structure of human lysozyme, whose variants are amyloidgenic, is known at atomic resolution and the physicochemical properties have been exhaustively analyzed. Thus, we chose human lysozyme as a model

protein for investigation of amyloid fibrillogenesis. First, we constructed the high expression system of human lysozyme using *Pichia pastoris*, because a large amount of protein is needed to study the conditions of amyloid formation. Amyloid fibril formation was found to occur in highly concentrated ethanol solution by human lysozyme. In addition to amyloidgenic mutant human lysozyme, the amyloid fibril formation was observed in the wild-type human lysozyme. Furthermore, we found that hen egg lysozyme which is non-disease-related protein forms amyloid fibrils in highly concentrated ethanol solution. This confirms that the amyloid fibril formation is a common property of globular proteins.

Chapter II shows the results of the high expression system of human lysozyme. *P. pastoris* expressed the human lysozyme at about 300 mg per L of broth, but four extra residues (Glu^{-4}-Ala^{-3}-Glu^{-2}-Ala^{-1}-) were added at the N-terminal of the expressed protein (EAEA-lysozyme). To determine the effect of the four extra residues on the stability, structures and folding of the protein, calorimetry, X-ray crystal analysis and GuHCl denaturation experiments were performed. The calorimetric studies showed that the EAEA-lysozyme was destabilized by 9.6 kJ/mol at pH 2.7 compared with the wild-type protein.

Chapter III shows the amyloid fibril formation of wild-type human lysoyme, amyloidgenic variant (I56T), EAEA-lysozyme and an amyloidgenic variant with four extra residues (EAEA-I56T) in ethanol solution. It was found that all human lysozymes precipitate in a highly concentrated ethanol solution. The precipitates were examined using three hallmarks of amyloid fibrils to determine whether amyloid fibrils are formed in the precipitates. These results of three hallmarks indicated that the precipitates of human lysozymes are amyloid protofilaments

and that the amyloid protofilament formation of human lysozyme follows closely on the destruction of the helical and tertiary structures.

The rate of amyloid formation was measured by the wild-type and three types of variant human lysozymes in 80 % ethanol solution at 25 °C. The wild-type protein did not form amyloid protofilaments after incubation for 30 hours in 80 % ethanol solution, but the amyloidgenic variants formed amyloid protofilaments up to 8 hours. EAEA-lysozyme and EAEA-I56T, which were largely destabilized as compared with the wild-type protein, formed amyloid protofilaments within one hour. This result suggests that the amyloidgenecity was strongly related to the stability of the proteins.

Chapter IV shows the amyloid fibril formation of hen egg lysozyme in highly concentrated ethanol solution. In highly concentrated ethanol solution, hen egg lysozyme, which is not related with amyloidosis, also formed amyloid protofilaments. This result suggests that the amyloid formation is a common property of globular proteins under appropriate conditions.

Chapter V summarizes the main results and conclusions obtained in this work.

The successive chapters, II to IV, correspond to each paper listed at the end of this thesis, [1] to [3], respectively.

Chapter II

Studies on the Stability and Folding of Human Lysozyme Expressed in *Pichia pastoris*

Introduction

Human lysozyme (EC 3.2.1.17) is widely distributed in several human tissues and secretions including milk, tears, and saliva (Peters *et al.*, 1989). It is composed of 130 amino acid residues and the molecular weight is 14.7 k. Its physico-chemical properties have been extensively studied (Artymiuk & Blake, 1981; Redfield & Dobson, 1990; Takano *et al.*, 1999a and references in these articles). Furthermore, two types of human lysozyme variants (Ile56Thr and Asp67His) are known to be amyloidogenic (Pepys *et al.*, 1993). Therefore, human lysozyme is expected to be a model protein in order to solve the mechanism of the amyloid disease caused by protein misfolding (Carell & Lomas, 1997). The expression systems have been reported using *Saccharomyces cerevisiae*, but the expression yield is about 2.4 mg per L of broth (Taniyama *et al.*, 1988; Muraki *et al.*, 1987). Therefore, we planned to construct the expression systems of the human lysozyme by *Pichia pastoris* GS115(His⁻) to get more human lysozyme variants in order to determine the characteristics of the amyloid formation.

The methylotropic yeast *P. pastoris* has recently attracted the attention to overexpress the proteins and has been used to express many kinds of proteins. Some proteins are expressed by several grams per L of broth (Tschopp *et al.*, 1987; Paifer *et al.*, 1994). However, the expression yields depend on the signal peptide and protein sequence in the yeast expression system (Hashimoto *et al.*, 1998). In some cases, a few residues are left at the N-terminal residue of the expressed protein derived from the signal peptide sequence problem (Steinlein *et al.*, 1995).

When a protein is expressed in *Escherichia coli*, a methionine residue is sometimes left at the N-terminal residue of an expressed protein when the penultimate residue is relatively bulky and/or charged (Flinta *et al.*, 1986;

Moerschell *et al.*, 1990). For lysozymes and α-lactoalbumins, this is also the case, because their N-terminal residues are lysine. It has been reported that the extra methionine residues at the N-terminal remarkably affect the conformational stability (Ishikawa *et al.*, 1998; Chaudhuri *et al.*, 1999; Takano *et al.*, 1999b). On the other hand, polyhistidine tags in the N/C terminal regions of proteins are widely used to easily isolate the proteins (Kuliopulos & Walsh, 1994). However, the effect of several elongation residues to N/C-terminal on the structure, stability and folding have not yet been well examined. Recently, Matsuura *et al.* (1999) have shown that the elongation to the N/C-terminal would lead to the construction of proteins with a higher stability and activity, because it provides a new protein sequence variety. More information on the stability-structure relationships of proteins with extra residues at the N/C terminals is then required.

The human lysozyme could be expressed by 300 mg/L of broth using the system of *P. pastoris* GS115(His⁻). However, four extra residues (Glutamic acid⁻⁴-Alanine⁻³-Glutamic acid⁻²-Alanine⁻¹-; EAEA-) derived from the signal peptide remained at the N-terminal residue of the expressed human lysozyme. It is called the EAEA-lysozyme. The EAEA-lysozyme also shows better amyloidgenic behavior than the wild-type protein (in Chapter III). It is important to know the physico-chemical properties of the protein which has good amyloidgenic behavior. In this paper, the effects of the four extra residues of the EAEA-lysozyme on stability, structure, and folding were examined using circular dichroism (CD), differential scanning calorimetry (DSC) and X-ray crystal diffraction. We will discuss the mechanism of changes in the conformational stability on the basis of the EAEA-lysozyme structure.

Materials and methods

Construction of expression vector and introduction into P. pastoris

The human lysozyme gene was amplified from pGEL125 (Taniyama *et al.*, 1988) using 5'-TTTGG<u>CTCGAG</u>AAAAGAGAGGCTGAAGCTAAGGTTTTCGAGAGATGC GAATTAGCC and 5'-AAGGATCCC<u>GAATTC</u>AGCTATTAAACACCAC as primers (underlining indicates *Xho*I and *Eco*RI site, respectively). The PCR product was digested with *Xho*I and *Eco*RI and the resulting fragment was cloned into pPIC9 (Invitrogen Inc., California, USA) digested with *Xho*I and *Eco*RI. In the resulting plasmid, designated Human lysozyme/pPIC9 (Fig. II-1), the human lysozyme gene was fused with the pre-pro sequence that originated from the α-factor of *S. cerevisiae*. The expression of the fused gene was controlled by the methanol-inducible *AOX1* promoter that originated from the alcohol oxidase gene of *P. pastoris*. The plasmid was digested with *Bgl*II and introduced into *P. pastoris* GS115 (*his4*) by electropolation according to the manufacturer's instructions (Invitrogen). A transformant slowly consuming methanol (Mut^s) was selected and used throughout this study.

Protein expression and purification

The protein expression was carried out using a methanol control system as described by Katakura *et al.* (1998), except that 1 % casamino acid was added to the basal salt medium and the methanol concentration in the medium was controlled at 0.3 % during the production phase.

For purification, the supernatant of the culture was diluted five times with water and loaded on a SP-Sepharose Fast Flow (26 mm x 50 mm, Pharmacia Biotch, Uppsala, Sweden) equilibrated with 20 mM sodium phosphate buffer (pH 6.5). The bound protein was eluted with a 0.5 M sodium chloride in 20 mM
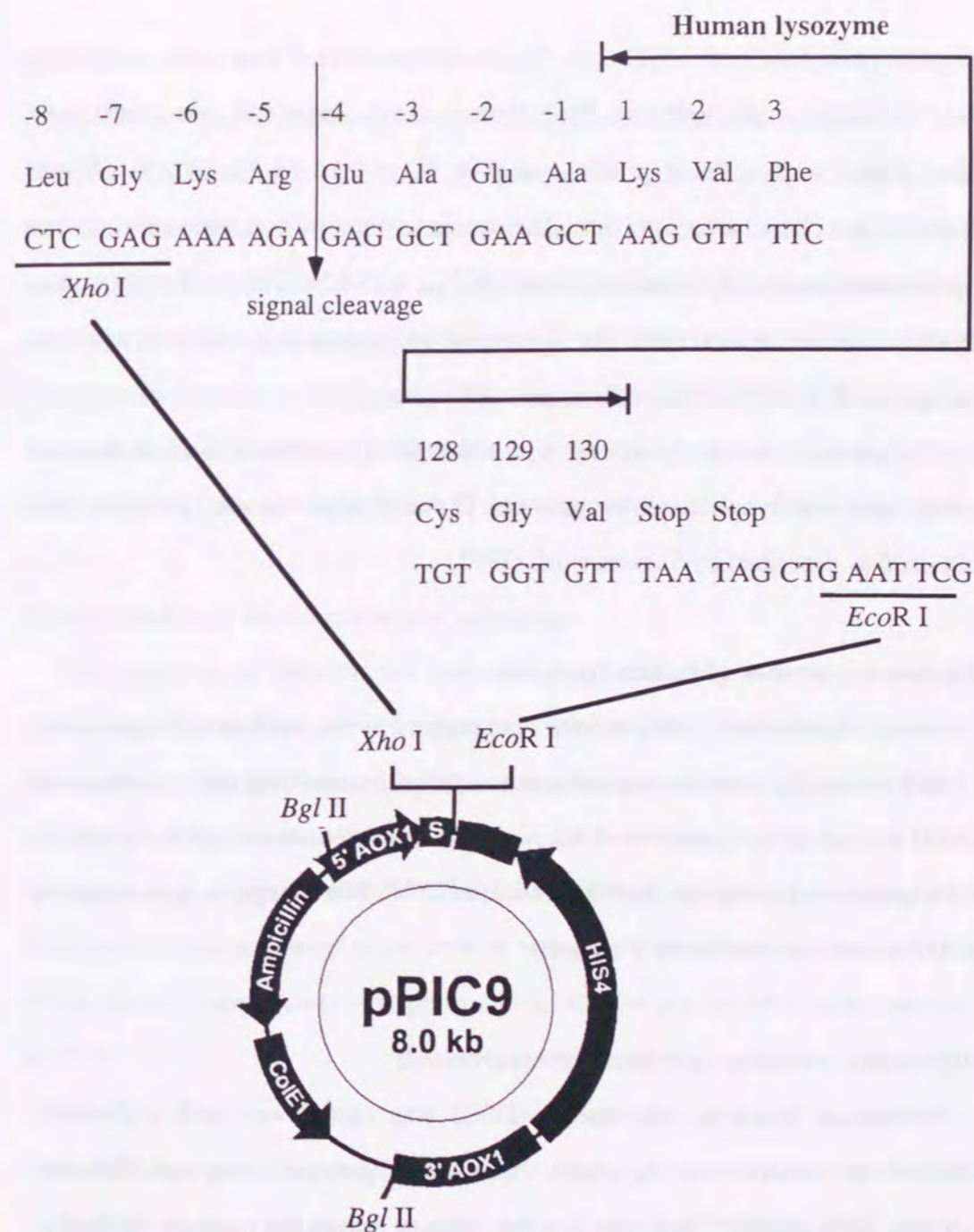
Fig. II-1. Restriction map of Human lysozyme/pPIC9. Human lysozyme genes were inserted between the *Xho*I site and *Eco*RI site of pPIC9.

sodium-phosphate buffer (pH 6.5). The eluent was diluted four times with water and loaded on a SP-Sepharose High Performance column (26 mm x 100 mm), then eluted with a linear gradient of 0.06 M to 0.36 M Na_2SO_4 in 50 mM sodium-phosphate buffer (pH 6.5). The concentration of the protein solution was spectrophotometrically determined using $E^{1\%}_{1cm} = 25.65$ at 280 nm for the human lysozyme (Parry et al., 1969). The N-terminal amino acid sequence was analyzed using the HP G1005A Protein Sequencing System.

The purified human lysozyme was exhaustively dialyzed against distilled water, and was lyophilized for storage. The wild-type human lysozyme was obtained as described by Takano et al. (1995).

Enzymatic activities of human lysozyme

Bacteriolytic activity of lysozyme was assayed by the method of Loquet et al. (1968) with slight modifications. A solution (25 µL) containing the lysozyme was added to 1 mL of a suspension of *Micrococcus lysodeikticus* cells (0.2 mg/mL) in 0.1 M potassium phosphate buffer (pH 6.2) at 25 °C. The change in optical density at 450 nm was measured for 3 minutes.

Differential scanning calorimetry measurements

Differential scanning calorimetry (DSC) was carried out with a DASM4 adiabatic microcalorimeter equipped with an NEC personal computer. The scan rate was 1.0 K/minute. This system is the same as previously reported (Yutani et al., 1991). The sample solution for the DSC measurements was prepared by dissolving the human lysozyme in 50 mM glycine-HCl buffer between pH 2.6 and 3.1. The concentration of the human lysozyme was 0.9 - 1.5 mg/mL. The data were analyzed by Origin software (Micro Cal Inc., Massachusetts, USA).

Equilibrium studies of guanidine hydrochloride-induced denaturation

The denaturation of proteins by guanidine hydrochloride (GuHCl) was monitored by changes in the circular dichroism (CD) values at 222 nm. The CD measurements were performed on a Jasco J-720 recording spectropolarimeter using a cell of 10 mm path length (Taniyama et al., 1992; Funahashi et al., 1996). The protein solution (0.05 mg/mL) was incubated for at least 24 hours in various concentrations of GuHCl at 25 °C and at a pH of 3.0, 4.0 or 7.0 (50 mM glycine-HCl buffer for pHs 3.0 and 4.0, and 50 mM sodium-phosphate buffer for pH 7.0).

Kinetic studies of denaturation and refolding

The reactions of denaturation and refolding by GuHCl were monitored by changes in the fluorescence intensity above 300 nm with excitation at 280 nm. Fluorescence stopped-flow experiments were carried out with a Photal RA-401 stopped-flow spectrophotometer equipped with a mixing device using 1:10 volumes of 2 solutions (Otsuka Electronics, Osaka, Japan). The system for fluorescence measurements is the same as previously described (Taniyama et al., 1992). Kinetic experiments were performed in 40 mM glycine-HCl buffer, pH 4.0, at 10 °C.

Crystallization and X-ray crystallography

Purified human lysozyme was crystallized by the hanging drop vapor-diffusion method. As crystals of the EAEA-lysozyme were not obtained from the usual crystallization conditions with a 2 M sodium chloride as the precipitant in 20 mM acetate buffer (pH 4.5), the sparse matrix approach (Jancarik & Kim, 1991) was used to search for the best crystallization conditions. A 3 µL drop of

aqueous protein (15 mg/mL) mixed with 3 μL of a reservoir solution containing 0.1 M cadmium chloride, 0.1 M sodium acetate (pH 4.6), and 30 % (v/v) Polyethylene Glycol #400. Crystals grew in several days at 10 °C. The data were collected at 100 k using synchrotron radiation on the beam line 18B of the Photon Factory (Tsukuba, Japan) with a Weissenberg camera (Sakabe, 1991). The data were processed with the program DENZO (Otwinowski, 1990). The structure of the EAEA lysozyme was solved by the molecular replacement technique using the program AMoRe (Navaza, 1994) with the wild-type structure (Takano *et al.*, 1995) as a search model. The structure was refined with the program X-PLOR (Brunger, 1992) as already described (Takano *et al.*, 1995; Yamagata *et al.*, 1998).

Results

Expression and purification of lysozyme

The protein expression was induced by the addition of methanol to broth and the methanol concentration was maintained at 0.3 % using the semiconductor methanol control system. Figure II-2 shows the time course of the cell concentration of *P. pastoris* monitored by its optical density at 600 nm and lysozyme concentration in broth evaluated from the enzymatic activity after induction. The cell concentration and lysozyme concentration in the culture increased exponentially (Fig. II-2). Although the production rate decreased later than 70 hours due to decrease of dissolved oxigen in the culture, the concentration of human lysozyme increased to 300 mg per L of broth.

In the final step of purification, the solution that contained the human lysozyme was applied to the SP-Sepharose high performance column and eluted by a single peak. The elution time was obviously faster than that of the wild-type protein. The N-terminal amino acid analysis showed that four extra residues
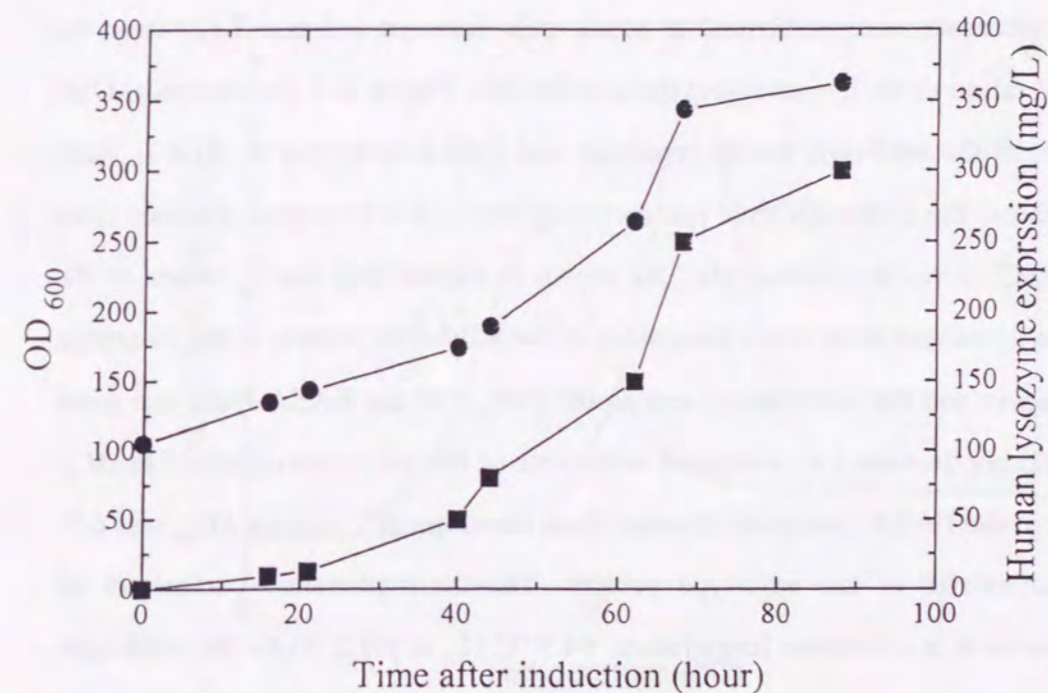

Fig. II-2. Time course of cell growth and expression of human lysozyme after induction. Circles and squares represent cell density and amount of lysozyme, respectively. Cell density is denoted by OD at 600 nm (left scale) and the amount of lysozyme in broth (right scale) was based on enzymatic activity.

(Glu^{-4}-Ala^{-3}-Glu^{-2}-Ala^{-1}-) were left at the N-terminal of the wild-type human lysozyme.

DSC measurements

In order to determine the effect of the four extra residues of the EAEA-lysozyme on the thermodynamic parameters of the denaturation, DSC measurements were performed at acidic pHs between 2.6 and 3.1, where the denaturation of the human lysozyme is reversible. Figure II-3 shows typical DSC curves of the wild-type human lysozyme and EAEA-lysozyme at pH 2.7. Table II-1 shows the thermodynamic parameters of the EAEA-lysozyme obtained from the DSC curves at different pHs. As shown in Figure II-4, the T_d values of the EAEA-lysozyme were lower than those of the wild-type protein in the measured pH region and the calorimetric enthalpies (ΔH_{cal}) of the EAEA-lysozyme were remarkably decreased as compared with those of the wild-type protein. The ΔCp value of the EAEA-lysozyme obtained from the slope of T_d versus ΔH_{cal} was 6.7, similar to that of the wild-type protein. The thermodynamic parameters of denaturation at a constant temperature, 64.9 °C (T_d at pH 2.70 for the wild-type protein) can be calculated using the equations I-1 to I-3 as shown in Table II-2.The differences in the   thermodynamic parameters between the wild-type and EAEA-lysozymes were $\Delta\Delta G$ = -9.6 kJ/mol, $\Delta\Delta H$ = -31 kJ/mol and $T\Delta\Delta S$ = -21 kJ/mol (Table II-2), indicating that the EAEA-lysozyme was remarkably destabilized due to the enthalpic effect.

Equilibrium experiments of denaturation by GuHCl

DSC measurements were carried out in the acidic pH region because of its high
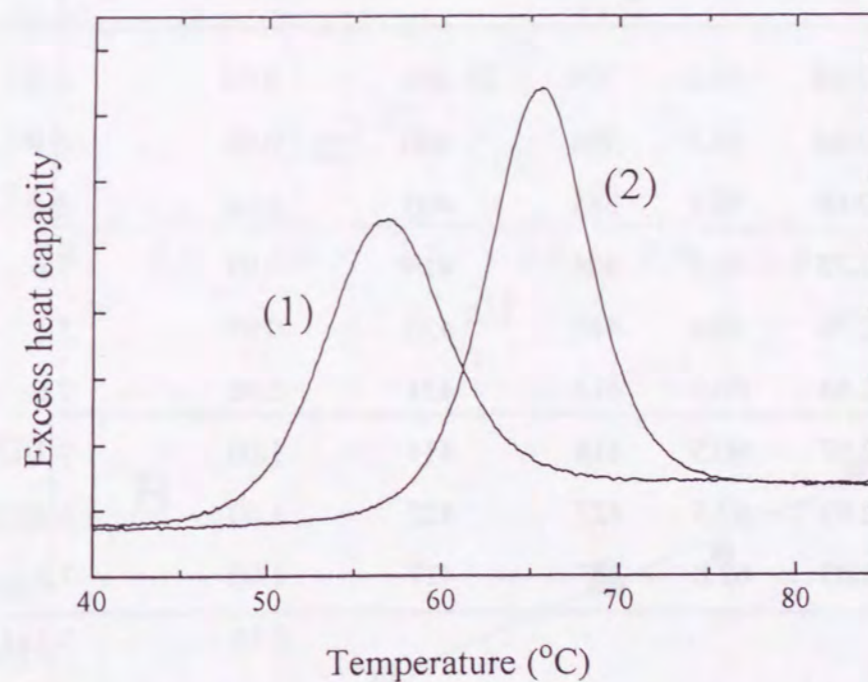
Fig. II-3. Typical excess heat capacity curves of the EAEA and wild-type human lysozymes. EAEA-lysozyme at pH 2.68 (1), wild-type lysozyme at pH 2.7 (2). The previously reported data of the wild-type protein were used (Takano *et al.*, 1995). The increments of excess heat capacity were 10 kJ/(mol K).

Table II-1. *Thermodynamic parameters for denaturation of the EAEA-lysozyme obtained from calorimetry at different pHs.*

pH	T_d (^{0}C)	ΔH_{cal} (kJ/mol)	ΔH_{VH} (kJ/mol)	ratio $\Delta H_{cal}/\Delta H_{VH}$	ΔC_p^a [kJ/(mol K)]
2.63	55.6	379	403	0.94	8.1
2.64	56.4	398	400	0.99	6.8
2.68	56.8	385	403	0.96	8.1
2.75	58.2	408	414	0.99	7.4
2.78	59.0	410	423	0.97	5.5
2.84	60.3	412	431	0.96	7.0
2.87	60.5	414	414	1.00	7.1
2.93	62.5	427	427	1.00	6.1
3.03	62.8	427	427	1.00	7.5
avg				0.99	7.1±1.3

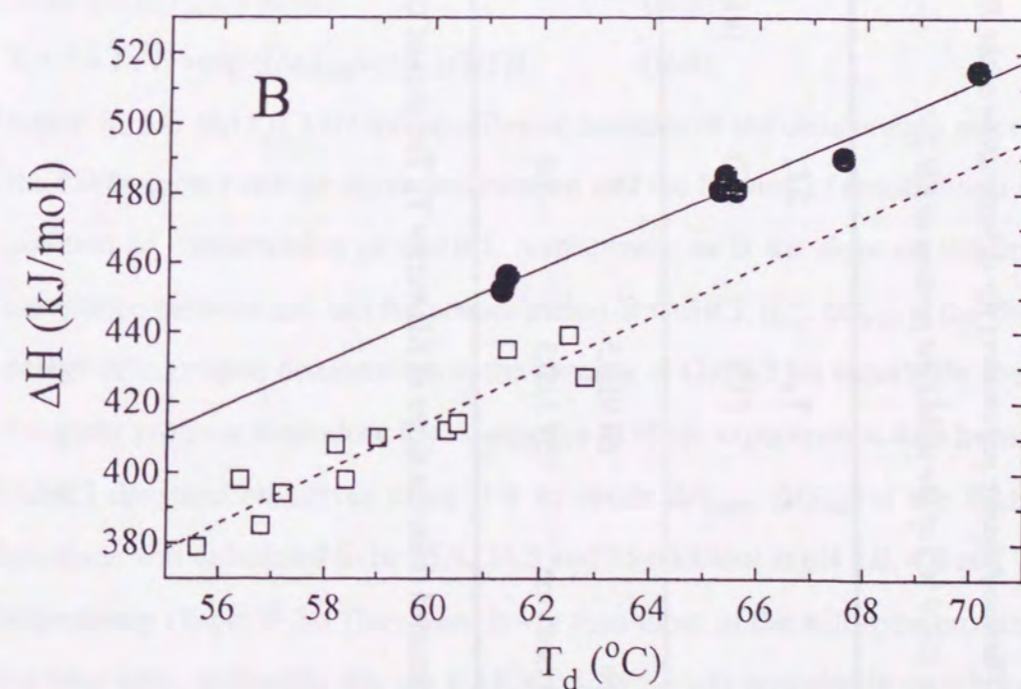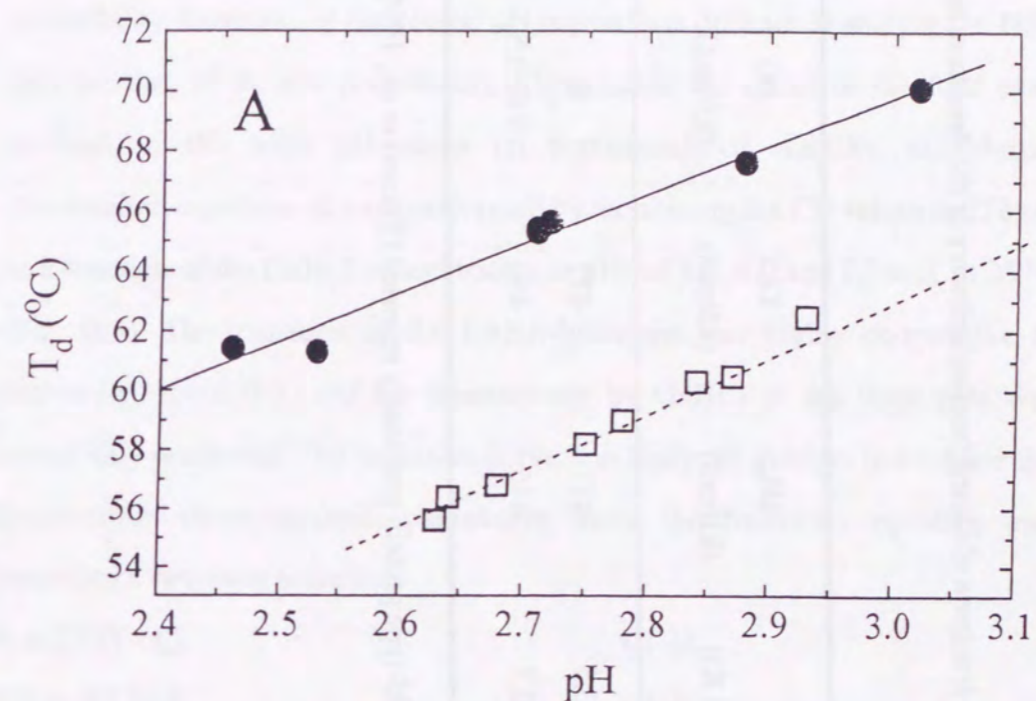$^a\Delta C_p$ was obtained from each calorimetric curve.

Fig. II-4. pH dependence of denaturation temperature (A) and the denaturation temperature dependence of calorimetric enthalpy change (B). Filled circles and open squares represent the wild-type and EAEA-lysozymes, respectively.

Table II-2. Thermodynamic parameters for denaturation of the EAEA-lysozyme obtained from calorimetry at the denaturation temperature (64.9 °C) of the wild-type protein at pH 2.7.

protein	T_d (°C)	ΔT_d (°C)	$\Delta C_p{}^a$ [kJ/(mol K)]	ΔH_{cal} (kJ/mol)	$T\Delta S$ (kJ/mol)	ΔG (kJ/mol)
wild-type	64.9±0.5		6.6±0.5	477	477	0
EAEA-lysozyme	57.3±0.3	-7.6	6.7±0.7	446	456	-9.6±0.5

$^a\Delta C_p$ was obtained from the slope of ΔH versus T_d. The data of the wild-type protein previously reported (Takano et al., 1995) was used.

-32-

reversibility. However, in the neutral pH region, it is difficult to analyze the DSC data because of its low reversibility. To examine the effect of the four extra residues in the wide pH range on conformational stability, equilibrium denaturation experiments were performed by monitoring the CD values at 222 nm as a function of the GuHCl concentration at pHs of 3.0, 4.0 and 7.0 and at 25 °C (Fig. II-5). The transition of the EAEA-lysozyme was highly cooperative as shown in Figure II-5, and the denaturation by GuHCl at the three pHs was completely reversible. The transition curve was analyzed in order to evaluate the denaturation thermodynamic parameters using the following equation and assuming a two-state transition.

$$K = f_u / (1 - f_u) \tag{II-1}$$

$$\Delta G = -RT \ln K \tag{II-2}$$

$$\Delta G(C) = \Delta G_{H2O} + m [C] \tag{II-3}$$

$$f_u(C) = 1 / [1+\exp ((\Delta G_{H2O}+m[C])/RT)] \tag{II-4}$$

where K, ΔG and $f_u(C)$ are the equilibrium constant of the denaturation reaction, the Gibbs energy change upon denaturation and the fraction of denaturation as a function of concentration of GuHCl, respectively. m is the slope of the linear correlation between ΔG and the concentration of GuHCl, [C]. ΔG_{H2O} is the Gibbs energy change upon denaturation in the absence of GuHCl (in water). We used a computer program to produce a least-squares fit of the experimental data from the GuHCl denaturation curves to eq II-4 to obtain ΔG_{H2O}. ΔG_{H2O} of the EAEA-lysozyme was calculated to be 25.9, 34.5 and 35.6 kJ/mol at pH 3.0, 4.0 and 7.0, respectively (Table II-3). They were lower than those of the wild-type protein at the three pHs, indicating that the EAEA-lysozyme was remarkably destabilized by the four extra residues, which was in agreement with the results of the heat denaturation in the acidic pH region (Table II-2).
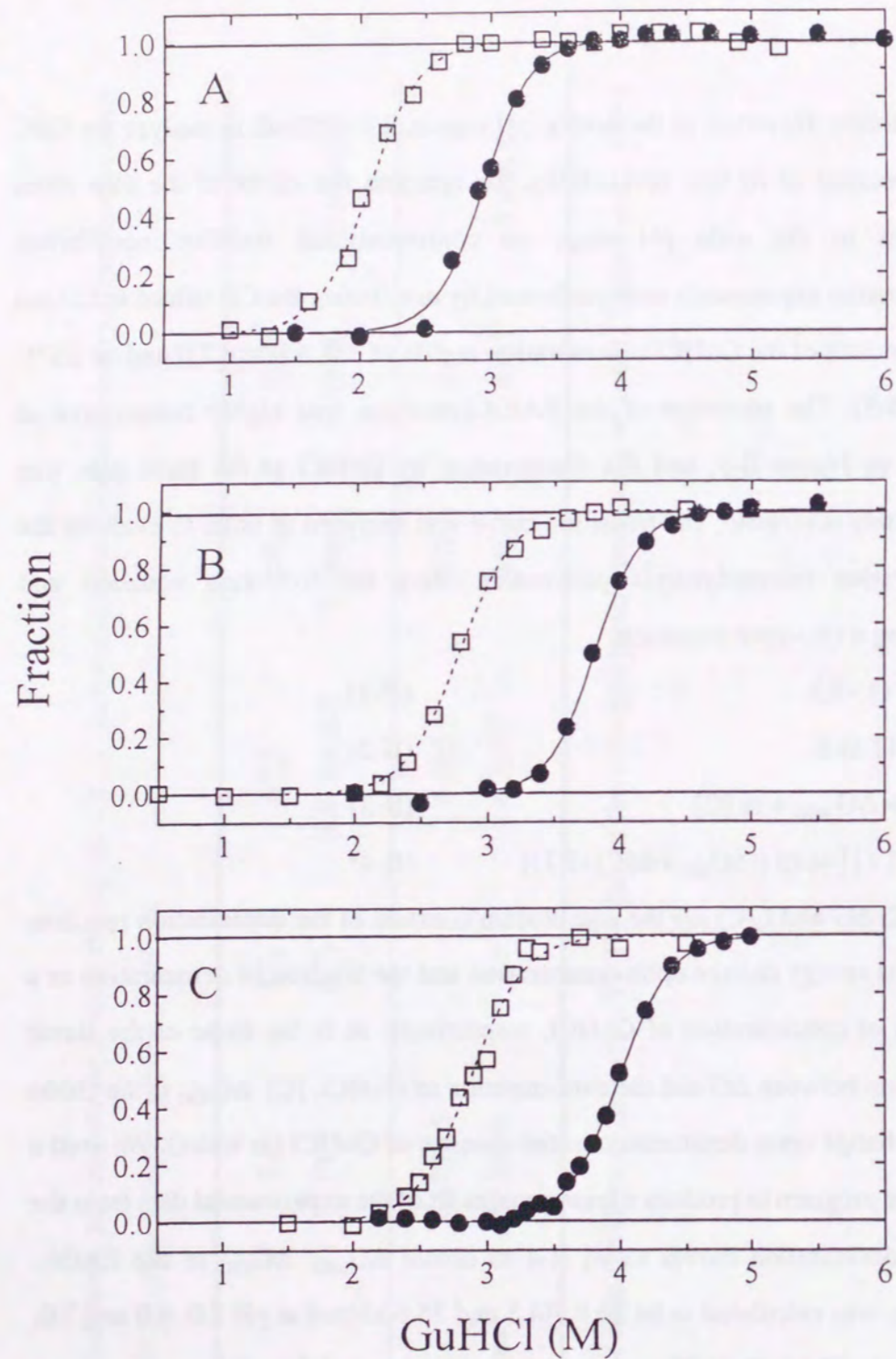
-33-

Fig. II-5. GuHCl denaturation curve of the EAEA and wild-type human lysozymes at various pHs and at 25 °C. (A) pH 3.0 in 50 mM Gly-HCl buffer, (B) pH 4.0 in 50 mM Gly-HCl buffer and (C) pH 7.0 in 50 mM sodium phosphate buffer. Filled circles and open squares represent the wild-type and EAEA-lysozymes, respectively.

Table II-3. *Thermodynamic parameters of the EAEA-lysozyme obtained from denaturation curves by GuHCl at 25 °C.*

	ΔG_{H2O} (kJ/mol)	m (kJ/mol·M)	C_m (M)	$\Delta\Delta G_{H2O}$[a] (kJ/mol)
wild-type				
pH 3.0	39.7±2.5	-13.5±0.8	2.9	——
pH 4.0	53.8±2.0	-14.1±0.5	3.8	——
pH 7.0	50.4±1.1	-12.6±0.3	4.0	——
EAEA-lysozyme				
pH 3.0	25.9±1.5	-12.6±0.7	2.1	13.8
pH 4.0	34.5±1.0	-12.4±0.4	2.8	19.3
pH 7.0	35.6±2.0	-12.4±0.7	2.9	14.8

[a] $\Delta\Delta G_{H2O}$ represents the difference in ΔG_{H2O} between the wild-type and EAEA-lysozyme.

Kinetic experiments of denaturation and refolding

To examine the effect of the four extra residues on the kinetic stability and the folding of the human lysozyme, kinetic experiments of the reversible denaturation-refolding of the EAEA-lysozyme were performed. The denaturation and refolding reactions were monitored by measuring the aromatic fluorescence intensity. The denaturation of the EAEA-lysozyme was followed by the concentration jump from 0 M to various concentrations of GuHCl. The denaturation rate of the EAEA-lysozyme was too fast to be precisely monitored in a stopped-flow apparatus at pH 3.0 and 25 °C. Therefore, all measurements were performed at pH 4.0 and 10 °C. The data were analyzed using the following equation

$$A(t) - A(\infty) = \Sigma A_i e^{-k_i t} \qquad (II\text{-}5)$$

where $A(t)$ is the fluorescence intensity at a given time, $A(\infty)$ is the value when no further change is observed, A_i is the amplitude of the ith phase, and k_i is the apparent rate constant of the ith phase. The denaturation kinetics of the EAEA-lysozyme was described by a single exponential, as reported for the wild-type protein (Taniyama *et al.*, 1992). The kinetic amplitudes of the denaturation reactions at various final concentrations of GuHCl were almost 100% as shown in Figure II-6(A). The logarithm of the apparent rate constant (k_{app}) of the EAEA-lysozyme linearly increased with increasing GuHCl concentration as shown in Figure II-7. The k_{app} values of the EAEA-lysozyme at all examined concentrations of GuHCl were 1 - 2 orders of magnitude higher than those of the wild-type protein, indicating that the addition of the four extra residues accelerates the denaturation rate of the human lysozyme.
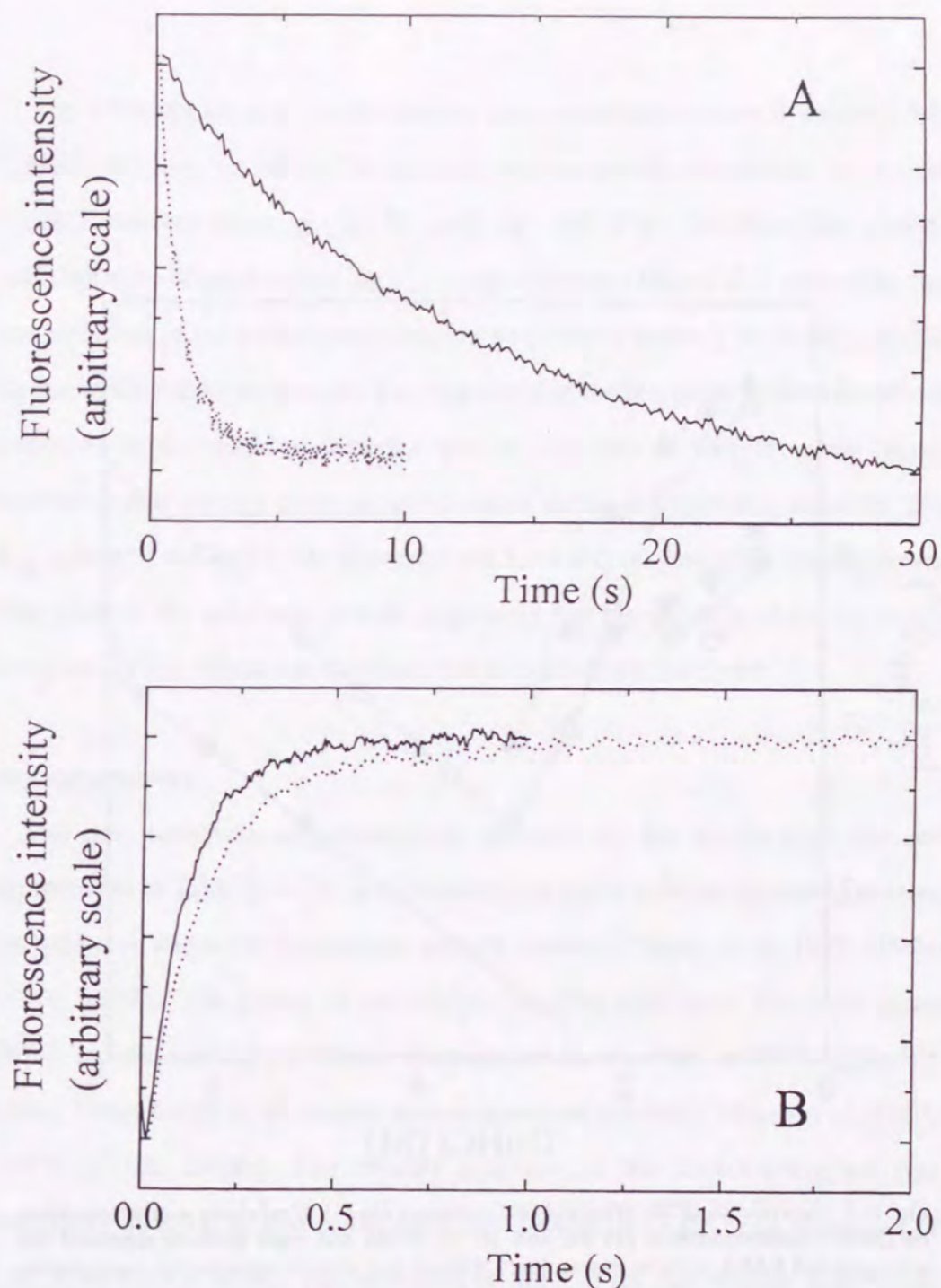

Fig. II-6. Typical GuHCl-induced denaturation and refolding kinetic progress curves of the wild-type and EAEA-lysozymes. (A) and (B) represent denaturation and refolding curves, respectively. Solid and dotted lines represent the wild-type and EAEA proteins, respectively. The denaturation was initiated by a concentration jump from 0 M to 4.51 M and the refolding process was initiated by a concentration jump of 5.0 M to 0.65 M at 10 °C in 40 mM glycine-HCl buffer at pH 4.0.
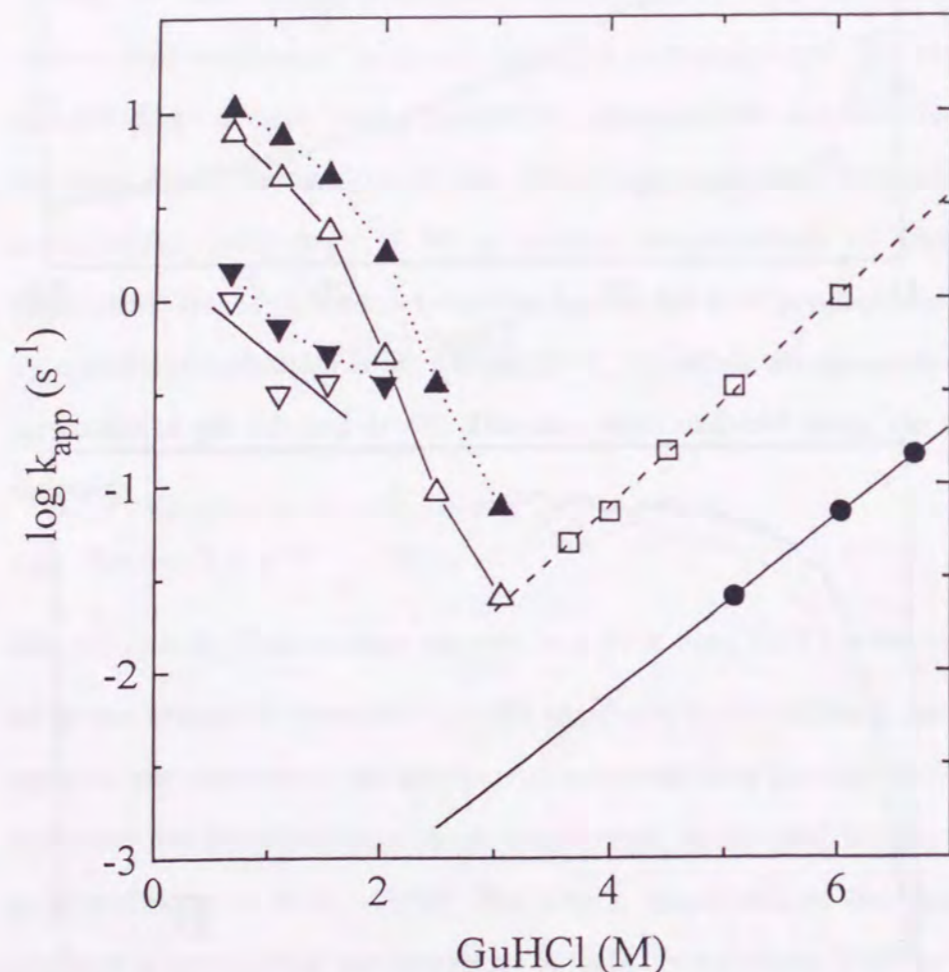
Fig. II-7. Dependence of the apparent rate constants (in s^{-1}) of refolding and denaturation on GuHCl concentration at pH 4.0 and 10 °C. Filled and open symbols represent the wild-type and EAEA proteins, respectively. Circles and squares represent the denaturation reactions. The up and down triangles refer to the slow and fast phases, respectively, in the biphasic refolding reactions.

The refolding kinetics was studied by the concentration jump from the 5.5 M GuHCl solution, in which the protein was completely denatured, to various GuHCl concentrations at 10 °C and pH 4.0 (Fig. II-6(B)). The GuHCl concentration dependence of log k_{app} is also shown in Figure II-7, indicating that the refolding of the EAEA-lysozyme has two phases below 2 M GuHCl, similar to that of the wild-type protein. The amplitude of the fast phase of the two phases observed in the refolding kinetics was greater than that of the slow phase, indicating that the fast phase is predominant during the refolding reaction. The k_{app} values of the major fast phase for the EAEA-lysozyme were slightly lower than those of the wild-type protein, indicating that the addition of the four extra residues slightly affects the refolding rate of the human lysozyme.

Crystal structure

The data collection and refinement statistics for the EAEA-lysozyme are summarized in Table II-4. The EAEA-lysozyme had a different crystal form from the wild-type and other mutant ones already reported (Takano *et al.*, 1995, 1997a, 1997b, 1999b). The crystal of the EAEA-lysozyme belongs to the space group P6$_1$22, and has the highest solvent content (Matthews, 1968) of 67 % of the six crystal forms found in the mutant human lysozyme crystals (Takano *et al.*, 1995, 1997a, 1997b, 1999b). The overall structure of the EAEA-lysozyme was essentially identical to that of the wild-type protein, with the r.m.s. deviation of 0.47 Å for the Cα atoms. The structural position of the first residue (Glu^{-4}) was not determined, because the electron density corresponding to the first residue was poor. As the space where the first residue would be located was open, the first Glu^{-4} residue should be flexible and disordered. There were large changes in the regions of the N-terminal residues (2.0 Å in r.m.s. deviations of mainchain atoms

Table II-4. *Data collection and refinement statistics of the EAEA-lysozyme.*

A. Data collection

crystal system	Hexagonal
space group	$P6_122$
a,c (Å)	91.08, 92.73
Z	12
resolution (Å)	2.4
no. of measured reflections	72761
no. of ind. Reflections	9367
completeness of data (%)	99.9
R merge (%)	4.4

B. Refinement

no. of protein atoms	1048
no. of solvent atoms	176
resolution range (Å)	5 – 2.4
no. of reflections used	8054
completeness of data (%)	98.1
R factor	0.197
Rmsd	
bonds (Å)	0.011
angles (°)	1.648

[a]R merge = $100\Sigma|I_{h,i}<I_h>|/\Sigma I_{h,i}I_{h,i}$ are individual values, and $<I_h>$ is the mean value of the intensity of reflection h.

[b]R factor = $\Sigma||F_o|-|F_c||/\Sigma|F_o|$.

between the wild-type and the EAEA-lysozyme) and of residue numbers 47-49 and 67-69 (1.5 Å in r.m.s. deviations) which are far from the N-terminal region. The regions of residue numbers 47-49 and 67-69 are on the surface area of the molecule and located in the loop structure, respectively. This suggests that changes in the regions of 47-49 and 67-69 reflect the conformational flexibility of these regions in addition to the difference in the crystal packings.

The structures in the vicinity of the N-terminal regions of the EAEA and the wild-type lysozymes are illustrated in Figure II-8. Three major structural changes were observed: changes in salt bridge pairs, those in the N-terminal β-sheet structure, and release of two water molecules. A salt bridge is observed between Lys1/Nζ and Glu7/Oε in the wild-type structure. However, in the EAEA-lysozyme, there were two salt bridges between Glu^{-2}/Oε (third residue of the four extra residues) and Lys1/Nζ, and between Glu7/Oε and Arg10/Nε. As a result, the side chain positions of these residues, especially the structural position of Lys1, were significantly changed. The N-terminal region of the wild-type human lysozyme forms a β-sheet structure with hydrogen bonds between Lys1/N and Thr40/Oγ1, between Lys1/O and Thr 40/Oγ1, and between Lys1/N and Asp87/Oδ1. In the EAEA-lysozyme structure, Lys1/N forms a hydrogen bond with Asn39/Oδ1 and Lys1/O for Thr40/Oγ1. The number of hydrogen bonds in the N-terminal region decreased from three to two bonds. In the wild-type protein, two water molecules were near the Lys^1 residue, however, they were lost in the EAEA-lysozyme.

Discussion

High level expression of human lysozyme

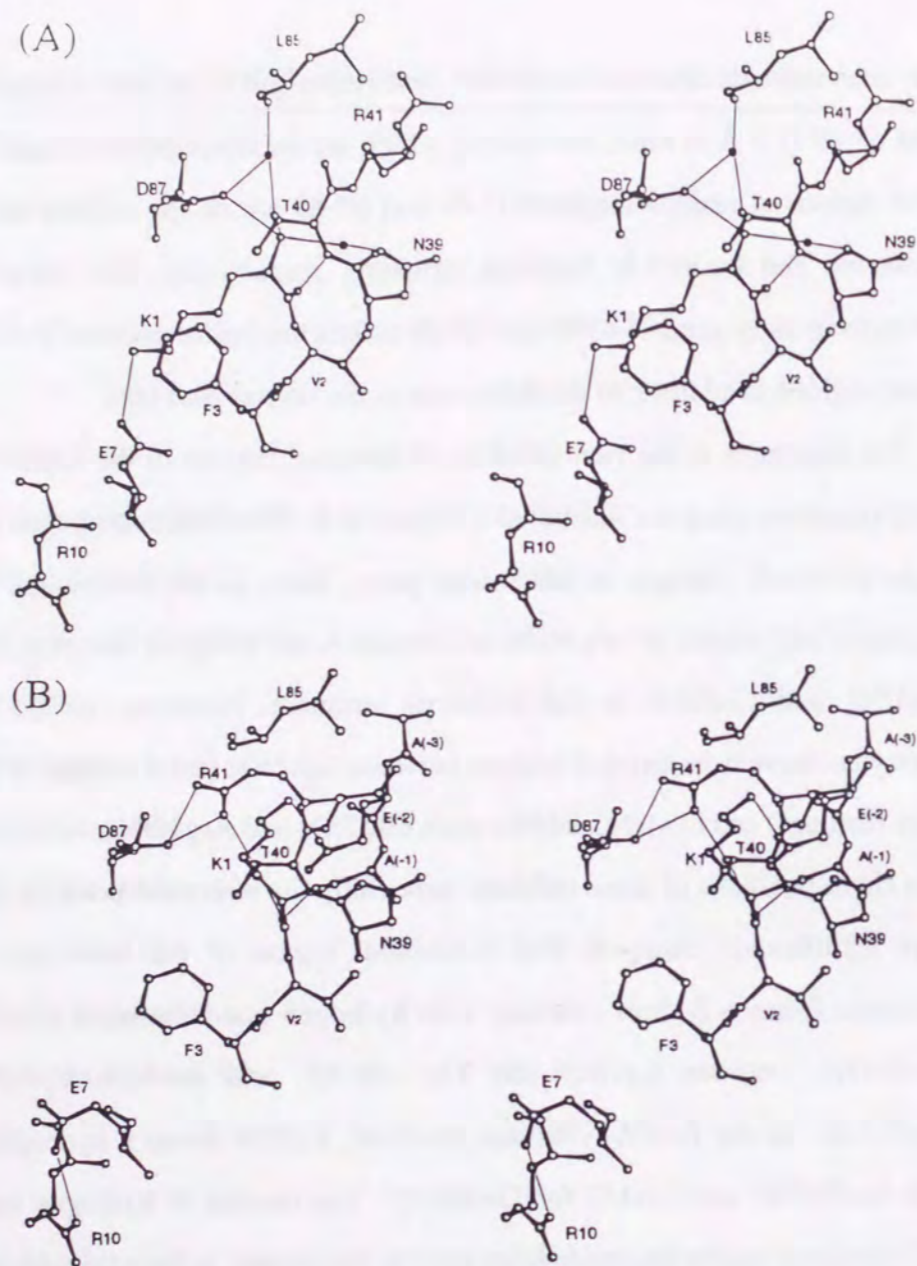The human lysozyme gene was cloned into the XhoI site of pPIC9 and the α-

(A)

(B)

Fig. II-8. Stereodrawings of the wild-type (A) and the EAEA human lysozyme (B) structures in the N-terminal region. Solvent water molecules are drawn as filled circles. The thin line represents a hydrogen bond. There are two water molecules in the wild-type protein, but none in the EAEA-lysozyme.

factor prepro sequence for the extracellular production of human lysozyme was regenerated for good processing efficiency. The processing of the prepro-sequence occurs in three steps (Julius *et al.*, 1983; Bussey, 1988; AnnaArriola & Herskowitz, 1994). (1) The pre-sequence is cleaved by a signal peptidase in endoprasmic reticulum. (2) The pro-sequence is cleaved between Arg^{-5} and Glu^{-4} by an endo-protease (Kex2p) in Golgi apparatus. (3) Finally, a repeat of spacer sequence Glu-Ala is cleaved by a dipeptidyl aminopeptidase (Ste13p). There is a case where the Ste13p cleavage of the Glu-Ala repeat is not efficient, and the (Glu-Ala) repeat is left at the N-terminal of the expressed protein. This is generally dependent on the expressed protein (Steinlein *et al.*, 1995). In the present study, four extra residues (EAEA) were left at the N-terminal of the expressed human lysozyme due to an inefficient cleavage of the Ste13p. The X-ray analysis showed that the Glu^{-2} forms a salt bridge with the Lys^{1}. This salt bridge might interfere the approach of the Ste13p to the cleavage sites. The EAEA spacer sequence was successful for high expression, but was left at the N-terminal residue.

Changes in the thermodynamic parameters of denaturation

The calorimetric studies showed that the EAEA-lysozyme was destabilized by 9.6 kJ/mol as compared with the wild-type protein due to the remarkable decrease in the enthalpy change (ΔH), although the conformational entropy in the denatured state should be increased when one or a few amino acid residues are added (inserted). Oobatake & Ooi (1993) have estimated the conformational entropy of each amino acid residue. Using these values, the change in conformational entropy ($T\Delta\Delta S_{conf}$) due to three extra residues ($-Ala^{-3}-Glu^{-2}-Ala^{-1}-$)

was estimated to be 31 kJ/mol at 64.9 °C. Among the additional EAEA residues, the first Glu^{-4} residue was excluded from the calculation, because the residue was estimated to be flexible in the native state based on the X-ray analysis. However, the experimental results showed an entropy change ($T\Delta\Delta S$) of -21 kJ/mol at 64.9 °C (Table II-2). The extra residues would affect not only the conformational entropy, but also the hydration effect. The hydration energy has been in proportion to changes in the accessible surface area (ASA) of each amino acid due to denaturation (Oobatake & Ooi 1993; Makhatadze & Privalov 1995). Using the parameters of Oobatake & Ooi (1993), the values of the hydration enthalpy ($\Delta\Delta H_h^u$) and hydration entropic energy ($T\Delta\Delta S_h^u$) were estimated to be -23 kJ/mol and -16 kJ/mol at 64.9 °C, respectively. Using the parameters reported by Makhatadze & Privalov (1995), they were -32 kJ/mol and -20 kJ/mol, respectively. The calculated values indicate that the entropic effect of the hydration energy ($T\Delta\Delta S_h^u$) due to the extra residues contributes to protein stabilization. On the other hand, it has been reported that the release of a water molecule from the protein inside stabilizes the protein due to the entropic effect by 7.5 kJ/mol at 64.9 °C ($T\Delta S$) (Takano et al., 1999b). In the case of the EAEA-lysozyme (Fig. II-9), the entropic effect due to the release of two water molecules is -15 kJ/mol ($T\Delta\Delta S_{H2O}$). The sum of the three effects, conformational entropy (31 kJ/mol), hydration entropy ($-16 \sim -20$ kJ/mol) and release of two water molecules (-15 kJ/mol), was 0 to -4 kJ/mol for $T\Delta\Delta S$ at 64.9 °C. This value did not agree with the experimental results ($T\Delta\Delta S = -21$ kJ/mol at 64.9 °C). Calorimetric studies of the EAEA-lysozyme showed a significant decrease in the enthalpy and entropy ($\Delta\Delta H = -31$ kJ/mol and $T\Delta\Delta S = -21$ kJ/mol at 64.9 °C), indicating that the significant decrease in enthalpy is largely compensated by the decrease in entropy. These thermodynamic parameters might include the enthalpy-entropy

-44-

compensation in the region except for the N-terminal, which would be affected due to the extra N-terminal. These results suggest that the contribution to $T\Delta\Delta S$ (-21 kJ/mol at 64.9 °C) can not be attributed to only the extra N-terminal residues, and the addition of four residues affects the conformation in other parts far from the N-terminal. This is supported by the X-ray crystal analysis results; the structural changes were observed in the regions of numbers 47-49 and 67-69 which are far from the N-terminal region.

On the other hand, Takano et al. (1999a) and Funahashi et al. (1999) have proposed parameters to estimate the difference in the denaturation Gibbs energy change on the basis of the structural information of a protein due to substitution. The contribution to the denaturation Gibbs energy change was divided into several stabilizing factors such as hydrophobic effect (ΔG_{HP}), conformational energy (ΔG_{conf}), hydrogen bonding (ΔG_{HB}) and introduction of a water molecule (ΔG_{H2O}). The value of $\Delta\Delta G_{HP}$ between the EAEA-lysozyme and the wild-type protein was calculated to be 7.7 kJ/mol. $\Delta\Delta G_{conf}$ was calculated to be -29.8 kJ/mol at 64.9 °C using the values reported by Schellman (1955) and Pickett & Sternberg (1993). $\Delta\Delta G_{HB}$ can be calculated from the change in hydrogen bonds. However, the present results showed that the hydrogen bonds decreased from three to two bonds, but the salt bridges increased from two to three. Therefore, in this case, $\Delta\Delta G_{HB}$ was assumed to be 0. Two water molecules around the Lys1 were lost in the EAEA-lysozyme (Fig. II-9). The entropic effect due to the release of two water molecules is 15.0 kJ/mol ($\Delta\Delta G_{H2O}$), as described above. The summation of the four effects ($\Delta\Delta G_{HP}$, $\Delta\Delta G_{conf}$, $\Delta\Delta G_{HB}$ and $\Delta\Delta G_{H2O}$) is -7.1 kJ/mol. This value is similar to the experimental data (-9.6 kJ/mol), suggesting that the contribution to $\Delta\Delta G$ is mainly due to the N-terminal region. The contribution of the conformational changes in other parts far from the N-terminal to $\Delta\Delta G$ could be

-45-

neglected by the enthalpy-entropy compensation.

It has been reported that extra methionine at the N-terminal residue of goat α-lactoalbumin expressed by *E. coli* destabilizes the protein due to a conformational entropy effect (Chaunduhri *et al.*, 1999). On the other hand, the extra methionine residue contributes to the large decrease in enthalpy ($\Delta\Delta H = -77$ kJ/mol, at 64.9 °C) in the human lysozyme (Takano *et al.*, 1999b).

Effects on folding of human lysozyme

The denaturation rate constant of the EAEA-lysozyme was significantly higher than that of the wild-type protein, but the refolding rate constant was slightly lower. Calorimetric studies and equilibrium studies indicate that the EAEA-lysozyme was significantly destabilized. These results indicate that the destabilization of the EAEA-lysozyme was mainly caused by the increase in the denaturation rate constant. In the studies of goat α-lactoalbumin, the addition of methionine at the N-terminal residue accelerates the denaturation rate constant and does not affect the refolding rate (Chaudhuri *et al.*, 1999). According to the H-D exchange experiments in the NMR studies, two helices and the 3_{10} helix near the C-terminal of the human lysozyme fold faster than the other sites. On the other hand, the N-terminal region does not play an important role in folding (Hooke *et al.*, 1994). In the present study, the refolding rate constant was slightly affected due to the four extra residues.

Conclusion

P. pastoris expressed the human lysozyme at about 300 mg per L of broth. However, at the N-terminal of the expressed protein, four extra residues (Glu^{-4}-Ala^{-3}-Glu^{-2}-Ala^{-1}-) were added (EAEA-lysozyme). Calorimetric studies showed

that the EAEA-lysozyme was destabilized by 9.6 kJ/mol as compared with the wild-type protein, mainly caused by the remarkably decrease in the enthalpy change ($\Delta\Delta H$). The obtained thermodynamic parameters obtained were analyzed on the basis of the structural information of the EAEA-lysozyme. The four extra residues also affected the thermodynamic properties in a region far from the N-terminal. However, the great change in enthalpy might be almost compensated by the changes in entropy. Therefore, changes in the Gibbs energy ($\Delta\Delta G$) could be explained by the summation of the Gibbs energies contributing to each stabilizing factor concerning the extra residues.

Chapter III

Studies on the Amyloid Formation of Amyloidgenic Human Lysozyme in Ethanol Solution

Introduction

Recently, the diseases caused by protein misfolding, such as Alzheimer's disease, late onset diabetes, prion-related transmissible spongiform encephalophathies and amyloidosis, have attracted considerable attention as conformational diseases (Carrell & Lomas, 1997). The extracellular insoluble deposits (amyloid fibrils), resulting from protein misfolding, damage tissues leading to disease (Tan & Pepys, 1994; Kelly, 1996; Pepys, 1996). The amyloid fibrils, independent of the amino acid sequence, native protein structure, and function of the constituent protein (Sunde *et al.*, 1997), are of indeterminate length, are unbranched with diameters of about 100 Å and display pathognomonic green birefringence when viewed in polarized light after staining with Congo red (Pepys, 1996). X-ray diffraction patterns of amyloid fibrils show simple patterns with a 4.7 Å meridional reflection and a 10 Å equatorial reflection (Sunde *et al.*, 1997). Sunde *et al.* (1997) have proposed that amyloid fibrils consist of a common core structure which is a cross-β-fiber structure, with β-strands perpendicular and β-sheets parallel to the fiber axis. However, the mechanism of the amyloid formation is still not clear.

The mutant human lysozymes, I56T and D67H, have been identified as fibril proteins in amyloid deposits that cause hereditary systemic amyloidosis (Pepys *et al.*, 1993). The native form of the I56T molecule is similar to the wild-type structure (Funahashi *et al.*, 1996; Booth *et al.*, 1997). However, the equilibrium and kinetic stabilities of the mutant protein are remarkably decreased due to the introduction of a polar residue (Thr) in the interior of the molecule. It has been reported that the amyloid formation of the mutant human lysozyme is due to a tendency to favor (partly or completely) denatured structures (Funahashi *et al.*, 1996). Lysozymes have been studied extensively and their physiochemical

properties have been examined in detail (Artymiuk & Blake, 1981; Redfield & Dobson, 1990; Radford *et al.*, 1992; Hooke *et al.*, 1994). Therefore, lysozymes are suitable as a model protein to elucidate the mechanism of amyloid fibril formation.

However, it is not easy to examine the process of amyloid formation, because we can not control artificially the rate of the formation. Recently, we found that amyloidgenic human lysozyme molecules associate and precipitate to form amyloid protofilaments in a high concentration of ethanol (> 80 %). In this paper, the amyloid formation of the amyloidgenic mutant human lysozyme (I56T), the wild-type and its mutant human lysozymes were examined in a high concentration of ethanol in order to analyze the mechanism of amyloid formation. We will discuss the relationship between amyloidgenecity and stability of the proteins.

Materials and methods
Protein Preparation

Three mutant human lysozymes: an amyloidgenic mutant (I56T), a mutant with four extra residues at the N-terminal (EAEA-lysozyme), and its point mutation (EAEA-I56T) were constructed as described (Chapter II). All human lysozymes which includes the wild-type, EAEA-lysozyme, I56T, and EAEA-I56T were obtained using *P. pastoris* as described in Chapter II.

Circular Dichroism

Circular dichroism (CD) spectra in the far-UV regions were obtained using a Jasco J-720 spectropolarimeter equipped with a water bath to control the temperature at 25 °C. The concentrations of human lysozymes were 0.1 mg/mL

for the far-UV experiments. Sixteen scans were averaged to obtain each spectrum. A cell with path lengths of 1 mm was used for far-UV data acquisition.

Congo Red Staining

For Congo red birefringence experiments, aliquots of protein were air-dried onto glass slides. The resulting films were stained by the reaction solution (10 mM phosphate buffer of pH 7.4, 2.7 mM KCl, and 137 mM NaCl, and 10 % ethanol), containing 5 μM Congo red. The stained slides were examined with an optical microscope between crossed polarizers. The Congo red solution was freshly prepared and filtered three times through a 0.2-μm filter before use.

For quantitative Congo red experiments, the samples were tested by the spectroscopic assay as described (Klunk *et al.*, 1999). Amyloid fibrils in the ethanol solution were collected by centrifugation and resuspended in the same solution as that of the birefringence experiments. The reaction samples were thoroughly mixed and incubated at room temperature for at least 30 minute before measurement.

Electron Microscopy

A suspension of the samples in ethanol was applied to carbon-coated copper grids, blotted, washed, negatively stained with 2 % uranyl acetate (wt/vol), air-dried, and then examined with a JEOL JEM1010 transmission electron microscope operating at an accelerating voltage of 100kV.

X-ray Diffraction of Amyloid Fibrils

The precipitates of the human lysozymes were put into a capillary of 1.0 mm in diameter. X-ray diffraction experiments were carried out using a RIGAKU

rotating anode X-ray generator, RU-300 (Tokyo), operated at 40 kV and 200 mA (λ=1.5418 Å). The specimen-to-film distance and the exposure time were 100 mm and 10 hours, respectively. X-ray diffraction patterns were recorded with a RIGAKU imaging plate detector R-AXIS IIc.

Differential scanning calorimetry measurements

Differential scanning calorimetry (DSC) was carried out same as Chapter II. The sample solution for the DSC measurements was prepared by dissolving the human lysozyme in 50 mM glycine-HCl buffer between pH 2.6 and 3.3. The concentration of the human lysozyme was 0.9 - 1.5 mg/mL.

Crystallization and X-ray crystallography

Purified human lysozyme was crystallized by the hanging drop vapor-diffusion method same as Chapter II.

Results and Discussion

CD spectra of human lysozymes in the ethanol solution

CD spectra of the wild-type and three mutant human lysozymes were measured in 50 or 60 % ethanol (Fig. III-1). The three mutant human lysozymes are EAEA-lysozyme with four extra residues (Glu-Ala-Glu-Ala) at the N-terminal, an amyloidgenic mutant (Ile56 -> Thr), and an amyloidgenic mutant with four extra residues at the N-terminal (EAEA-I56T). Protein solutions (0.1 mg/mL) were incubated at 25 °C for one week for CD measurements. The CD spectra show that the values of negative peaks at [θ] 208 nm and 222 nm which reflect the characteristic of the α-helix structure increase in ethanol solution. Under these conditions, all solutions were clear and no precipitation was observed.
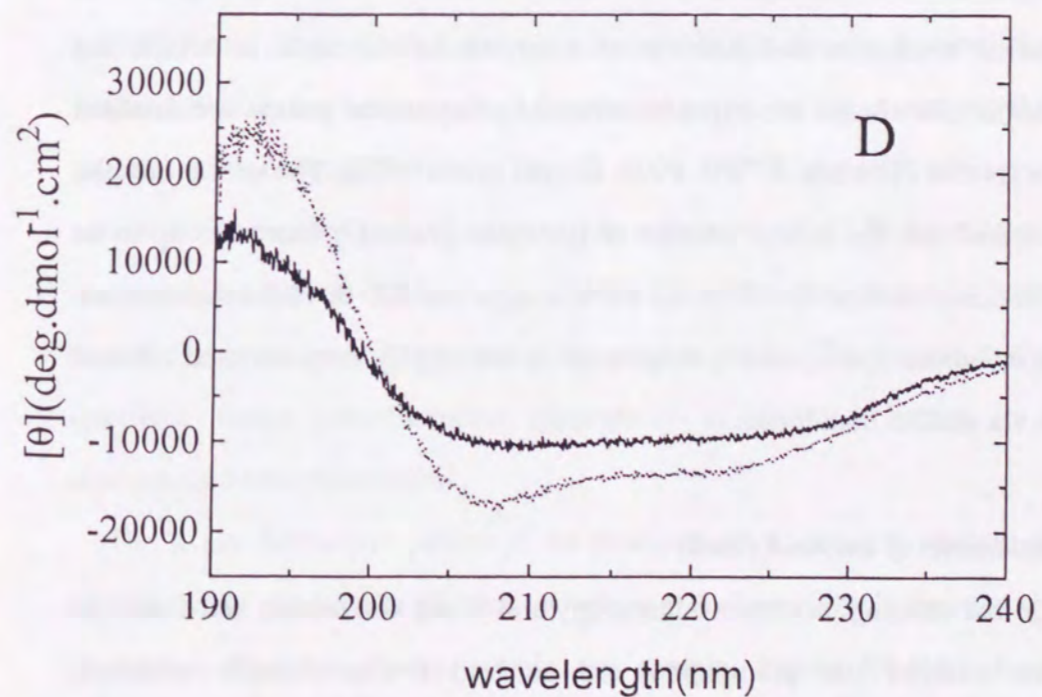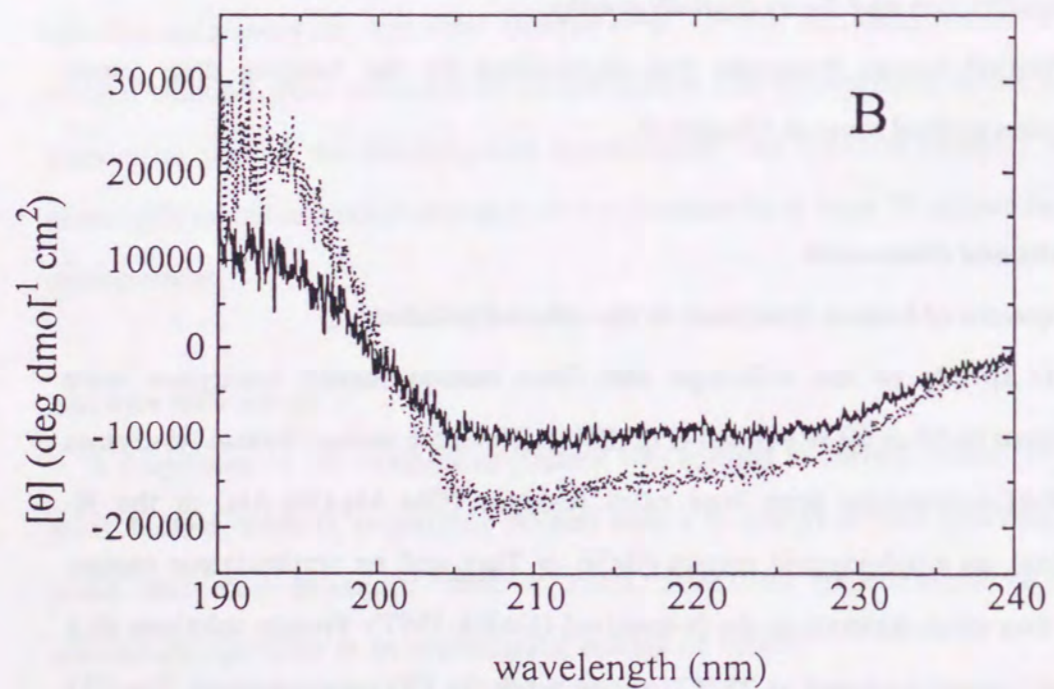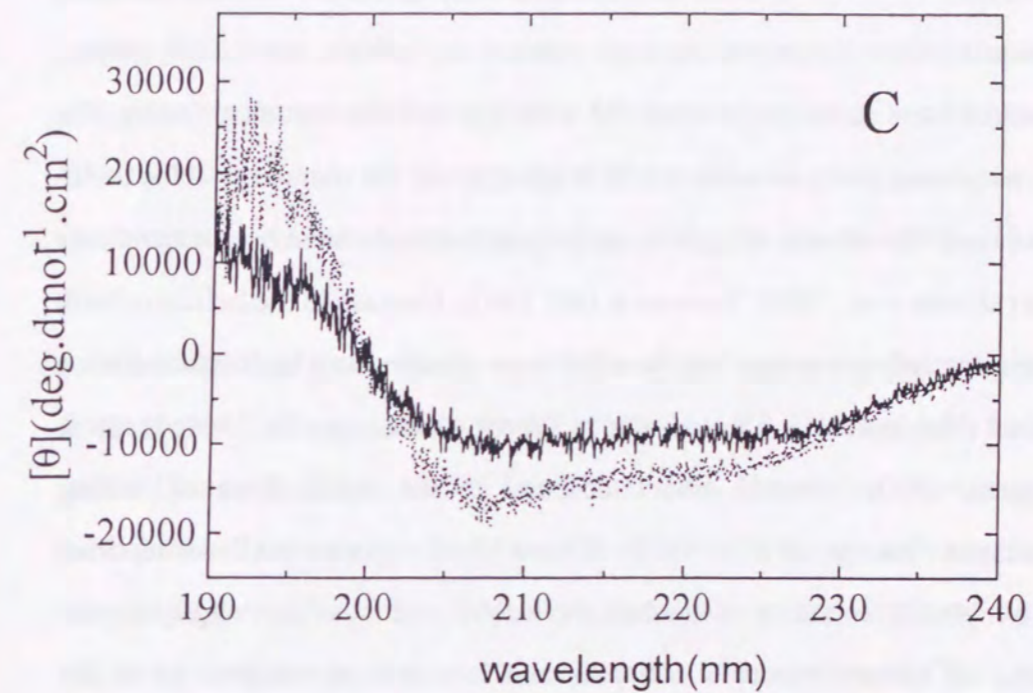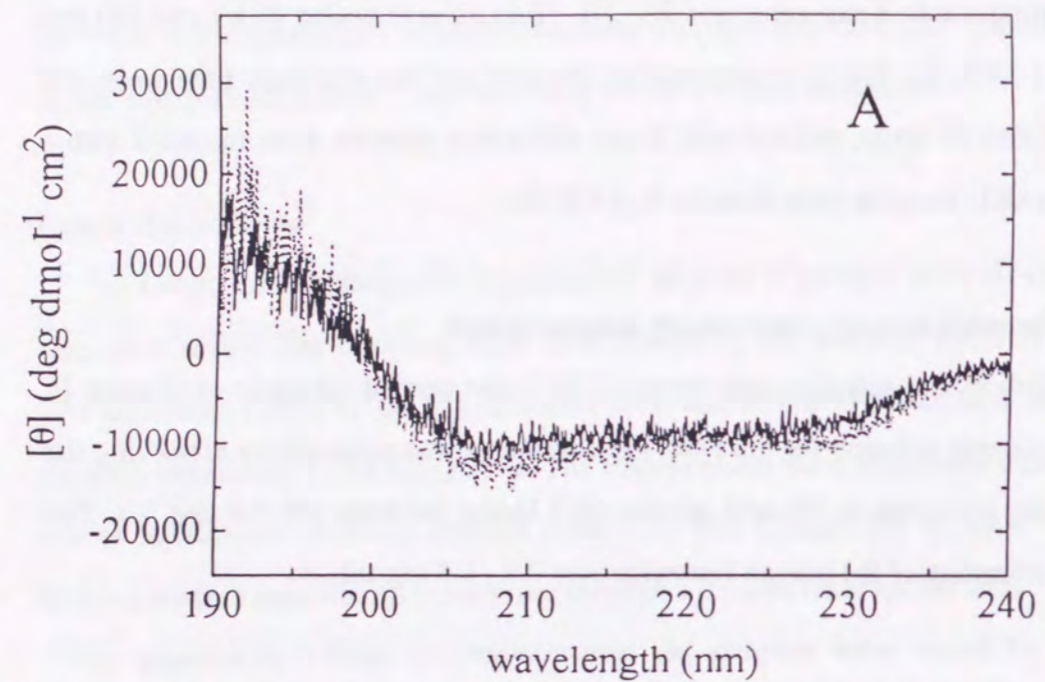
Fig. III-1. Far-UV CD spectra of the wild-type and three mutant human lysozymes (0.1 mg/mL) in 50 % or 60 % ethanol solution. The wild-type protein was incubated for 24 h at 25 °C in 60 % ethanol and the three mutants in 50 % ethanol. The solid line was the spectrum in water, and the dotted line was that in the 50 % or 60 % ethanol solution.
A: wild-type, B: EAEA-lysozyme, C: I56T, D: EAEA-I56T

Fig. III-1. (Continued)

Furthermore, when the ethanol concentration was increased, human lysozyme precipitated. The concentrations of ethanol in which human lysozyme precipitated were different between the wild-type and the mutant proteins. The wild-type protein precipitated in 60-70 % ethanol and the mutant proteins in 50-60 % ethanol. The effects of alcohol on protein structures have been extensively studied (Shiraki *et al.*, 1995; Thomas & Dill, 1993). Increase in the helical content of proteins including hen egg lysozyme has been observed in a high concentration of ethanol (Hamaguchi & Kurono, 1963; Kurono & Hamaguchi, 1964; Ikeda & Hamaguchi, 1970). Alcohol also contributes to the stabilization of folding intermediates (Thomas & Dill, 1993). Recent NMR experiments have reported that in a high concentration of alcohol, the helical content of hen egg lysozyme increases, its tertiary structure collapses and it is not as compact as in the molten-globule state (Kamatari *et al.*, 1998). In many cases, alcohol-induced denaturation results in stabilization of extended helical rods in which the hydrophobic side chains are exposed, whereas polar amide groups are shielded from the solvent (Thomas & Dill, 1993; Shiraki *et al.*, 1995). The present results also indicated that the helical content of lysozyme gradually increases up to an ethanol concentration of 60 - 70 % for the wild-type and 50 - 60 % for the mutants. After that, human lysozymes precipitated in the highly concentrated ethanol solution via alcohol denaturation.

Three hallmarks of amyloid fibrils

Congo red staining, electron microscopy and X-ray diffraction were used to determine whether the precipitates are amyloid fibrils. Sample solutions containing 10 mg/mL of human lysozymes were incubated at 25 °C for a week in ethanol of 80 % for the wild-type and 70 % for mutants. The precipitates obtained

were used for the following experiments.

Fig. III-2 shows optical microscope images of human lysozymes stained by Congo red under cross-polarized light. All the precipitates of human lysozymes (the wild-type and all mutant proteins) displayed pathognomonic green birefringence and filamentous aggregations. They are characteristics of amyloid fibrils.

All known amyloid fibrils, regardless of the nature of the main protein component or the source of the fibrils, are about 100 Å wide and have no branch points (Sunde & Blake 1997). The observation of electron microscopy was carried out only the EAEA-lysozyme. Those of the wild-type and other mutants have been carring out. The EAEA-lysozyme precipitates displayed a typical amyloid protofilament form, having a diameter of approximately 70 Å with no branching (Fig. III-3). The lengths of the human lysozyme fibrils were about 1000 to 2000 Å and shorter than that of transthyretin fibrils already reported (Sunde & Blake, 1997). It has been reported that transthyretin, which causes amyloidosis, consists of four protofilaments (Serpell *et al.*, 1995), electron micrographs of transthyretin amyloid protofilaments show a diameter of 40-50 Å, and the length is also around 1000 Å (Lashuel *et al.*, 1998). These features are similar to those of human lysozyme protofilaments in the present study. This means that human lysozyme forms protofilaments (precursors of amyloid fibrils) in highly concentrated ethanol solution.

The X-ray diffraction pattern of the precipitates of human lysozyme showed one sharp and one broad reflection, which appeared as a ring because of the lack of relative fibril orientation within the sample. Figure III-4(A) shows the diffraction patterns of the wild-type and mutant human lysozymes. Figure III-4(B) shows the radial intensity profile of the circular average (Vonderviszt *et al.*,
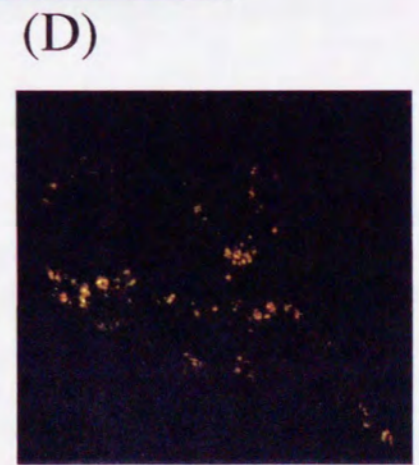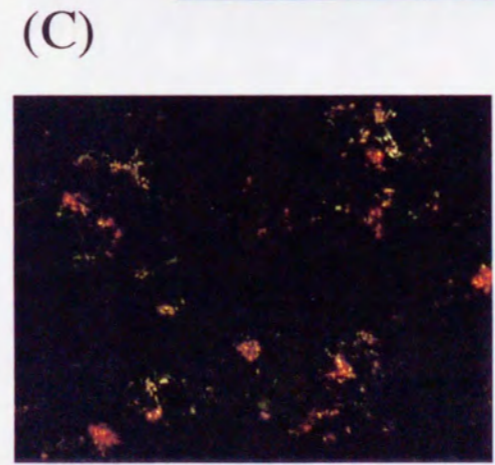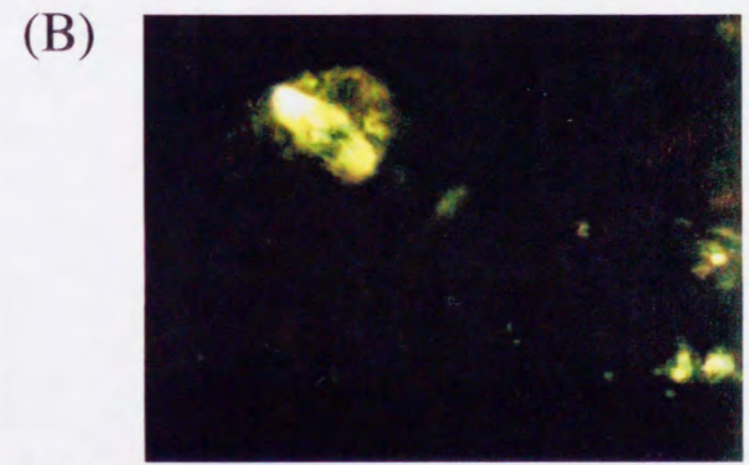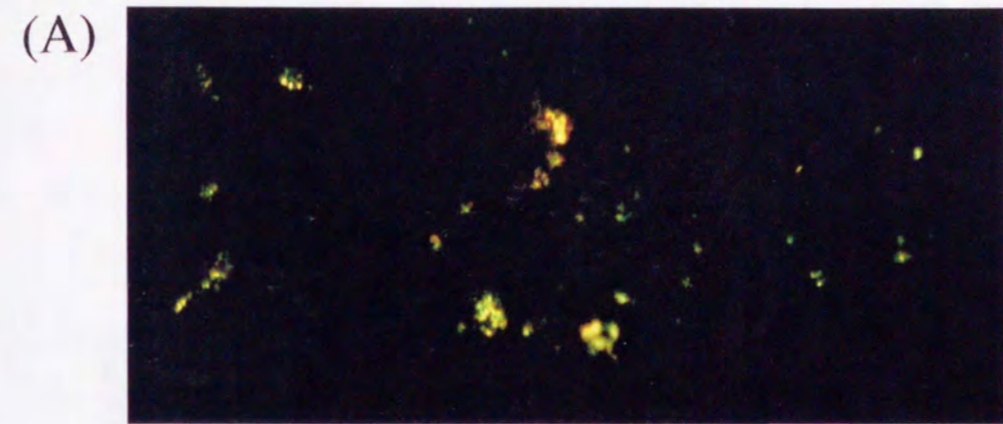
Fig. III-2. Optical microscopy image obtained under cross-polarized light. The precipitates of the wild-type and mutants of human lysozymes were obtained after 1 week of incubation in 70 % and 80 % ethanol solution for the mutants and wild-type, respectively, and were stained with Congo red. The photograph shows the blots of green birefringence coming from regions rich in amyloid fibrils.

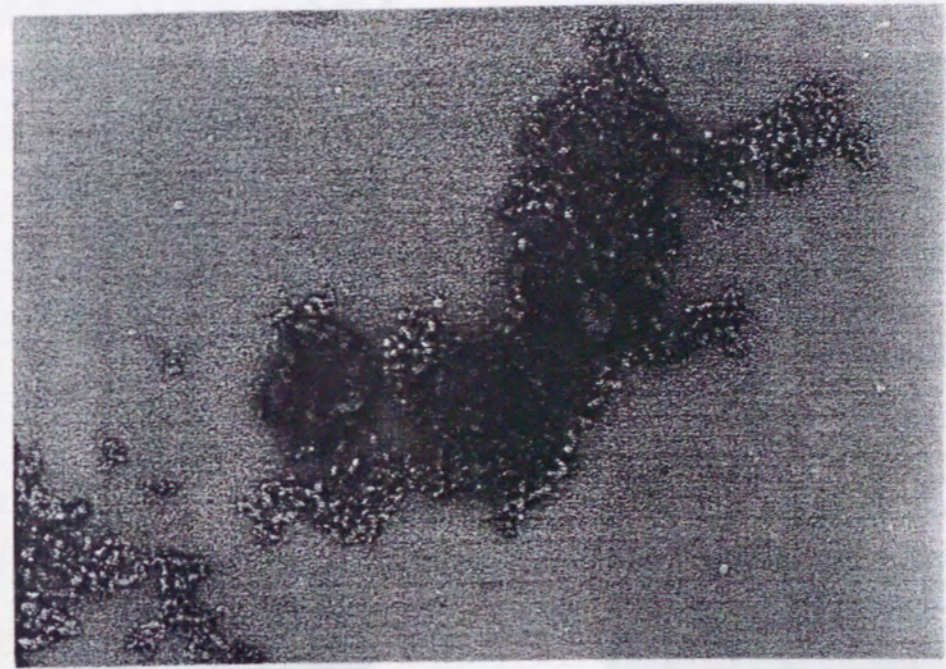A: wild-type, B: EAEA-lysozyme, C: I56T, D: EAEA-I56T

Fig. III-3. Electron micrograph of a negatively stained preparation of 1 mg/mL EAEA-lysozyme in 70 % ethanol solution incubated at 25 °C for a week (bar = 100 nm).
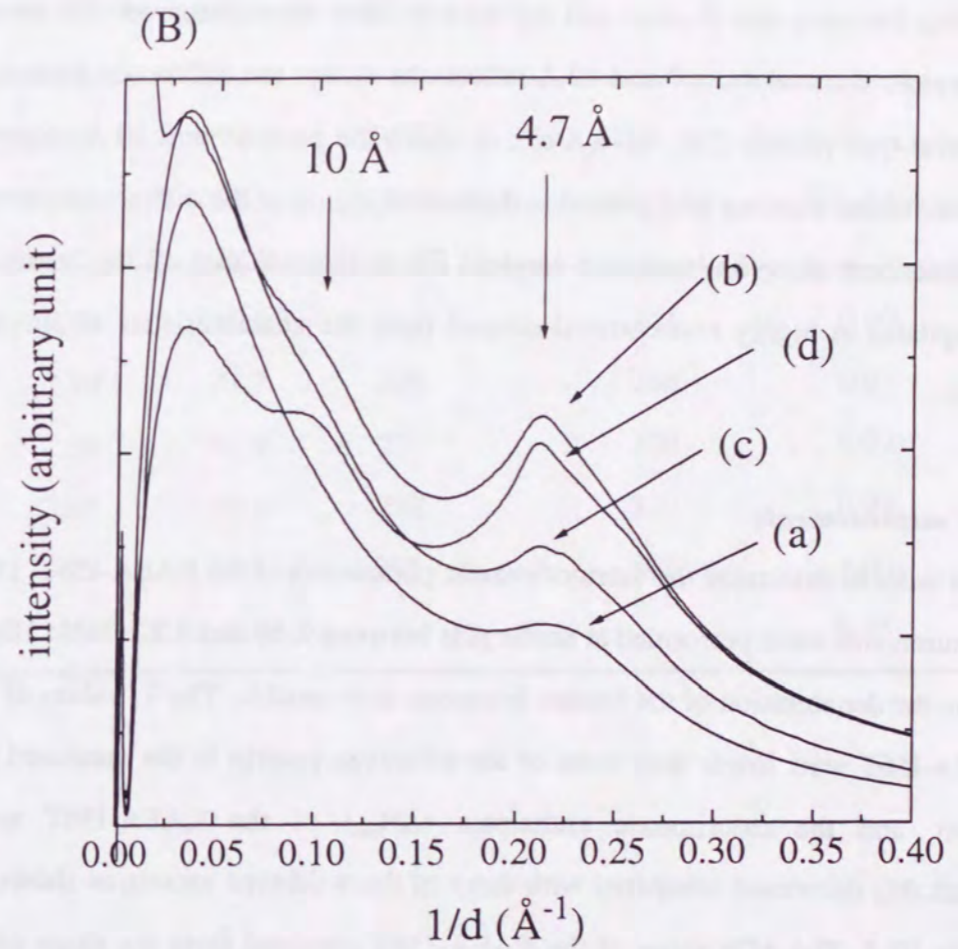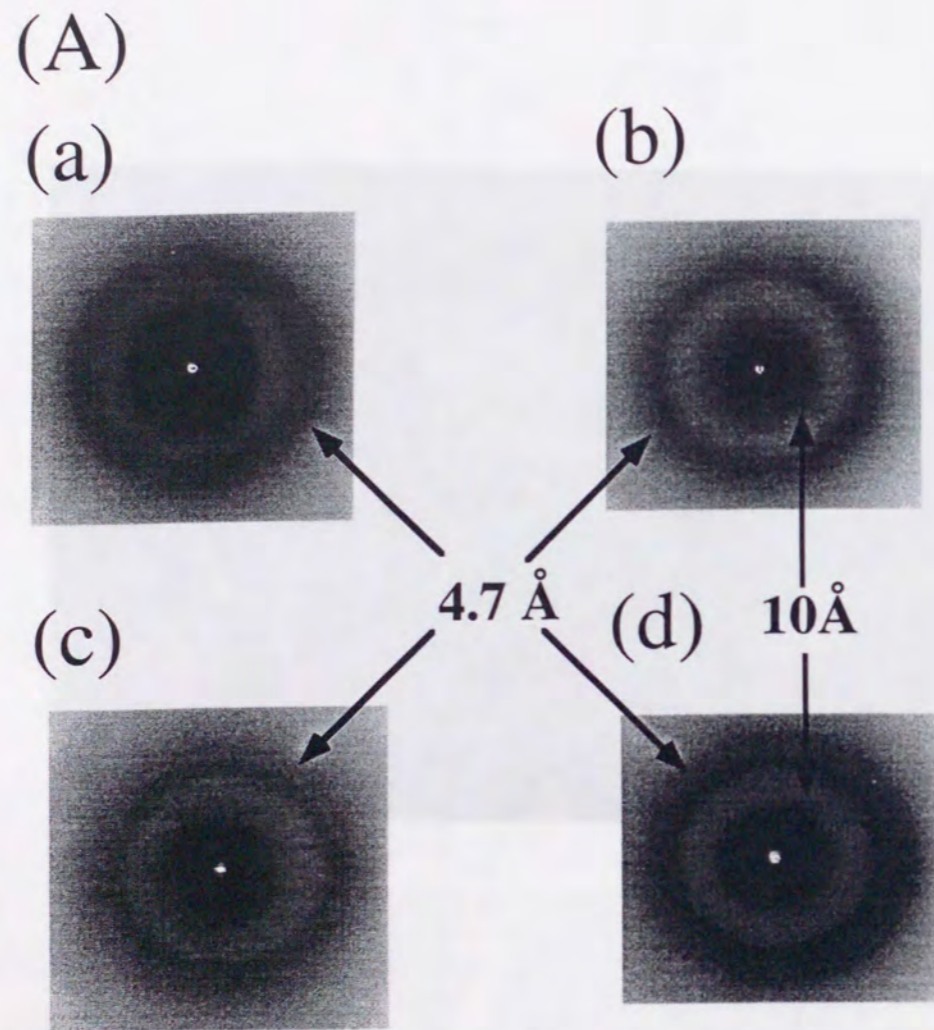
Fig. III-4. (A) X-ray diffraction pattern of the wild-type and mutant human lysozymes. Because of no alignment of the fibrils, these reflections appear as rings and do not display a meridional or equatorial character. (B) Radial intensity distribution profile of the X-ray diffraction pattern from human lysozyme fibrils. The X-ray diffraction patterns were mostly circular symmetric with no tendency of orientation. Therefore, circular averaging was done to create the plot of the radial intensity distribution. The reflections generated by the interstrand spacing (4.7 Å) and the intersheet spacing (about 10 Å) typical of amyloid fibrils are marked by arrows.
a: wild-type, b: EAEA-lysozyme, c: I56T, d: EAEA-I56T

1992). One sharp reflection at 4.7 Å which arises from the interstrand spacing in the β-sheets and a broad reflection around 10 Å which arises from the intersheet spacing between one β-sheet and the next β-sheet were observed. All human lysozymes showed the 4.7 and 10 Å reflections except the diffraction pattern of the wild-type protein (Fig. III-4(A-a)), in which the peak around 10 Å might be hidden behind a strong background in the central region of the diffraction pattern. As described, three hallmarks of amyloid fibrils indicate that all the lysozyme precipitates in highly concentrated ethanol have the characteristics of amyloid fibrils.

DSC measurements

In order to determine the thermodynamic parameters of the EAEA-I56T, DSC measurements were performed at acidic pHs between 2.69 and 3.22 (Table III-1), where the denaturation of the human lysozyme is reversible. The T_d values of the EAEA-I56T were lower than those of the wild-type protein in the measured pH region, and the calorimetric enthalpies (ΔH_{cal}) of the EAEA-I56T were remarkably decreased compared with those of the wild-type protein as shown in Figure III-5. The ΔCp value of the EAEA-I56T obtained from the slope of T_d versus ΔH_{cal} was 7.0 kJ/mol K, similar to that of the wild-type protein. The thermodynamic parameters of denaturation at a constant temperature, 64.9 °C (T_d at pH 2.70 for the wild-type protein) can be calculated using equations I-1 to I-3 as shown in Table III-2. The differences in the thermodynamic parameters between the wild-type and EAEA-I56T were $\Delta\Delta G$ = -23.7 kJ/mol and $\Delta\Delta H$ = -87 kJ/mol (Table III-2), indicating that the EAEA-I56T was remarkably destabilized. The thermodynamic parameters of other mutant proteins (I56T and EAEA-lysozyme) are also listed in Table III-2. The stability of EAEA-I56T was the

Table III-1 *Thermodynamic parameters for denaturation of the EAEA-I56T obtained from calorimetry at different pHs.*

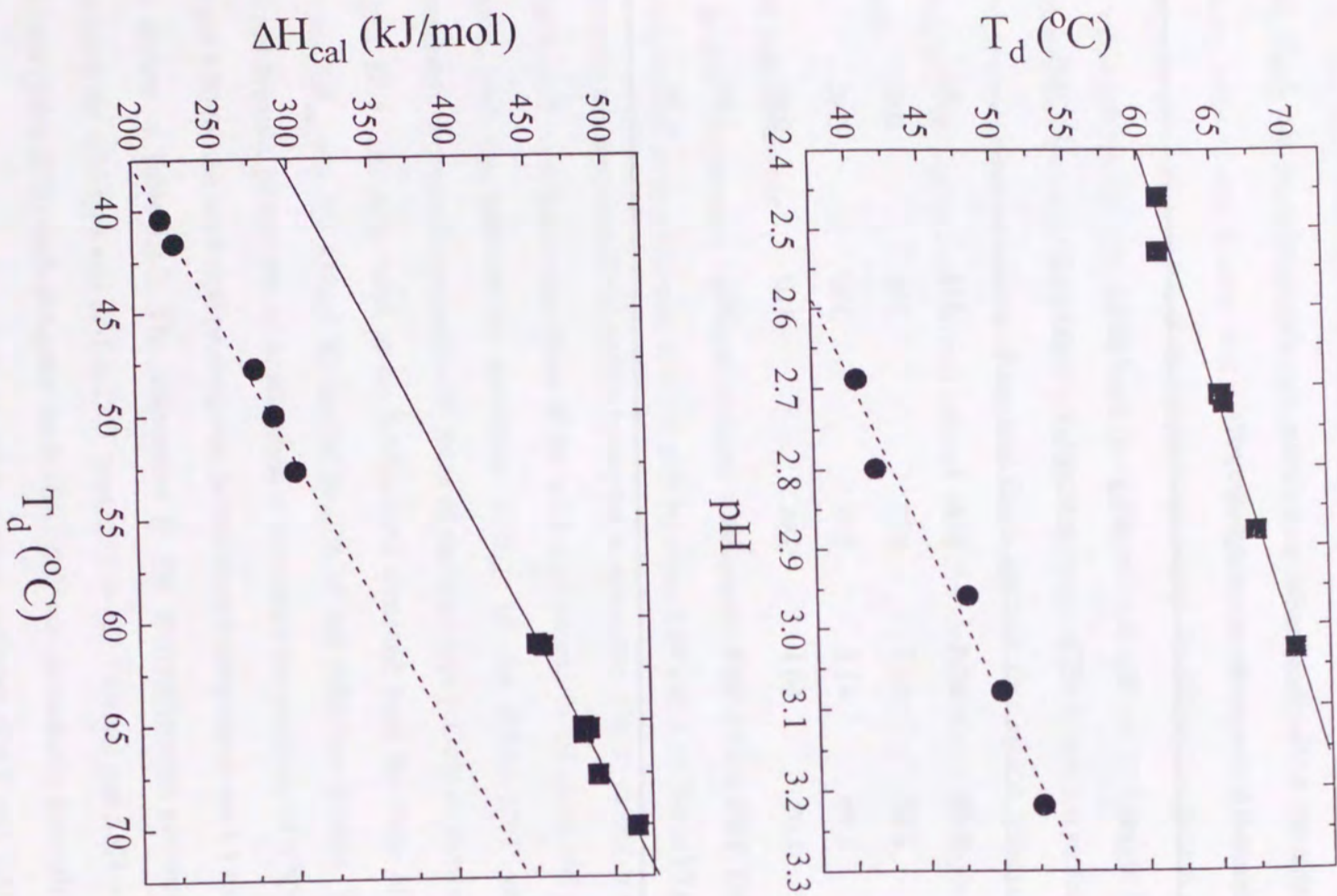| pH	T_d (^{0}C)	ΔH_{cal} (kJ/mol)	ΔH_{VH} (kJ/mol)	ratio $\Delta H_{cal}/\Delta H_{VH}$
2.69	40.5	218	241	0.90
2.80	41.7	226	246	0.92
2.96	47.8	277	300	0.92
3.08	50.1	288	310	0.93
3.22	52.7	301	302	1.00
avg				0.93

Fig. III-5. pH dependence of denaturation temperature (A) and the denaturation temperature dependence of calorimetric enthalpy change (B) of EAEA-I56T. Squares and circles represent the wild-type and EAEA-I56T, respectively.

-64-

Table III-2 Thermodynamic parameters for denaturation of the EAEA-lysozyme, I56T and EAEA-I56T obtained from DSC at the denaturation temperature (64.9 °C) of the wild-type protein at pH 2.7.

Protein	T_d (°C)	ΔT_d (°C)	ΔC_p^a [kJ/(mol K)]	ΔH_{cal} (kJ/mol)	$\Delta\Delta H_{cal}$ (kJ/mol)	$\Delta\Delta G$ (kJ/mol)
wild-type[b]	64.9±0.5	(0)	6.6±0.5	477	(0)	(0)
EAEA-lysozyme[c]	57.3±0.3	-7.6	6.7±0.7	446	-31	-9.6±0.5
I56T[d]	52.4	-12.5	5.2±0.5	425	-52	-15.2
EAEA-I56T	40.4±1.0	-24.5	7.0±0.4	390	-87	-23.7±1.1

[a]ΔC_p was obtained from the slope of ΔH against T_d. [b]The data for the wild-type protein reported previously (Takano *et al.*, 1995) were used. [c]The data for the EAEA-lysozyme reported Chapter II were used. [d]The data for the I56T reported previously (Funahashi *et al.*, 1996) were used.

lowest among the wild-type and three mutant proteins.

Crystal structure

The crystal of EAEA-I56T belonged to the space group P6₁22, and had the highest solvent content of 67 % in the six crystal forms found in the mutant human lysozyme crystals (Takano *et al.*, 1995, 1997a, 1997b, 1999b). The structure of the EAEA-I56T was essentially identical to that of EAEA-lysozyme in the N-terminal region (Fig. III-6) and identical to that of I56T in the vicinity of the mutation site (Fig. III-7). The structures of I56T (Funahashi *et al.*, 1996) and EAEA-lysozyme (Chapter II) have already been analyzed. The structural position of the first residue (E(-4)) was not determined, because the electron density corresponding to the first residue was poor. Because the space where the first residue would be located was open, the first E(-4) residue should be flexible and disordered.

The structures in the vicinity of the N-terminal regions of the wild-type, EAEA and EAEA-I56T lysozymes are illustrated in Figure III-6. Three major structural changes between EAEA-I56T and the wild-type protein were observed in the vicinity of the N-terminal regions and these changes were the same as the following between the wild-type and EAEA-lysozyme: changes in the salt bridge pairs, those in the N-terminal β-sheet structure, and the release of two water molecules. The striking feature is that the side chain of the threonine is rotated ca. 111° (χ1 angle, -51° in the EAEA-I56T, -47° in the I56T and -162° in the wild-type) so that the hydroxyl group of Thr 56 forms a hydrogen bond with one of the internal water molecules found in the wild-type and mutant structures. The hydrogen bonding distance was 2.96 Å in EAEA-I56T and 3.06 Å in I56T.
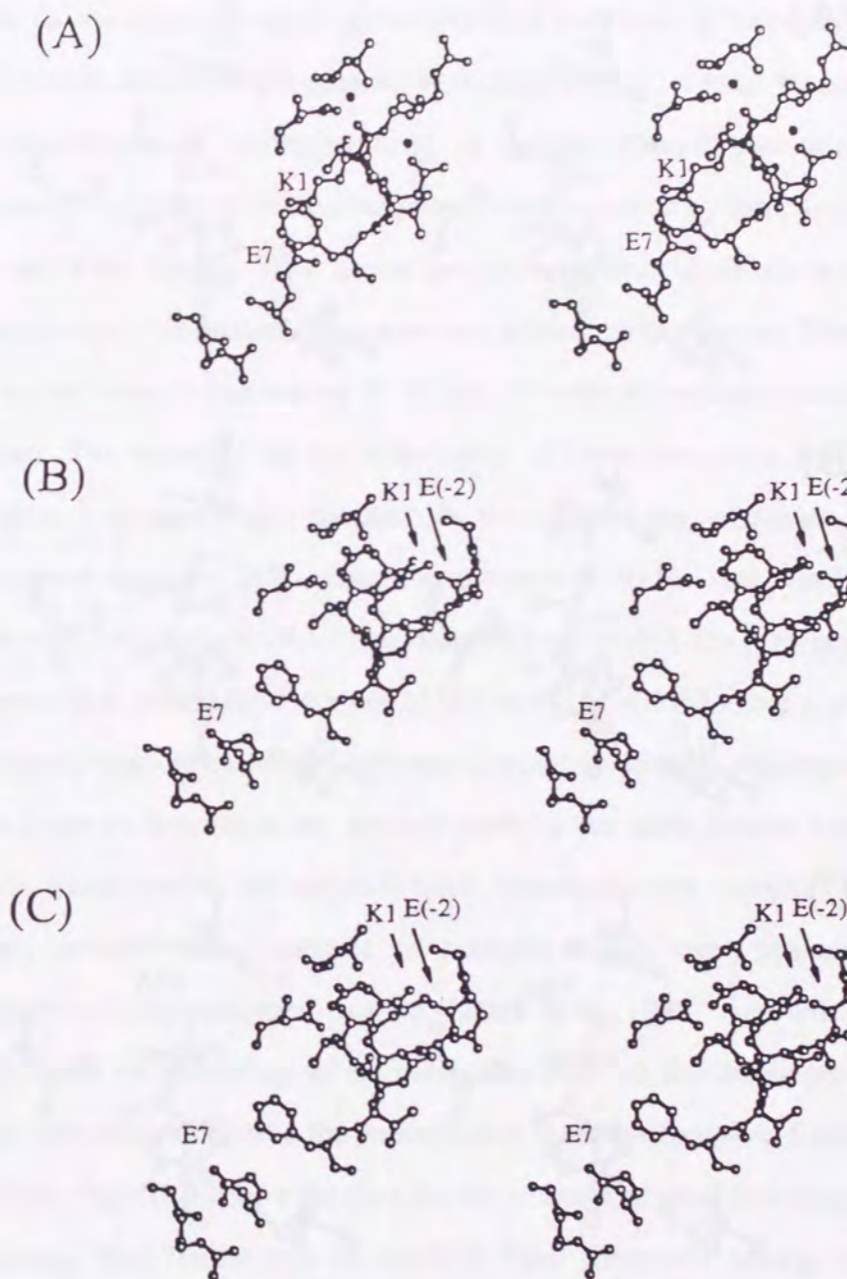

Fig. III-6. Stereodrawings of the wild-type (A), EAEA (B) and EAEA-I56T (C) human lysozyme structures in the N-terminal region. Solvent water molecules are drawn as filled circles. There are two water molecules in the wild-type protein, but none in the EAEA-lysozyme and EAEA-I56T.

(A)

156   156

(B)
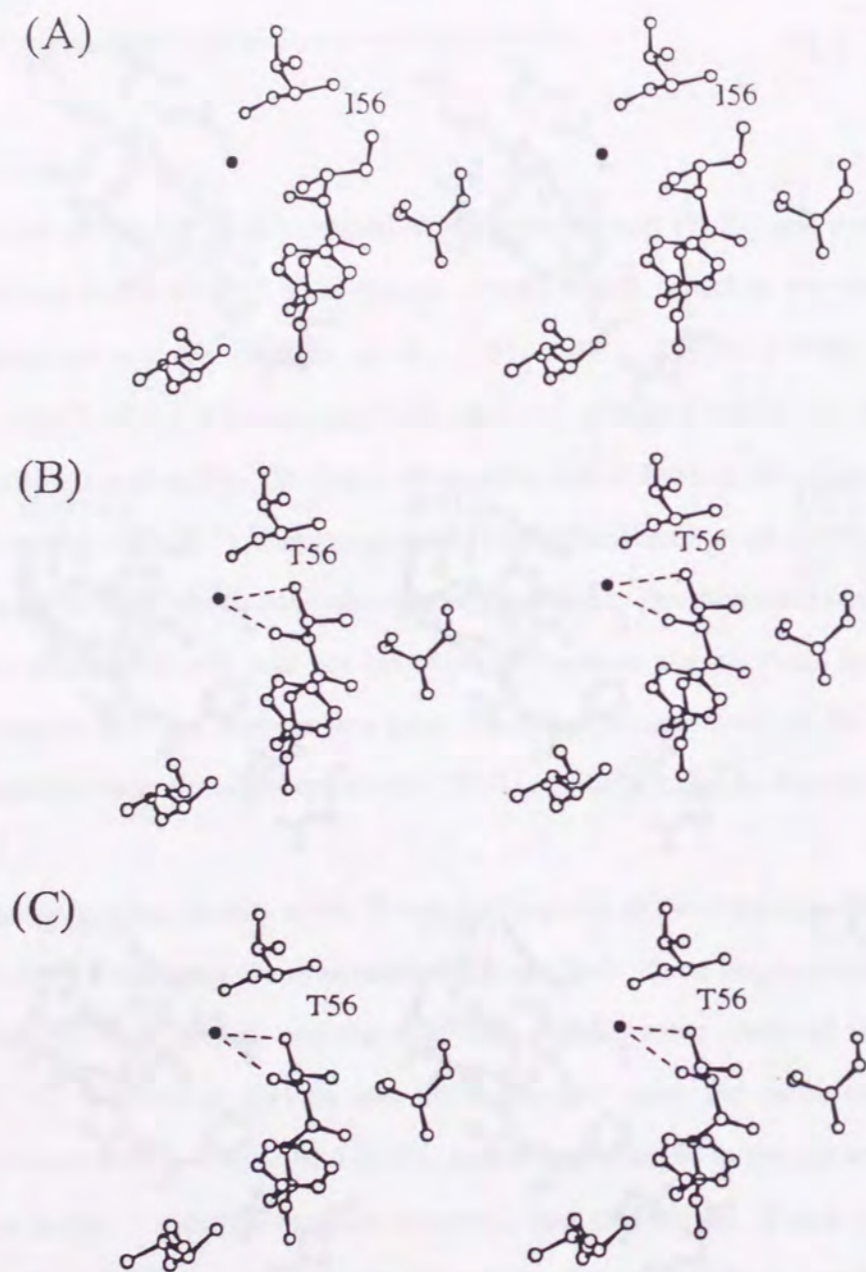
T56   T56

(C)

T56   T56

Fig. III-7. Stereodrawings of the wild-type (A), I56T (B) and EAEA-I56T (C) human lysozyme structures in the mutation site. Solvent water molecules are drawn as filled circles.

Time-course measurements of amyloid fibril formation of human lysozymes

In order to evaluate the amount of fibril formation for each human lysozyme, the absorbance of the supernatant at various ethanol concentrations were measured at 280 nm after the precipitates were separated by centrifugation (for 30 min at 13000 G). Fig. III-8 shows the relationship between the amount of the precipitates of the human lysozymes and ethanol concentration. The proteins of 0.1 mg/mL were incubated at 25 °C for 15 hours in various concentrations of ethanol. The decrease in the absorbance of the supernatant means that the precipitates appear in the solution. In the case of the wild-type protein, the precipitates appeared at an ethanol concentration 80 %. That was about 75 %, 75 % and 70 % for the EAEA-lysozyme, I56T and EAEA-I56T, respectively. This indicates that the EAEA-lysozyme, I56T and EAEA-I56T have a propensity to form precipitates at an ethanol concentration lower than the wild-type protein.

In order to determine the amyloidgenecity for each human lysozyme, the kinetic measurements of amyloid fibril formation were carried out in 80 % ethanol solution. The amounts of amyloid fibrils were evaluated by the quantitative Congo red stain method (Klunk *et al.*, 1999). Amounts of amyloid fibrils could be quantified at the maximum point of the difference spectra of Congo red solution between the presence and absence of amyloid fibrils (Klunk *et al.*, 1999). Fig. III-9 shows the time course of amyloid fibril formation of human lysozymes. The fastest rate of amyloid fibril formation among four human lysozymes was that of EAEA-I56T and the next EAEA-lysozyme. After 30 hours, all mutant lysozymes formed amyloid fibrils, but the wild-type protein still did not form amyloid fibrils. These results corresponded to the decreases in the absorbance of the supernatant as shown in Figure III-8. This means that all precipitates were amyloid fibrils.
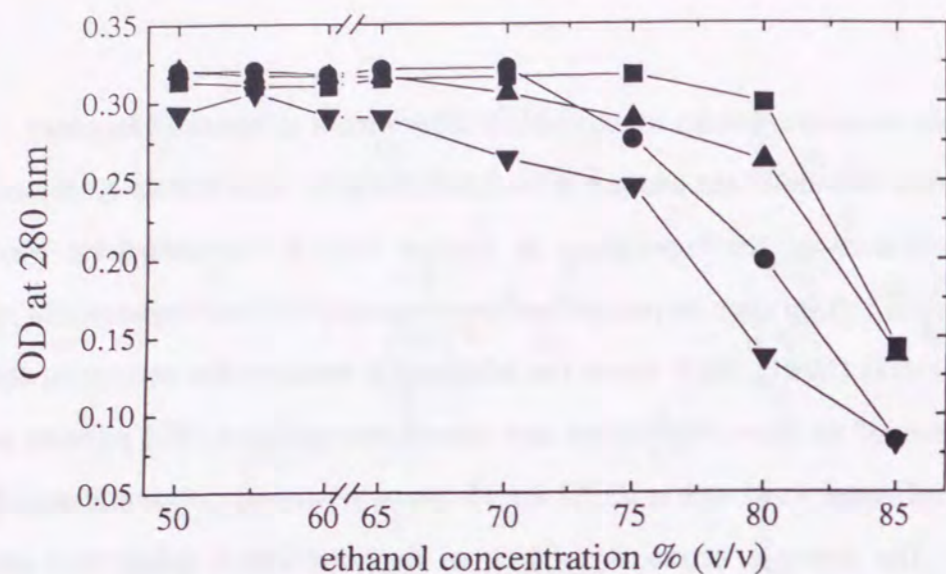
Fig. III-8. The relationship between the OD at 280 nm of the supernatant and ethanol concentration. The concentration of human lysozymes was 0.1 mg/mL. After incubation at 25 °C for 15 hours, centrifugation was carried out for 13000 G for 30 minutes. The changes in OD at 280 nm of the supernatant of the wild-type and mutant human lysozymes solutions in the various concentrations of ethanol were measured. Squares, circles, up triangles and down triangles represent the wild-type, EAEA, I56T and EAEA-I56T lysozymes, respectively.
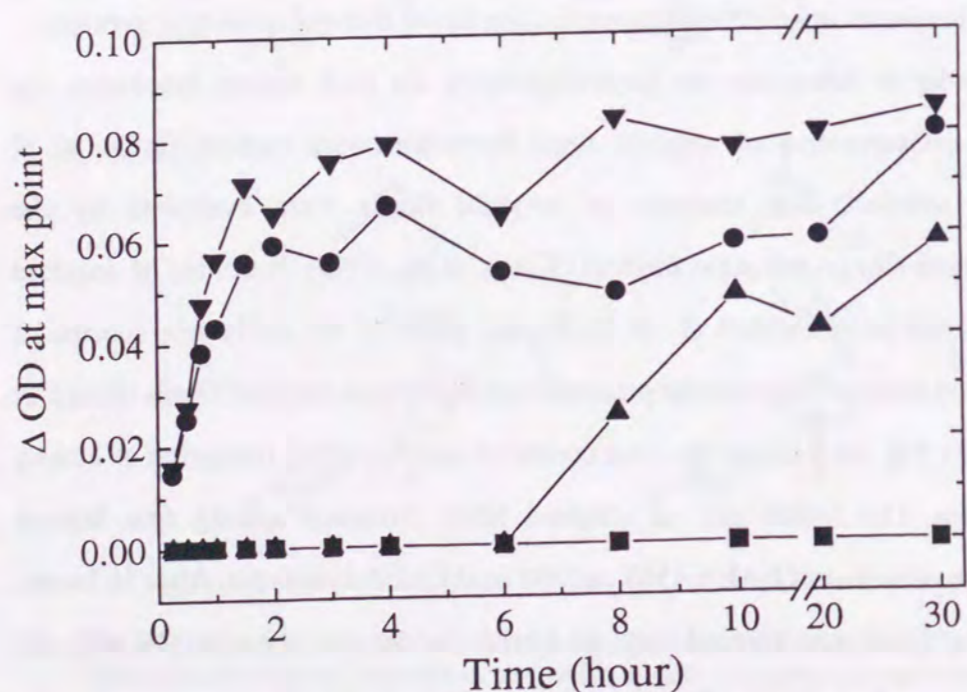

Fig. III-9. The time course of amyloid fibril formation of the wild-type and mutant human lysozymes. The amounts of amyloid fibrils were quantified by quantitative Congo red staining method. Squares, circles, up triangles and down triangles represent the wild-type, EAEA, I56T and EAEA-I56T lysozymes, respectively.

*The relation between the amyloidgenicity and stability*

Previous reports suggest that the amyloidgenecity of human lysozyme is related to the stability (Funahashi *et al.*, 1996; Booth *et al.*, 1997). The reason is that the amyloidgenic mutants of human lysozyme were more unstable than the wild-type between the native and denatured states. In the present results, the transition between native and amyloid forms of human lysozyme was measured for the first time. As shown in Fig. III-9, the wild-type protein did not form amyloid at a given concentration of the protein (0.1 mg/mL) after incubation for 30 hours in 80 % ethanol solution. The other three mutants (I56T) formed amyloid up to eight hours. EAEA-lysozyme and EAEA-I56T which were largely more unstable than the wild-type protein formed amyloid within one hour. This result also confirms that the amyloidgenecity was strongly related to the stability of the proteins.

Mechanism of Amyloid Fibril Formation by Human Lysozymes in Ethanol Solution

The amyloid formation of EAEA-lysozyme was faster than that of I56T whose stability was lower than that of the EAEA-lysozyme (Table III-2). This indicates that the amyloid formation is not related only to the instability of its protein. Why and how do the four extra residues (EAEA) affect the amyloid formation? Previous reports propose that the mechanism of the amyloid formation is divided into the two steps. (1) Monomer protein forms nuclei and (2) elongates into fibrils (Bishop & Ferrone, 1984; Walsh *et al.*, 1997; Wall *et al.*, 1999; Lashuel *et al.*, 1999). In the first step, the monomer protein transforms to the prototype of amyloid formation form via denaturation. Therefore, the nucleation might be

strongly related to the instability of the proteins. However, the rate of elongation might be affected by other factors. Amyloid fibrils consist of a number of β-sheets. The rate of elongation may be related to the formation of the β-sheets. The elongation rate of EAEA-lysozyme might be faster than that of I56T, although the stability of the former protein was lower.
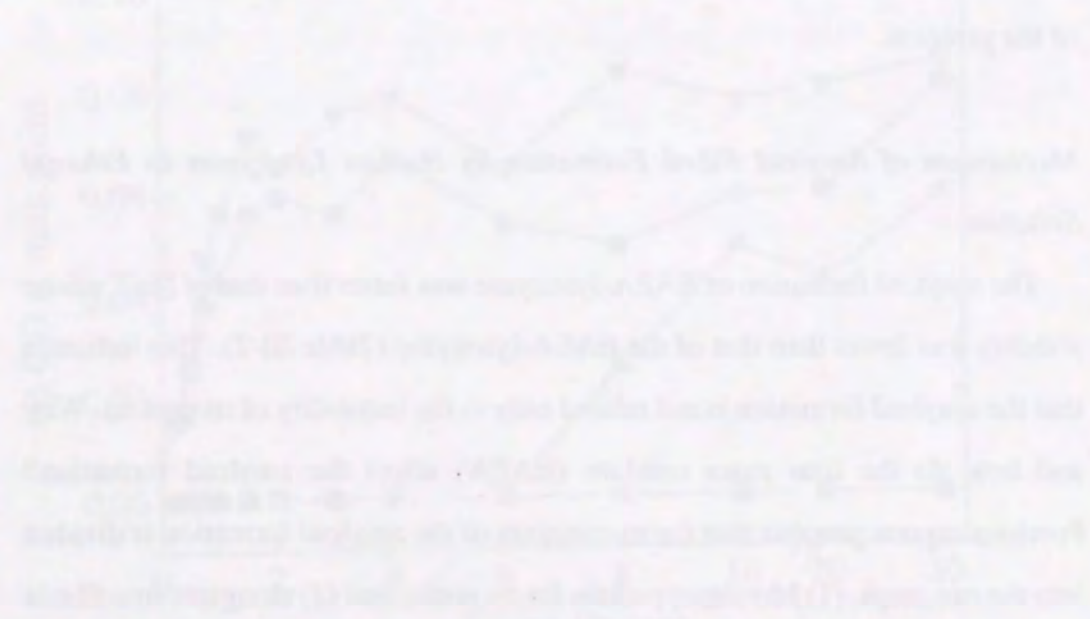
Chapter IV

Studies on Amyloid Protofilament Formation of Hen Egg Lysozyme in Highly Concentrated Ethanol Solution

Introduction

Recently, the diseases caused by protein misfolding, such as Alzheimer's disease, late onset diabetes, prion-related transmissible spongiform encephalophathies and amyloidosis, have attracted considerable attention as conformational diseases (Carrell & Lomas, 1997). The extracellular insoluble deposits (amyloid fibrils), resulting from protein misfolding, damage tissues leading to disease (Tan & Pepys, 1994; Kelly, 1996; Pepys, 1996). The amyloid fibrils, independent of the amino acid sequence, native protein structure, and function of the constituent protein (Sunde *et al.*, 1997), are of indeterminate length, are unbranched with diameters of about 100 Å and display pathognomonic green birefringence when viewed in polarized light after staining with Congo red (Pepys, 1996). X-ray diffraction patterns of amyloid fibrils show simple patterns with 4.7 Å meridional reflection and 10 Å equatorial reflection (Sunde *et al.*, 1997). Sunde *et al.* (1997) have proposed that amyloid fibrils consist of a common core structure which is a cross-β-fiber structure, with β-strands perpendicular and β-sheets parallel to the fiber axis.

The mutant human lysozymes, Ile56Thr and Asp67His, have been identified as fibril proteins in amyloid deposits that cause hereditary systemic amyloidosis (Pepys *et al.*, 1993). The native form of the Ile56Thr molecule is similar to the wild-type structure (Funahashi *et al.*, 1996; Booth *et al.*, 1997). However, the equilibrium and kinetic stabilities of the mutant protein are remarkably decreased due to the introduction of a polar residue (Thr) in the interior of the molecule. It has been reported that the amyloid formation of the mutant human lysozyme is due to a tendency to favor (partly or completely) denatured structures (Funahashi *et al.*, 1996). However, the mechanism of the amyloid formation is still not clear.

Fortunately, lysozymes have been studied extensively and their physiochemical properties have been examined in detail (Artymiuk & Blake, 1981; Redfield & Dobson, 1990; Radford *et al.*, 1992; Hooke *et al.*, 1994). Therefore, lysozymes are suitable as a model protein to elucidate the mechanism

of amyloid fibril formation. Hen egg lysozyme is known to increase in helical content in ethanol (alcohol) solution (Hamaguchi & Kurono, 1963; Kurono & Hamaguchi, 1964; Ikeda & Hamaguchi, 1970; Kamatari *et al.*, 1998). During re-examinations of ethanol effects on the conformational stability of hen egg lysozyme, we found that in higher concentrations of ethanol (> 80 %), hen egg lysozyme molecules associate and form a β-structure. Furthermore, white precipitates appeared when 10 mM NaCl was added to the lysozyme solution in which the lysozyme is in a β-rich conformation in 90 % ethanol. Congo red staining, electron microscopy and X-ray diffraction all indicate that the precipitates were amyloid protofilament.

Recently, it has been reported that non-disease-related protein can also form amyloid fibrils in extreme environments, for example, in alcohol or acidic pH (Litvinovich *et al.*, 1998; Guijarro *et al.*, 1998; Chiti *et al.*, 1999). It is important to elucidate whether amyloid formation is a property common to many proteins and how amyloid fibrils form to understand the mechanism of the misfolding of proteins. In this paper, the mechanism of amyloid protofilament formation from hen egg lysozyme in highly concentrated ethanol solution will be discussed.

Materials and methods
Protein Preparation

Hen egg lysozyme (6x Crystallization) was purchased from Seikagaku Kogyo (Tokyo, Japan). Further purification was carried out using cation-exchange column chromatography, SP-sepharose (Pharmacia), in 50 mM sodium acetate (pH 4.0) with a gradient from 0.3 M to 0.5 M NaCl.

Circular Dichroism

Circular dichroism (CD) spectra in the near-UV and far-UV regions were obtained using a Jasco J-720 spectropolarimeter equipped with a water bath to control the temperature at 25 °C. The concentration of hen egg lysozyme was 5

mg/ml for the near- and far-UV experiments. Sixteen scans were averaged to obtain each spectrum. Cells with path lengths of 1 mm and 0.1 mm were used for near- and far-UV data acquisition, respectively.

Ultracentrifugation

Sedimentation equilibrium data were collected on a temperature-controlled Beckman XL-A analytical ultracentrifuge equipped with an An60Ti rotor and a photoelectric scanner. Sedimentation equilibrium runs were performed on 29-μL samples at 20000-25000 rpm using a double sector cell equipped with a 3-mm charcoal-filled Epon centerpiece and quartz windows. The partial specific volume of hen egg lysozyme (0.703 cm^3/g) reported previously was used (Sophianopoulos *et al.*, 1964). For the measurements, the protein solution contained 150 mM KCl in various concentrations of ethanol less than 80 %, but not in 85 % ethanol. The concentration of the protein solution was 10 mg/ml.

Congo red Staining

Congo red staining method was same as quantitative Congo red experiments in Chapter III.

Electron Microscopy

Suspensions of hen egg lysozyme in concentrated ethanol solution were applied to carbon-coated copper grids, blotted, washed, negatively stained with 2 % uranyl acetate (wt/vol), air-dried, and then examined with a JEOL JEM1010 transmission electron microscope operating at an accelerating voltage of 100kV.

X-ray Diffraction

X-ray diffraction experiments were carried out using a RIGAKU FRD rotating anode X-ray generator, operated at 50kV and 70mA. Double mirror optics (RIGAKU-MSC/Yale) were used to produce a well-collimated beam of CuKα

radiation (λ=1.5418 Å). Precipitates were put into a capillary with a diameter of 0.5 mm. The specimen-to-film distance and the exposure time were 275 mm and 10 hours, respectively. X-ray diffraction patterns were recorded with a RIGAKU imaging plate detector R-AXIS IV.

NMR Spectroscopy

^{1}H-NMR spectra at 600 MHz were recorded with a Bruker DRX600 NMR spectrometer at 25 °C. The concentration of hen egg lysozyme was 5.0 mg/ml. The mixture of H$_2$O and C$_2$^{2}H$_5$OH (^{2}H 98 %, Cambridge Isotope Laboratories, Inc.) was used as a solvent. 10 % ^{2}H$_2$O was used for the 0 % ethanol solution

Results

Characterization of hen egg lysozyme in a highly concentrated ethanol solution

CD spectra of hen lysozyme were measured in various concentrations of ethanol. Protein solutions (5 mg/mL) were incubated at 25 °C for 24 hours for CD measurements. Figure IV-1 shows the far-UV CD spectra of hen egg lysozyme in various concentrations of ethanol. The values of negative peaks at [θ] 208 nm and 222 nm which reflect the characteristic of the α-helix structure were increased with an increase in ethanol concentration up to 80 %. Under these conditions, all solutions were clear and no precipitation was observed. These ethanol effects on the lysozyme structure are well-known (Hamaguchi & Kurono, 1963, Kurono & Hamaguchi, 1964, Ikeda & Hamaguchi, 1970). Whereas, CD values at 208 and 222 nm of samples containing 85 % ethanol were decreased, and the spectra showed a single negative peak around 215 nm (Curve 5 in Fig. IV-1). In order to analyze the features of the structural changes, secondary structure compositions of the protein were calculated from the CD spectra by the method of Provencher (1982). As shown in Table IV-1, the α-helical content increased with increasing ethanol concentration up to 80 %, but at 90 % it decreased and the content of β-structure increased. These results suggest that the conformation of lysozyme
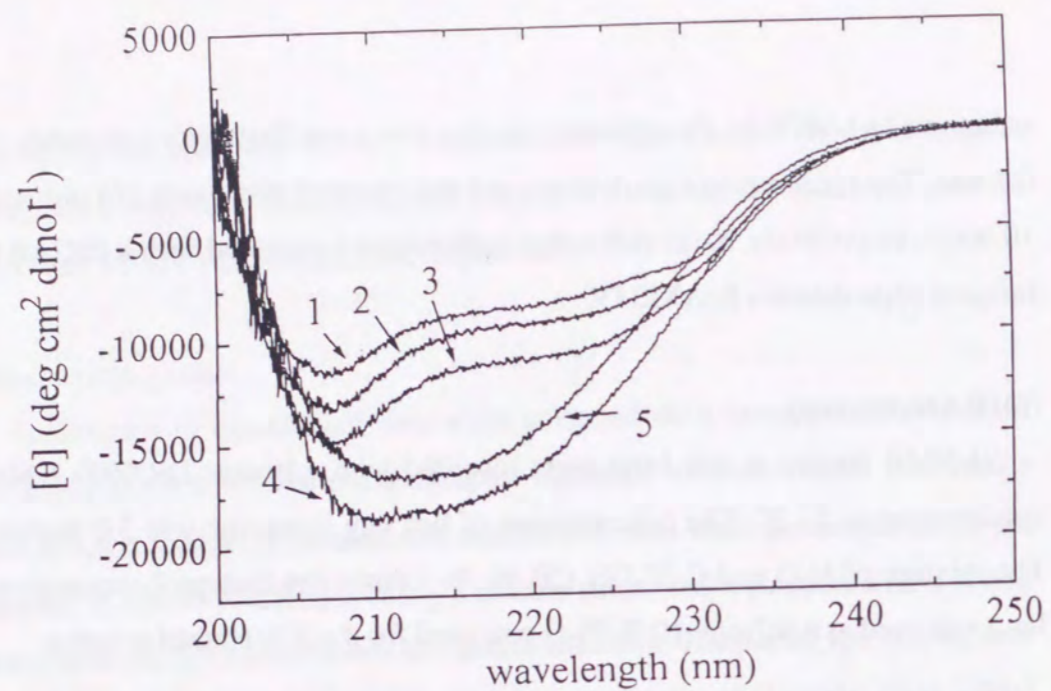
Fig. IV-1. Far-UV CD spectra of hen egg lysozyme (5 mg/mL) in various concentrations of ethanol incubated for 24 h at 25 °C.
1 : 0 %, 2 : 50 %, 3 : 70 %, 4 : 80 %, 5 : 85 % ethanol solution.
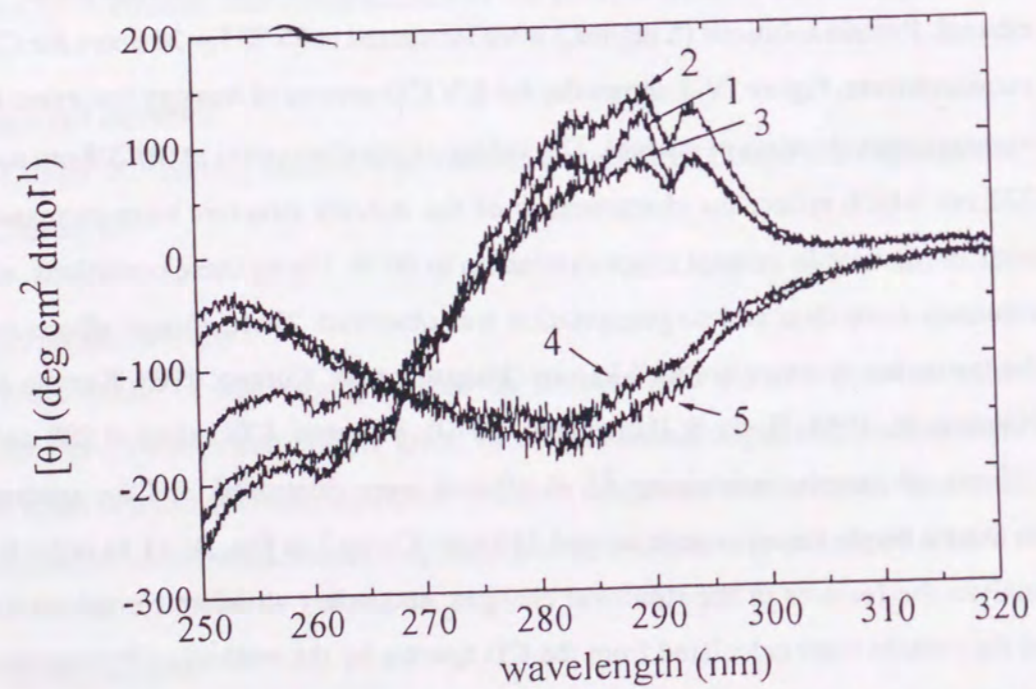
Fig. IV-2. Near-UV CD spectra of hen egg lysozyme (5 mg/mL) in various concentrations of ethanol incubated for 24 h at 25 °C.
1 : 0 %, 2 : 50 %, 3 : 70 %, 4 : 80 %, 5 : 85 % ethanol solution.

Table IV-1. CD values at 208 nm, 222 nm and secondary structure compositions[a] in various ethanol concentrations.

ethanol concentration (%)	$[\theta]$ 208 nm	$[\theta]$ 222 nm	α helix (%)	β-structure (%)	$[\theta]$ 288 nm
0	-11397	-8208	31	6	98.42
70	-14782	-10860	52	6	68.08
80	-18090	-15361	54	15	-123.9
85	-15592	-13409	48	16	-118.6
90	-15087	-12874	44	26	-116.8

[a]Conditions were the same as those of Figure IV-1 in various ethanol concentrations.

transforms from an α-helical structure to a β-sheet structure in highly concentrated ethanol solution.

In order to examine the changes in the tertiary structure, CD spectra in the near-UV region were measured under the same conditions as those in the far-UV region (Fig. IV-2). The positive peak around 288 nm slightly increased at 50 % ethanol. At ethanol concentration higher than 80 %, a broad negative peak around 280 nm appeared. The spectra were similar to that of the denatured state in 5 M urea (Kamatari *et al.*, 1998). These results indicate that the tertiary structure collapses in high concentration ethanol solution and that the transition point is between 70 and 80 %. One-dimensional NMR spectra of hen egg lysozyme at the same concentration as the sample for CD were also measured in the 0 %, 40 %, and 60 % ethanol-d_5 solutions (in H_2O). The spectrum essentially did not change up to 40 % ethanol-d_5 except for the broadening of the signals. At 60 % ethanol, however, a significant broadening was observed in the amide proton region (data not shown). This fact suggests that the exchange of the amide protons is significantly enhanced at 60 % ethanol. NMR results were consistent with those of the CD spectra in the near-UV region.

In order to examine the protein concentration dependence of the α-to-β structure transition, CD spectra in the far-UV region were measured at various protein concentrations (Fig. IV-3). At the lower protein concentration, the structure transition was not observed after incubation for 24 hours at 25 °C in 85 % ethanol solution. The spectrum still showed a helix-rich character at a protein concentration of 1 mg/mL, but at 3 mg/mL, it changed to a β-rich structure. The extent of association was examined by analytical ultracentrifugation. At less than 80 % concentration of ethanol, the apparent molecular weight was that of a monomer. In 85 % ethanol, precipitates appeared when the solution contained 10 mM NaCl. Without salt in the 85 % ethanol solution, the apparent molecular weight was calculated to be 260,000. These results indicate that lysozyme molecules associate in 85 % ethanol solution and that the α-to-β structure
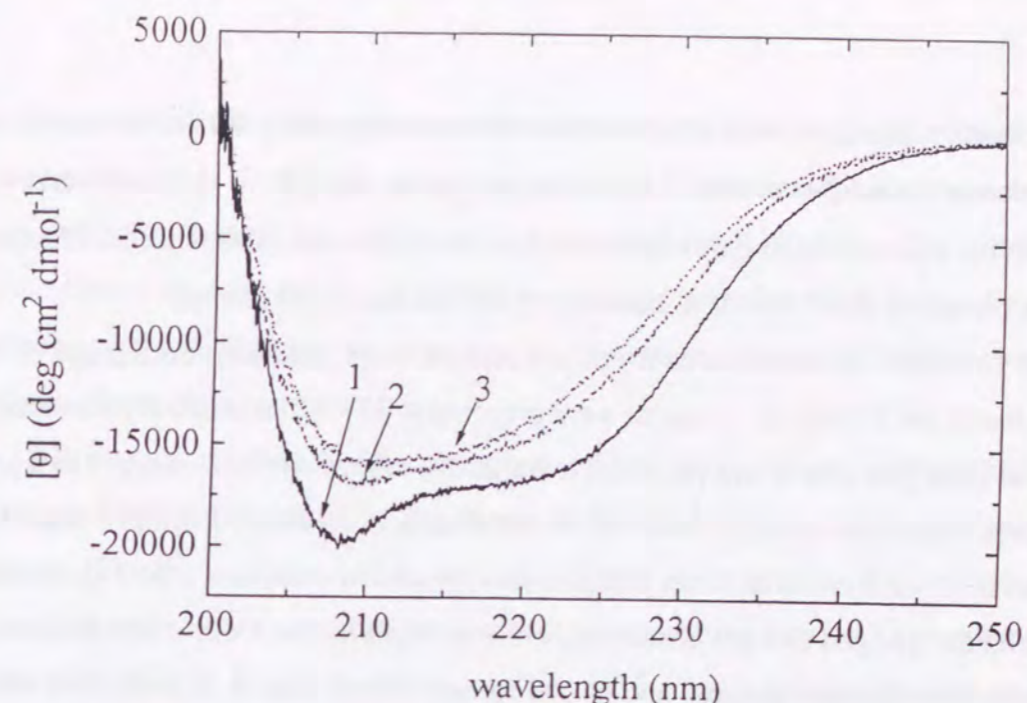
Fig. IV-3. Protein concentration dependence of CD spectra in the far-UV region. All solutions were incubated at 25 °C for 24 h in 85 % ethanol solution.
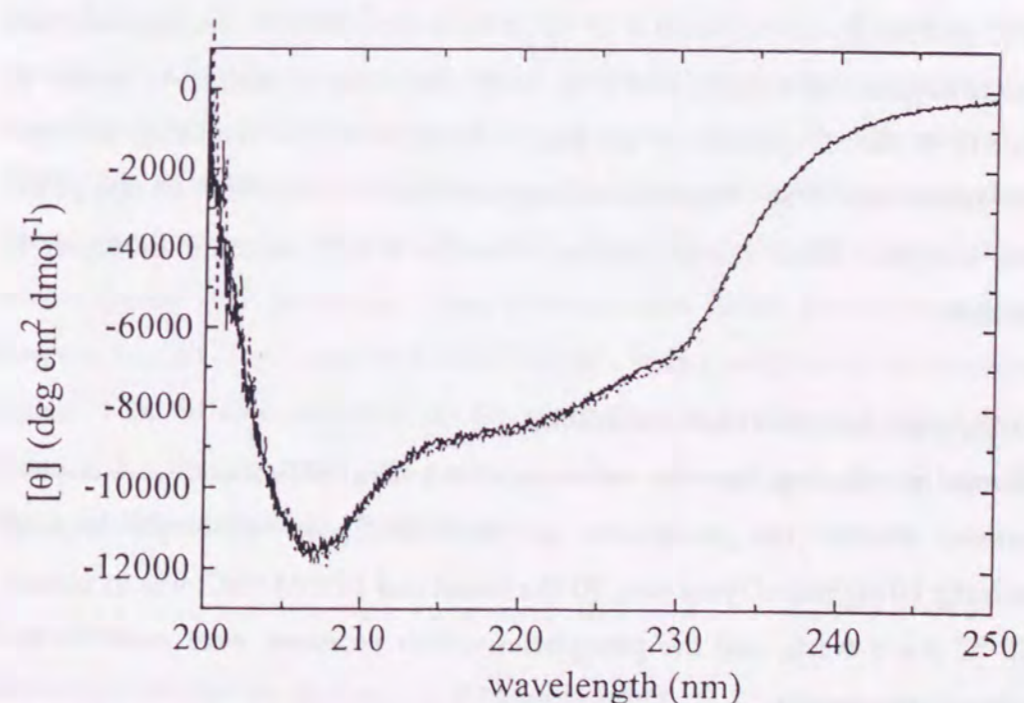1 : 1 mg/mL 2 : 2 mg/mL 3 : 3 mg/mL hen egg lysozyme.

Fig. IV-4. Far-UV CD spectra of native and refolded forms from precipitant hen egg lysozyme. Protein concentration was 7 mg/mL. Solid line, native fold; Dashed line, refolded from precipitant in 90 % ethanol containing 10 mM NaCl solution.

transition proceeds with molecular association, suggesting the formation of an intermolecular β-structure. These phenomena are similar to those of amyloid fibrils; intermolecular β-structures and protein concentration dependence (Harper & Lansbury, 1997, Jarrett & Lansbury, 1993, Lashuel *et al.*, 1998).

In order to examine the effect of salt concentration, solutions containing 90 % ethanol and 10 mg/mL lysozyme were prepared at 25 °C. The solution without salt was clear just after it was prepared, but after 1 week the solution changed to a gel form. When the solution contained 0.1 mM NaCl, a gel formed within 1 hour. In 0.5 mM NaCl solution, white precipitates appeared at once, and after 1 week the solution changed to a gel containing white precipitates. In 1 mM NaCl solution, white precipitates appeared and no gel formed. These results indicate that salts promote the association of proteins. Whether the precipitates are dissolved and recover to the native structure when ethanol concentration is diluted was examined. The protein solution of 7 mg/mL lysozyme containing 90 % ethanol and 10 mM NaCl was incubated at 25 °C for three days. The precipitates collected by centrifugation at 13000g could be easily dissolved in water. As shown in Figure IV-4, the CD spectrum of the dissolved sample was almost identical to that of the native state. The enzymatic activity also recovered to 50 % of that of the native enzyme. These results indicate that the α-to-β structure transition is reversible.

Hen egg lysozyme fibril characterization

Congo red staining, electron microscopy and X-ray diffraction were used to determine whether the precipitates are amyloid fibrils. A sample solution containing 10 mg/mL of lysozyme, 90 % ethanol and 10 mM NaCl was incubated at 25 °C for a week, and the precipitates which appeared were used for the following experiments.

Figure IV-5 (A) shows the absorption spectra of the mixture of Congo red and lysozyme precipitates, Congo red alone and lysozyme precipitates alone. The

difference spectrum was obtained by subtraction of the scattering due to precipitates (Fig. IV-5B). The maximum point of the difference spectrum was 541 nm, which is one of the characteristic features of amyloid fibrils. The stained precipitates were examined by optical microscope under cross-polarized light. The precipitates displayed pathognomonic green birefringence and filamenteous aggregations (data not shown).

All known amyloid fibrils, regardless of the nature of the main protein component or the source of the fibrils, are about 100 Å wide and have no branch points (Sunde & Blake 1997). In the electron micrographs, the lysozyme precipitates displayed a typical amyloid protofilament form, having a diameter of approximately 70 Å with no branching (Fig. IV-6). The lengths of the hen egg lysozyme fibrils were shorter by about 1000 to 2000 Å than that of transthyretin fibrils already reported (Sunde & Blake, 1997).

The X-ray diffraction pattern of the lysozyme precipitates showed one sharp reflection, which appeared as a ring because of the lack of relative fibril orientation within the sample. Figure IV-7 shows the radial intensity profile of the circular average after subtraction of the solvent scattering (Vonderviszt *et al.*, 1992). The reflection at 4.7 Å which arises from the interstrand spacing in the β-sheets, was observed as shown in Figure IV-7B. A broad intensity maxima should appear around 10 Å in the case of multilayer β-sheet fibrils. In the present case, the peak around 10 Å might be hidden behind a strong background in the central region of the diffraction pattern. As described, three hallmarks of amyloid fibrils indicate that the lysozyme precipitates in highly concentrated ethanol have the characteristics of amyloid protofilament.

Discussion

Structural changes in lysozyme in ethanol solution

The effects of alcohol on protein structures have been extensively studied (Shiraki *et al.*, 1995; Thomas & Dill, 1993). Increase in the helical content of
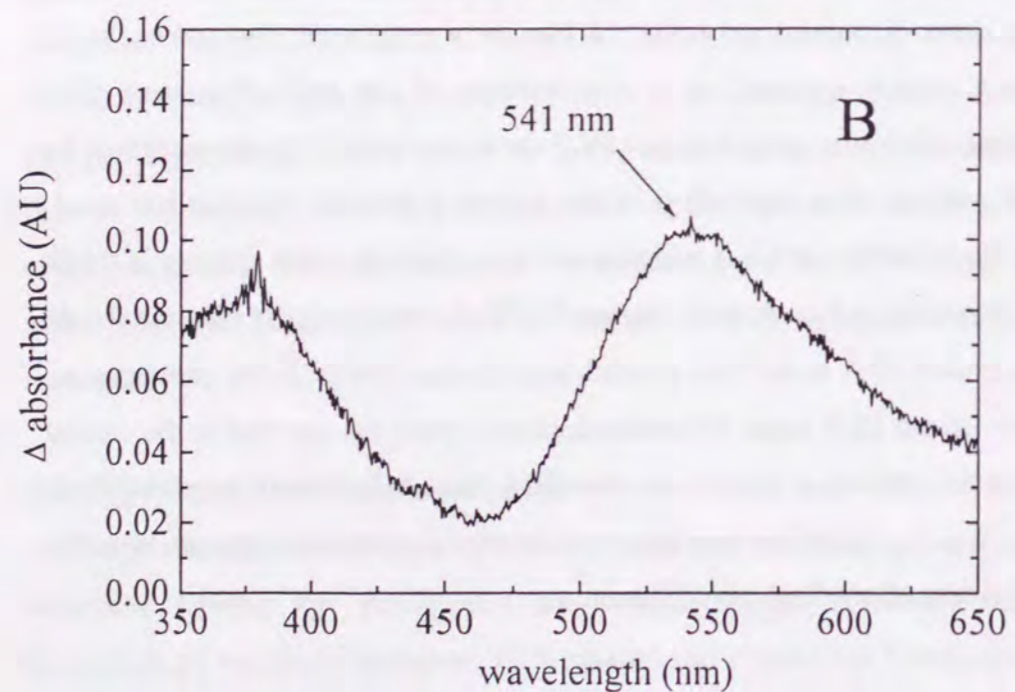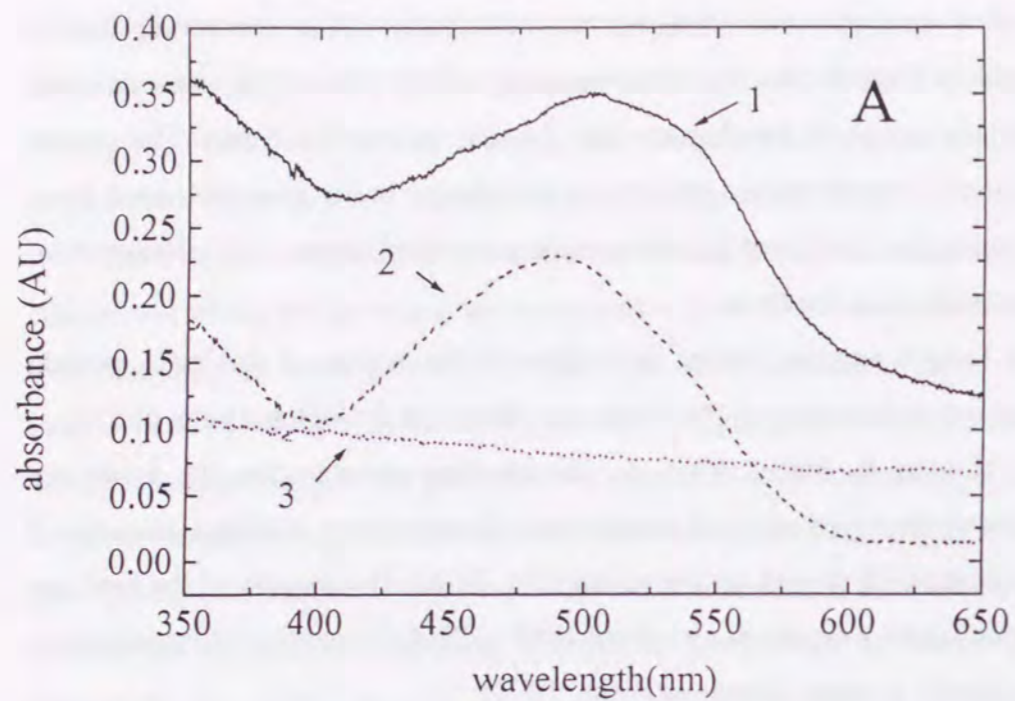
Fig. IV-5. (A) Absorbance spectra of Congo red (CR) solution in the presence (1) and absence (2) of hen egg lysozyme fibers and lysozyme fibers alone (3). (B) Difference spectra obtained by subtracting the spectra of CR alone and lysozyme alone from the spectrum of lysozyme + CR. The maximal point of difference spectrum is around 541 nm.
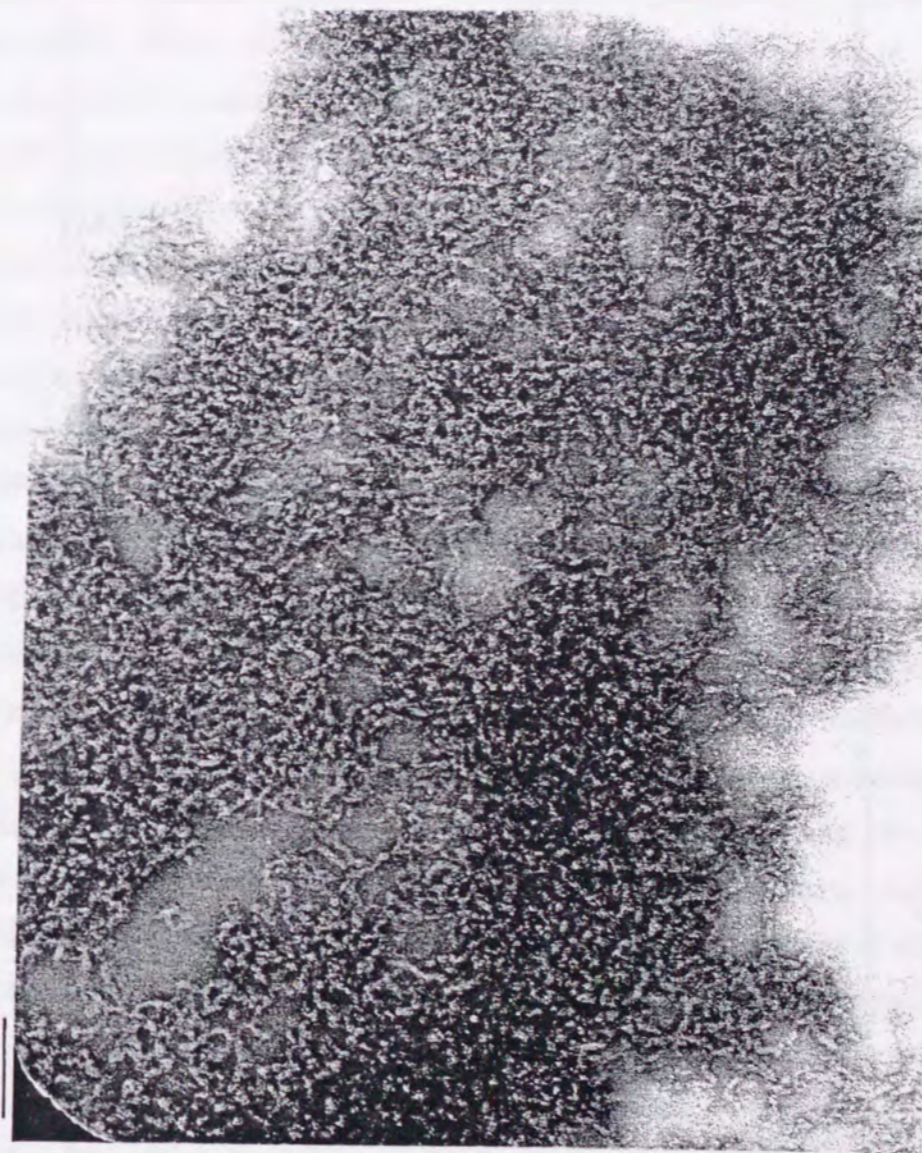
Fig. IV-6. Electron micrograph of a negatively stained preparation of 10 mg/mL hen egg lysozyme in 90 % ethanol solution incubated at 25 °C for a week (bar = 100 nm).

Fig. IV-7. (A) Radial intensity distribution profile of X-ray diffraction pattern from hen egg lysozyme fibrils. The X-ray diffraction patterns were mostly circular symmetric with a little tendency of orientation. Therefore, circular averaging was done to make the plot of the radial intensity distribution. The peak is sharp on the broad background scattering from the radial intensity distribution.(B) Difference intensity was obtained by subtracting 90 % ethanol 90 % ethanol solution from hen egg lysozyme fibrils. The peak (4.7 Å) indicated by an arrow is of the interstrand spacing and is typical of amyloid fibrils.

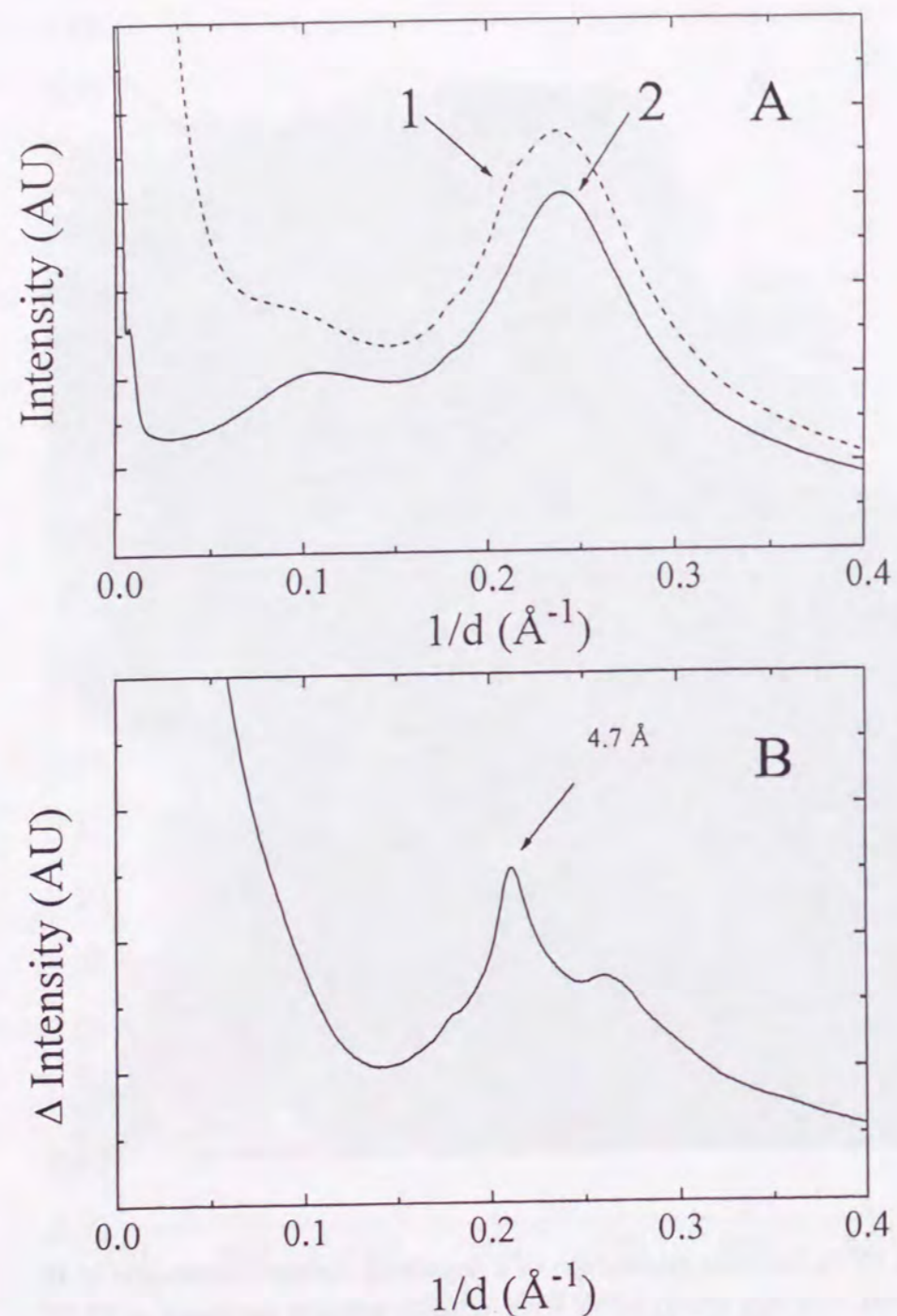proteins including lysozymes have been observed in high concentrations of ethanol (Hamaguchi & Kurono, 1963; Kurono & Hamaguchi, 1964; Ikeda & Hamaguchi, 1970). Alcohol also contributes to the stabilization of folding intermediates (Thomas & Dill, 1993). Recent NMR experiments have reported that in high concentration of alcohol, the helical content of hen egg lysozyme increases, its tertiary structure collapses and it is not as compact as the molten-globule state (Kamatari *et al.*, 1998). In many cases, alcohol-induced denaturation results in stabilization of extended helical rods in which the hydrophobic side chains are exposed, whereas polar amide groups are shielded from the solvent (Thomas & Dill, 1993; Shiraki *et al.*, 1995).

The present results also indicated that the helical content of lysozyme gradually increases up to an ethanol concentration of 80 %. However, over 80 %, we found that the helical content decreases and the β-structure increases. The tertiary structure was destroyed as reported (Parodi *et al.*, 1973; Velicelebi & Sturtevant, 1979; Kamatari *et al.*, 1998). In this high ethanol environment, hen egg lysozyme with a β-rich structure associated into amyloid protofilament. Recently, it has been reported that acylphosphatase, which does not cause amyloidosis, can form amyloid fibrils in a solution containing moderate concentrations of trifluoroethanol (Chiti *et al.*, 1999). In the process of amyloid formation of acylphosphatase, the CD spectra in the far-UV region show a slow two-state transition between two conformations containing significant amounts of α-helical and β-sheet structures. These observations suggest that the transformation from α- to β-conformation is a common property for kinds of proteins under appropriate concentrations of alcohol (Chiti *et al.*, 1999).

Amyloid formation of hen egg lysozyme

The examinations by Congo red staining, electron microscopy and X-ray diffraction support that the precipitates of hen egg lysozyme are in an amyloid

protofilament form. In electron micrographs, the diameter of the fibrils was 70 Å and the length was from 1000 to 2000 Å. It has been reported that transthyretin, which causes amyloidosis, consists of four protofilaments (Serpell *et al.*, 1995), electron micrographs of transthyretin amyloid protofilaments show a diameter of 40-50 Å, and the length is also around 1000 Å (Lashuel *et al.*, 1998). These features are similar to those of lysozyme protofilament in the present study. This means that hen egg lysozyme form protofilament (precursor of amyloid fibrils) in highly concentrated ethanol solution.

Generally, amyloid fibrils *in vitro* are stable and hardly susceptible to protease (Badman *et al.*, 1998). In the case of amyloid fibrils of mutant human lysozyme (Asp67His), however, the fibrils can be dissolved in strong denaturant (6 M GuHCl) and the protein refolds to the native conformation on dilution, with its enzymatic activity also recovered (Booth *et al.*, 1997). On the other hands, insulin fibrils do not cause amyloidosis but possess the three hallmarks of amyloid fibrils (Burke & Rougvie, 1972). The polymerization process of insulin fibrils has been reported to be reversible (Waugh, 1957). The protofilaments of transthyretin amyloid also recover to a monomer (Lashuel *et al.*, 1998), suggesting that the transformation to amyloid protofilaments is reversible. The precipitates of hen egg lysozyme in the present study, which look very similar to the protofilaments as judged by an electron micrograph, could recover the native conformation with its enzymatic activity by removal of ethanol. These results indicate that amyloid fibrils, especially the protofilaments, can recover the original monomer conformation under appropriate conditions.

The mechanism of amyloid fibril formation by hen egg lysozyme

Dobson's group has proposed that amyloid formation is a common property of globular proteins under appropriate conditions (Guijarro *et al.*, 1998; Chiti *et al.*, 1999). For example, the SH3 domain of the p85α subunit (Guijarro *et al.*, 1998)

and acylphosphatase (Chiti *et al.*, 1999) form amyloid fibrils in an acid pH region and in the presence of trifluoroethanol, respectively, which are environments far from physiological conditions. Recently, our group also discovered that even the extremely stable methionine aminopeptidase (MAP) from a hyperthermophile, *Pyrococcus furiosus*, forms amyloid-like fibrils in the presence of guanidine hydrochloride (about 3 M) in an acidic region. In the case of MAP, it is clearly demonstrated that the amyloid-like form appears just after the protein is almost completely denatured (Yutani *et al.*, 2000). This means that the β-structure of amyloid fibrils forms after destruction of the α-helical structure. This mechanism was confirmed by the present results. On the other hand, proteins that known to cause amyloidosis were independent of the amino acid sequence, native protein structure, and function of the constituent protein (Sunde *et al.*, 1997). These results indicate that the amyloid fibrils formation is not caused by a specific sequence but proteins generally form amyloid fibril under conditions in which population of partially (or completely) denatured state is increased.

The process of amyloid formation by hen egg lysozyme in ethanol solutions is summarized in Fig. IV-8. In the first step, the helical content of the lysozyme increases with an increase in the concentration of ethanol. In the second step at higher concentrations of ethanol, the helical content further increases but the tertiary structure is destroyed. In the third step in highly concentrated ethanol solution, the helical structures are partly destroyed. Finally, in lysozyme the β-sheets associate with one another and form the protofilament of amyloid fibrils (step IV). The rate of the formation is highly dependent on protein concentration and the concentration of salts.

In this paper, we could find the conditions for amyloid protofilament formation by hen egg lysozyme and demonstrate that amyloid protofilament formation of hen egg lysozyme occurs after the destruction of the helical and tertiary structures.
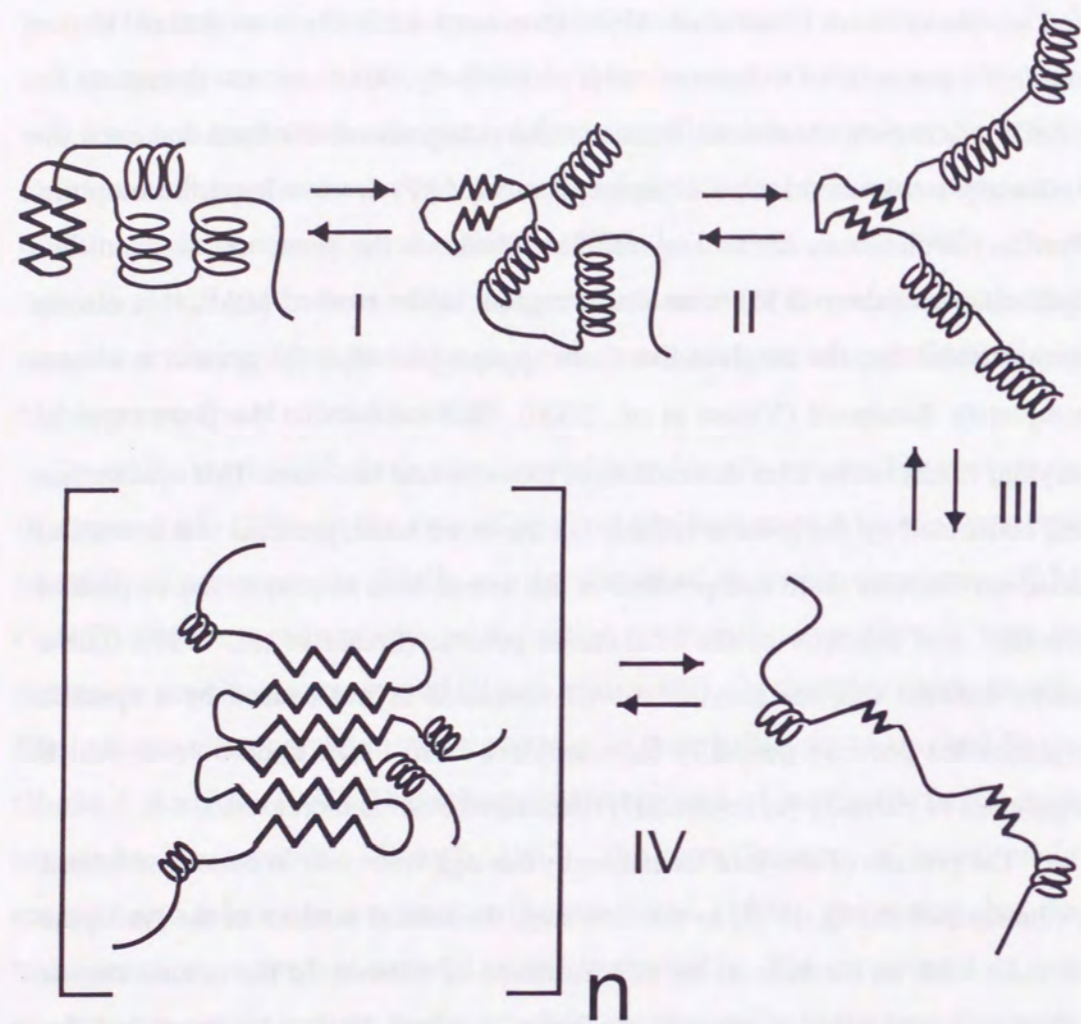
Fig. IV-8. Proposed mechanism for hen egg lysozyme amyloid fibril formation in ethanol solution. Helices and sheets are shown by spirals and zigzag lines, respectively. First, the helical content increases with perturbation of the tertiary structure (step I and II). In highly concentrated ethanol solution, the helical structure are partly destroyed (step III). Finally, the lysozyme assembles to form amyloid fibrils (step IV).

Chapter V

Summary and Conclusions

In this thesis, the relationship between the amyloidgenecity and stability of the human lysozyme was investigated to elucidate how and why the amyloid formation of human lysozyme occurs. The main results obtained in Chapters II to IV are summarized as follows.

Chapter II   The construction of a human lysozyme expression system by *P. pastoris*. *P. pastoris* expressed the human lysozyme at about 300 mg per L of broth, but four extra residues (Glu^{-4}-Ala^{-3}-Glu^{-2}-Ala^{-1}-) were added at the N-terminal of the expressed protein (EAEA-lysozyme). To determine the effect of the four extra residues on the stability, structures and folding of the protein, calorimetry, X-ray crystal analysis and GuHCl denaturation experiments were performed. The calorimetric studies showed that the EAEA-lysozyme was destabilized by 9.6 kJ/mol at pH 2.7 as compared with the wild-type protein, mainly caused by the remarkable decrease in the enthalpy change (ΔH). On the basis of the structural information of the EAEA-lysozyme, thermodynamic analyses show that (1) the addition of the four residues slightly affected the conformation in other parts far from the N-terminal, (2) the remarkable decrease in the enthalpy change due to the conformational changes was almost compensated by the decrease in the entropy change, and (3) the decrease in the Gibbs energy change between the EAEA and wild-type human lysozymes could be explained by the summation of each Gibbs energy change contributing to the stabilizing factors concerning the extra residues.

Chapter III   In order to analyze the mechanism of amyloid fibril formation, the wild-type human lysoyme, amyloidgenic variant (I56T), EAEA-lysozyme and an amyloidgenic variant with four extra residues (EAEA-I56T) were examined in high concentration of ethanol. It was found that all human lysozymes precipitated in a highly concentrated ethanol solution. The three hallmarks of amyloid fibrils were examined to determine whether amyloid fibrils were formed in the precipitates. These results indicated that the precipitates of human lysozymes are amyloid protofilaments.

The rate of amyloid formation was measured by the wild-type and three types of variant human lysozymes in 80 % ethanol solution at 25 °C. The wild-type protein did not form amyloid protofilaments after incubation for 30 hours in 80 % ethanol solution at protein concentration of 0.1 mg/mL, but the amyloidgenic variants formed amyloid protofilaments up to 8 hours. The EAEA and EAEA-I56T lysozymes, which were largely destabilized as compared with the wild-type protein, formed amyloid protofilaments within one hour of incubation. This result suggests that the amyloidgenecity was strongly related to the stability of the proteins.

Chapter IV   In order to determine the whether hen egg lysozyme, which is not related with amyloidosis, forms amyloid fibrils in high ethanol concentration or not, CD spectra, ultracentrifugation and the three hallmarks of amyloid fibril were carried out in various concentrations of ethanol solution. It was found that the CD spectra in the far-UV region of the hen egg lysozyme changed to those characteristic of a β-structure from the native α-helix rich spectra in 90 % ethanol solution. When the concentration of protein was increased to 10 mg/mL, the protein solution formed a gel in the presence of 90 % ethanol and precipitated on further addition of 10 mM NaCl. The results of three hallmarks of amyloid fibril indicate that the precipitates of hen egg lysozyme are amyloid protofilament and that the amyloid protofilament formation of hen egg lysozyme follows closely on the destruction of the helical and tertiary structures. This result suggests that the amyloid formation is a common property of globular proteins under appropriate conditions.

Amyloidgenic mutant human lysozyme was found to form the amyloid fibril in highly concentrated ethanol solution. The amyloid fibril formation in ethanol solution was also found in other mutant human lysozymes, the wild-type human lysozyme and even in the hen egg lysozyme, which is not related with amyloidosis. The present studies conclude that the amyloid formation is not caused by a specific sequence but proteins generally form

amyloid fibrils under specific conditions in which population of partially (or completely) denatured state is increased. That is, the amyloid fibril formation occurs after the destruction of the helical (secondary) and tertiary structures.

References

Anna-Arriola SS, Herskowitz I. 1994. Isolation and DNA sequence of the STE13 gene encoding dipeptidyl aminopeptidase. *Yeast* **10**:801-810.

Anfinsen CB. 1973. Principles that govern the folding of protein chains. *Science* **181**:223-30.

Artymiuk PJ, Blake CC. 1981. Refinement of human lysozyme at 1.5 Å resolution analysis of non-bonded and hydrogen-bond interactions. *J Mol Biol* **152**:737-762.

Arvinte T, Cudd A, Drake AF. 1993. The structure and mechanism of formation of human calcitonin fibrils. *J Biol Chem* **268**:6415-22.

Badman MK, Pryce RA, Charge SB, Morris JF, Clark A. 1998. Fibrillar islet amyloid polypeptide (amylin) is internalised by macrophages but resists proteolytic degradation. *Cell Tissue Res* **291**:285-294.

Bayreuther K, Masters CL. 1996. Alzheimer's disease. Tangle disentanglement. *Nature* **383**:476-477.

Becktel WJ, Schellman JA. 1987. Protein stability curves. *Biopolymers* **26**:1859-1877.

Bishop MF, Ferrone FA. 1984. Kinetics of nucleation-controlled polymerization. A perturbation treatment for use with a secondary pathway. *Biophys J* **46**:631-644.

Blake C, Serpell L. 1996. Synchrotron X-ray studies suggest that the core of the transthyretin amyloid is a continuous β-sheet helix. *Structure* **4**:989-998.

Bonar L, Cohen AS, Skinner MM. 1969. Characterization of the amyloid fibril as a cross-β protein. *Proc Soc Exp Biol Med* **131**:1373-1375.

Booth DR, Sunde M, Bellotti V, Robinson CV, Hutchinson WL, Fraser PE, Hawkins PN, Dobson CM, Radford SE, Blake CCF, Pepys MB. 1997. Instability, unfolding and aggregation of human lysozyme variants underlying amyloid fibrillogenesis. *Nature* **385**:787-793.

Burke MJ, Rougvie MA. 1972. Cross-β protein structures. I. Insulin fibrils. *Biochemistry* **13**:2435-2439.

Brunger AT. 1992. X-PLOR Manual, Ver. 3.1, Yale University, New Haven, CT.

Bussey H. 1988. Proteases and the processing of precursors to secreted proteins in yeast. *Yeast* **4**:17-26.

Canet D, Sunde M, Last AM, Miranker A, Spencer A, Robinson CV, Dobson CM. 1999. Mechanistic studies of the folding of human lysozyme and the origin of amyloidogenic behavior in its disease-related variants. *Biochemistry* **38**:6419-6427.

Carrell RW, Lomas DA. 1997. Conformational disease. *The Lancet* **350**:134-138.

Chaudhuri TK, Horii K, Yoda T, Arai M, Nagata S, Terada TP, Uchiyama H, Ikura T, Tsumoto K, Kataoka H, Matsusima M, Kuwajima K, Kumagai I. 1999. Effect of the extra N-terminal methionine residue on the stability and folding of recombinant α-lactalbumin expressed in *Escherichia coli*. *J Mol Biol* **285**:1179-1194.

Chiti F, Webster P, Taddei N, Clark A, Stefani M, Ramponi G, Dobson CM. 1999. Designing conditions for *in vitro* formation of amyloid protofilaments and fibrils. *Proc Natl Acad Sci USA* **96**:3590-3594.

Cohen AS, Calkins E. 1959. Electron microscopic observations on a fibrous component in amyloid of diverse origins. *Nature* **183**:1202-1203.

Cohen AS. 1965. The constitution and genesis of amyloid. *Int Rev Exp Pathol* **4**:159-243.

Collee JG. 1996. A dreadful challenge. *Lancet* **347**:917-918.

Collinge J, Rosser M. 1996. A new variant of prion disease. *Lancet* **347**:916-917.

Eanes ED, Glenner GG. 1968. X-ray diffraction studies on amyloid filaments. *J Histochem Cytochem* **16**:673-677.

Flinta C, Persson B, Jornvall H, von Heijne G. 1986. Sequence determinants of cytosolic N-terminal protein processing. *Eur J Biochem* **154**:193-196.

Funahashi J, Takano K, Ogasahara K, Yamagata Y, Yutani, K. 1996. The structure, stability, and folding process of amyloidogenic mutant human lysozyme. *J Biochem* **120**:1216-1223.

Funahashi J, Takano K, Yamagata Y, Yutani K. 1999. Contribution of amino acid substitutions at two different interior positions to the conformational stability of human lysozyme. *Protein Engng* **12**:841-850.

Gilchrist PJ, Bradshaw JP. 1993. Amyloid formation by salmon calcitonin. *Biochim Biophys Acta* **4**:111-114.

Glenner GG, Eanes ED, Page DL. 1972. The relation of the properties of Congo red-stained amyloid fibrils to the -conformation. *J Histochem Cytochem* **20**:821-826.

Glenner GG. 1980. Amyloid deposits and amyloidosis. The β-fibrilloses (First of two parts). *New Engl J Med* **302**:1283-1292.

Goldsbury C, Kistler J, Aebi U, Arvinte T, Cooper GJ. 1999. Watching amyloid fibrils grow by time-lapse atomic force microscopy. *J Mol Biol* **285**:33-39.

Gross M, Wilkins DK, Pitkeathly MC, Chung EW, Higham C, Clark A, Dobson CM. 1999. Formation of amyloid fibrils by peptides derived from the bacterial cold shock protein CspB. *Protein Sci* **8**:1350-1357.

Guijarro JI, Sunde M, Jones JA, Campbell ID, Dobson CM. 1998. Amyloid fibril formation by an SH3 domain. *Proc Natl Acad Sci USA* **95**:4224-4228.

Hamaguchi K, Kurono A. 1963. Structure of muramidase (lysozyme) III Effect of 2-Chloroethanol, ethanol and dioxane on the stability of muramidase. *J Biochem* **54**:497-505.

Harper JD, Lansbury PT Jr. 1997. Models of amyloid seeding in Alzheimer's disease and scrapie : Mechanistic truths and physiological consequences of the time-dependent solubility of amyloid proteins. *Annu Rev Biochem* **66**:385-407.

Hashimoto Y, Koyabu N, Imoto T. 1998. Effects of signal sequences on the secretion of hen lysozyme by yeast: construction of four secretion cassette vectors. *Protein Engng* **11**:75-77.

Hawkes R, Grutter MG, Schellman J. Thermodynamic stability and point mutations of bacteriophage T4 lysozyme. *J Mol Biol* **175**:195-212.

Hooke SD, Radford SE, Dobson CM. 1994. The refolding of human lysozyme: a comparison with the structurally homologous hen lysozyme. *Biochemistry* **33**:5867-5876

Ikeda K, Hamaguchi K. 1970. Interaction of alcohols with lysozyme. I. Studies on circular dichroism. *J Biochem* **68**:785-794.

Ishikawa N, Chiba T, Chen LT, Shimizu A, Ikeguchi M, Sugai S. 1998. Remarkable destabilization of recombinant α-lactalbumin by an extraneous N-terminal methionyl residue. *Protein Engng* **11**:333-335.

Jancarik J, Kim SH. 1991. Sparse matrix sampling: a screening method for crystallization of proteins. *J Appl Cryst* **24**:409-411.

Jarrett JT, Lansbury PT Jr. 1993. Seeding "one-dimensional crystallization" of amyloid : A pathogenic mechanism in Alzheimer's disease and scrapie? *Cell* **73**:1055-1058.

Jimenez JL, Guijarro JI, Orlova E, Zurdo J, Dobson CM, Sunde M, Saibil HR. Cryo-electron microscopy structure of an SH3 amyloid fibril and model of the molecular packing. *EMBO J* **18**:815-821.

Julius D, Blair L, Brake A, Sprague G, Thoner J. 1984. Isolation of the putative structural gene for the lysine-arginine-cleaving endopeptidase required for processing of yeast prepro-α-factor. *Cell* **32**:839-852.

Kamatari YO, Konno T, Kataoka M, Akasaka K. 1998. The methanol-induced transition and the expanded helical conformation in hen lysozyme. *Protein Sci* **7**:681-688.

Katakura Y, Zhang W, Zhuang G, Omasa T, Kishimoto M, Goto Y, Suga K. 1998. Effect of methanol concentration on the production of human β2-glycoprotein I domain V by a recombinant *Pichia pastoris*: a simple system for the control of methanol concentration using a semiconductor gas sensor. *J Ferm Bioeng* **86**:482-487.

Kelly JW. 1996. Alternative conformations of amyloidogenic proteins govern their behavior. *Curr Opin Struct Biol* **6**:11-17.

Kirschner DA, Abraham C, Selkoe DJ. X-ray diffraction from intraneuronal paired helical filaments and extraneuronal amyloid fibers in Alzheimer disease indicates cross-β conformation. *Proc Natl Acad Sci U S A* **83**:503-7. Published erratum appears in 1986. *Proc Natl Acad Sci U S A* **83**:2776.

Klunk WE, Pettegrew JW, Abraham DJ.1989. Quantitative evaluation of congo red binding to amyloid-like proteins with a β-pleated sheet conformation. *J Histochem Cytochem* **37**:1273-1281.

Klunk WE, Jacob RF, Mason RP. 1999. Quantifying amyloid β-peptide (Aβ) aggregation using the Congo red-Aβ (CR-Aβ) spectrophotomeric assay. *Anal Biochem* **266**:66-76.

Kowalewski T, Holtzman DM. 1999. In situ atomic force microscopy study of Alzheimer's β-amyloid peptide on different substrates: new insights into mechanism of β-sheet formation. *Proc Natl Acad Sci U S A* **96**:3688-3693.

Kuliopulos A, Walsh CT. 1994. Production, purification, and cleavage of tandem repeats of recombinant peptides. *J Am Chem Soc* **116**:4599-4607.

Kurono A, Hamaguchi K. 1964. Structure of muramidase (lysozyme) VII. Effect of alcohols and the related compounds on the stability of muramidase. *J Biochem* **56**:432-440.

Kuwajima K. 1989. The molten globule state as a clue for understanding the folding and cooperativity of globular-protein structure. *Proteins* **6**:87-103.

Lansbury PT Jr, Costa PR, Griffiths JM, Simon EJ, Auger M, Halverson KJ, Kocisko DA, Hendsch ZS, Ashburn TT, Spencer RGS, Tidor B, Griffin RG. 1995. Structural model for the β-amyloid fibril based on interstrand alignment of an antiparallel-sheet comprising a C-terminal peptide. *Nat Struct Biol* **2**:990-998.

Lashuel HA, Lai Z, Kelly JW. 1998. Characterization of the transthyretin acid denaturation pathways by analytical ultracentrifugation : implications for wild-type, V30M, and L55P amyloid fibril formation. *Biochemistry* **37**:17851-17864.

Lashuel HA, Wurth C, Woo L, Kelly JW. 1999. The most pathogenic transthyretin variant, L55P, forms amyloid fibrils under acidic conditions and protofilaments under physiological conditions. *Biochemistry* **38**:13560-13573.

Lazo ND, Downing DT. 1998. Amyloid fibrils may be assembled from β-helical protofibrils. *Biochemistry* **37**:1731-1735.

Litvinovich SV, Brew SA, Aota S, Akiyama SK, Haudenschild C, Ingham KC. 1998. Formation of amyloid-like fibrils by self-association of a partially unfolded fibronectin type III module. *J Mol Biol* **280**:245-258.

Lomakin A, Teplow DB, Kirschner DA, Benedek GB. Kinetic theory of fibrillogenesis of amyloid β-protein. *Proc Natl Acad Sci U S A* **94**:7942-7.

Loquet LP, Saint-Blancard J, Jolles P. 1968. Apparent affinity constants of lysozymes from different origins for *Micrococcus lysodeikticus* cells. *Biochim Biophys Acta* **167**:150-153.

Makhataze GI, Privalov PL. 1995. Energetics of protein structure. *Adv Protein Chem* **47**:307-425.

Matsuura T, Miyai K, Trakulnaleamsai S, Yomo T, Shima Y, Miki S, Yamamoto K, Urabe I. 1999. Evolutionary molecular engineering by random elongation mutagenesis. *Nat Biotechnol* **17**:58-61.

Matthews BW. 1968. Solvent content of protein crystals. *J Mol Biol* **33**:491-497.

Missmahl HP. 1968. *In* "amyloidosis" (E Mandera, L Ruinen, JH Scholten, AS Cohen, eds.), pp. 22-29. Excerpta Medica, Amsterdam.

Missmahl HP, Hartwig M. 1953. Polarisationsoptische untersuchungen an der amyloidsubstanz. *Virchows Arch. Path. Anat.* **324**:489-508.

Moerschell RP, Hosokawa Y, Tsunasawa S, Sherman F. 1990. The specificities of yeast methionine aminopeptidase and acetylation of amino-terminal methionine *in vivo*. Processing of altered iso-1-cytochromes c created by oligonucleotide transformation. *J Biol Chem* **265**:19638-19643.

Muraki M, Jigami Y, Morikawa M, Tanaka H. 1987. Engineering of the active site of human lysozyme: conversion of aspartic acid 53 to glutamic acid and tyrosine 63 to tryptophan or phenylalanine. *Biochim Biophys Acta* **911**:376-380.

Navaza J. 1994. AmoRe: an automated package for molecular replacement. *Acta Cryst* **A50**:157-163.

Nguyen JT, Inouye H, Baldwin MA, Fletterick RJ, Cohen FE, Prusiner SB, Kirschner DA. X-ray diffraction of scrapie prion rods and PrP peptides. *J Mol Biol* **252**:412-422.

Oobatake M, Ooi T. 1993. Hydration and heat stability effects on protein unfolding. *Prog Biophys Molec Biol* **59**:237-284.

Otwinowski Z. 1990. DENZO data processing package, Yale University, New Haven, CT.

Pace CN. 1986. Determination and analysis of urea and guanidine hydrochloride denaturation curves. *Methods Enzymol* **131**:266-280.

Paifer E, Margolles E, Cremata J, Montesino R, Herrera L, Delgado J. 1994. Efficient expression and secretion of recombinant alpha amylase in *Pichia pastoris* using two different signal sequences. *Yeast* **10**:1415-1419.

Parodi RM, Bianchi E, Ciferri A. 1973. Thermodynamics of unfolding of lysozyme in aqueous alcohol solutions. *J Biol Chem* **11**:4047-4051.

Parry RM Jr., Chandon RC, Shahani KM. 1969. Isolation and characterization of human milk lysozyme. *Arch Biochem Biophys* **130**:59-65

Pauling L, Corey RB. 1951. Configurations of polypeptide chains with favored orientations around single bonds: two new pleated sheets. *Proc Natl Acad Sci U S A* **37**:729-740.

Pepys MB, Hawkins PN, Booth DR, Vigushin DM, Tennent GA, Soutar AK, Totty N, Nguyen O, Blake CCF, Terry CJ, Feest TG, Zalin AM, Hsuan JJ. 1993. Human lysozyme gene mutations cause hereditary systemic amyloidosis. *Nature* **362**:553-557.

Pepys MB. 1996. Amyloid, familial Mediterranean fever, and acute phase response. In The Oxford Textbook of Medicine (Weatherall DJ, Ledingham JGG, Warell DA. eds), 3rd edit., **2**:1512-1524, Oxford University Press, Oxford.

Peters CW, Kruse U, Pollwein R, Grzeschik KH, Sippel AE. 1989. The human lysozyme gene. Sequence organization and chromosomal localization. *Eur J Biochem* **182**:507-516.

Peterson SA, Klabunde T, Lashuel HA, Purkey H, Sacchettini JC, Kelly JW. 1998. Inhibiting transthyretin conformational changes that lead to amyloid fibril formation. *Proc Natl Acad Sci U S A* **95**:12956-12960.

Pickett SD, Sternberg MJE. 1993. Empirical scale of side-chain conformational entropy in protein folding. *J Mol Biol* **231**:825-839.

Plotnikov VV, Brandts JM, Lin LN, Brandts JF. 1997. A new ultrasensitive scanning calorimeter. *Anal Biochem* **250**:237-244.

Privalov PL. 1974. Thermal investigations of biopolymer solutions and scanning microcalorimetry. *FEBS Lett* **40S**:S140-53.

Privalov PL, Khechinashvili NN. 1974. A thermodynamic approach to the problem of stabilization of globular protein structure: a calorimetric study. *J Mol Biol* **86**:665-684.

Privalov PL, Potekhin SA. 1986. Scanning microcalorimetry in studying temperature-induced changes in proteins. *Methods Enzymol* **131**:4-51.

Privalov G, Kavina V, Freire E, Privalov PL. 1995. Precise scanning calorimeter for studying thermal properties of biological macromolecules in dilute solution. *Anal Biochem* **232**:79-85.

Provencher SW. 1982. A constrained regularization method for inverting data represented by linear algebraic or integral equations. *Comput Phys Commun* **27**:213-227.

Puchtler H, Sweat F, Levine M. 1962. On the binding of Congo red by amyloid. *J Histochem Cytochem* **10**:355-364.

Radford SE, Dobson CM, Evans PA. 1992. The folding of hen lysozyme involves partially structured intermediates and multiple pathways. *Nature* **358**:302-307.

Radford SE, Dobson CM. 1999. From computer simulations to human disease: emerging themes in protein folding. *Cell* **97**:291-298.

Redfield C, Dobson CM. 1990. 1H NMR studies of human lysozyme: spectral

assignment and comparison with hen lysozyme. *Biochemistry* **29**:7201-14.

Sakabe N. 1991. X-ray diffraction data collection system for modern protein crystallography with a Weissenberg camera and an imaging plate using synchrotron radiation. *Nucl Instr Methods Phys Res* **A303**:448-463.

Schellman JA. 1955. The stability of hydrogen-bonded peptide structures in aqueous solution. *Compt Rend Trav Lab Carlsberg Ser Chim* **29**:230-259.

Serpell LC, Sunde M, Fraser PE, Luther PK, Morris E, Sandgren O, Lundgren E, Blake CCF. 1995. Examination of the structure of the transthyretin amyloid fibril by image reconstruction from electron micrographs. *J Mol Biol* **254**:113-118.

Shen CL, Scott GL, Merchant F, Murphy RM. 1993. Light scattering analysis of fibril growth from the amino-terminal fragment β(1-28) of β-amyloid peptide. Biophys J **65**:2383-2395.

Shirahama T, Cohen AS. 1967. High-resolution electron microscopic analysis of the amyloid fibril. *J Cell Biol* **33**:679-708.

Shiraki K, Nishikawa K, Goto Y. 1995. Trifluoroethanol-induced stabilization of the α-helical structure of β-lactoglobulin: implication for non-hierarchical protein folding. *J Mol Biol* **245**:180-194.

Sophianopoulos AJ, Rhodes CK, Holcomb DN, Van Holde KE. 1964. Phisical studies of muramidase (lysozyme) II. pH-dependent dimerization. *J Biol Chem* **239**:2516-2524.

Steinlein LM, Graf TN, Ikeda RA. 1995. Production and purification of N-terminal half-transferrin in *Pichia pastoris*. *Protein Expr Purif* **6**:619-624.

Sunde M, Blake CCF. 1997. The structure of amyloid fibrils by electron microscopy and X-ray diffraction. *Adv Protein Chem* **50**:123-159.

Sunde M, Serpell LC, Bartlam M, Fraser PE, Pepys MB, Blake CCF. 1997. Common core structure of amyloid fibrils by synchrotron X-ray diffraction. *J Mol Biol* **273**:729-739.

Takano K, Ogasahara K, Kaneda H, Yamagata Y, Fujii S, Kanaya E, Kikuchi M, Oobatake M, Yutani K. 1995. Contribution of hydrophobic residues to the stability of human lysozyme: calorimetric studies and X-ray structural analysis of the five isoleucine to valine mutants. *J Mol Biol* **254**:62-76.

Takano K, Yamagata Y, Fujii S, Yutani K. 1997a. Contribution of the hydrophobic effect to the stability of human lysozyme: calorimetric studies and X-ray structural analyses of the nine valine to alanine mutants. *Biochemistry* **36**:688-698.

Takano K, Funahashi J, Yamagata Y, Fujii S, Yutani K. 1997b. Contribution of water molecules in the interior of a protein to the conformational stability. *J Mol Biol* **274**:132-142.

Takano K, Yamagata Y, Funahashi J, Hioki Y, Kuramitsu S, Yutani K. 1999a. Contribution of intra- and intermolecular hydrogen bonds to the conformational stability of human lysozyme. *Biochemistry* **38**:12698-12708.

Takano K, Tsuchimori K, Yamagata Y, Yutani K. 1999b. Effect of foreign N-terminal residues on the conformational stability of human lysozyme. *Eur J Biochem* **266**:675-682.

Tan SY, Pepys MB. 1994. Amyloidosis. *Histopathology* **25**:403-414.

Taniyama Y, Yamamoto Y, Nakano M, Kikuchi M, Ikehara M. 1988. Role of disulfide bonds in folding and secretion of human lysozyme in *Saccharomyces cerevisiae*. *Biochem Biophys Res Commun* **152**:962-967.

Taniyama Y, Ogasahara K, Yutani K, Kikuchi M. 1992. Folding mechanism of mutant human lysozyme C77/95A with increased secretion efficiency in yeast. *J Biol Chem* **267**:4619-4624.

Thomas PD, Dill KA. 1993. Local and nonlocal interactions in globular proteins and mechamisms of alcohol denaturation. *Protein Sci* **2**:2050-2065.

Tschopp JF, Sverlow G, Kosson R, Craig W, Grinna l. 1987. High level secretion of glycosylated invertase in the methylotrophic yeast *Pichia pastoris*. *Bio/Technology* **5**:1305-1308.

Turnell W, Sarra R, Baum JO, Caspi D, Baltz ML, Pepys MB. 1986. X-ray scattering and diffraction by wet gels of AA amyloid fibrils. *Mol Biol Med* **3**:409-24.

Velicelebi G, Sturtevant JM. 1979. Thermodynamics of the denaturation of lysozyme in alcohol-water mixtures. *Biochemistry* **7**:1180-1186.

Virchow R. 1854. Zur cellulose-frage. *Virchows Arch* **6**:416-426.

Vonderviszt F, Sonoyama M, Tasumi M, Namba K. 1992. Conformational adaptability of the terminal regions of flagellin. *Biophys J* **63**:1672-1677.

Wall J, Schell M, Murphy C, Hrncic R, Stevens FJ, Solomon A. 1999. Thermodynamic instability of human λ6 light chains: correction with fibrillogenecity. *Biochemistry* **38**:14101-14108

Wolman M, Bubis JJ. 1965. The cause of the green polarization color of amyloid stained with Congo red. *Histochemie* **4**:351-356.

Walsh DM, Lomakin A, Benedek GB, Condron MM, Teplow DB. 1997. Amyloid β-protein fibrillogenesis. *J Biol Chem* **272**:22364-22372.

Waugh DF. 1957. A mechanism for the formation of fibrils from protein molecules. *J Cell Comp Physiol* **49**:145.

Yamagata Y, Kubota M, Sumikawa Y, Funahashi J, Takano K, Fujii S, Yutani K. 1998. Contribution of hydrogen bonds to the conformational stability of human lysozyme: calorimetry and X-ray analysis of six tyrosine --> phenylalanine mutants. *Biochemistry* **37**:9355-9362.

Yutani K, Hayashi S, Sugisaki Y, Ogasahara K. 1991. Role of conserved proline residues in stabilizing tryptophan synthase α subunit: analysis by mutants with alanine or glycine. *Proteins: Struct Funct Genet* **9**:90-98.

Yutani K, Takayama G, Goda S, Yamagata Y, Maki S, Namba K, Tsunasawa S, Ogasahara K. 2000. The process of amyloid-like fibril formation by methionine aminopeptidase from a hyperthermophile, *Pyrococcus furiosus*. *Biochemistry* in press.

List of Publications

[1] **Amyloid Protofilament Formation of Hen Egg Lysozyme in Highly Concentrated Ethanol Solution**

Shuichiro Goda, Kazufumi Takano, Yuriko Yamagata, Ryou Nagata, Hideo Akutsu, Saori Maki, Keiichi Namba, and Katsuhide Yutani

Protein Sci. 2000. in press.

[2] **Effect of the Extra N-terminal Residues on the Stability and Folding of Human Lysozyme Expressed in *Pichia pastoris***

Shuichiro Goda, Kazufumi Takano, Yuriko Yamagata, Yoshio Katakura, and Katsuhide Yutani

Submitted to *Protein Engng*

[3] **Amyloid Formation of Amyloidgenic Human Lysozyme in Ethanol Solution**

Shuichiro Goda, Kazufumi Takano, Yuriko Yamagata, and Katsuhide Yutani

in preparation

List of Related Publications

[4] **The Process of Amyloid-like Fibril Formation by Methionine Aminopeptidase from a Hyperthermophile, *Pyrococcus furiosus***

Katsuhide Yutani, Goh Takayama, Shuichiro Goda, Yuriko Yamagata, Saori Maki, Keiichi Namba, Susumu Tsunasawa, and Kyoko Ogasahara.

Biochemistry 2000. in press.

[5] **Importance of van der Waals Contact Between Glu 35 and Trp 109 to the Catalytic Action of Human Lysozyme**

Michiro Muraki, Shuichiro Goda, Hitoshi Nagahora, and Kazuaki Harata.

Protein Sci 1997. **6**:473-476.

[6] **The Superreactive Disulfide Bonds in α-Lactalbumin and Lysozyme**

Shuichiro Gohda, Akio Shimizu, Masamichi Ikeguchi, and Shintaro Sugai.

J Protein Chem 1995. **14**:731-737.